DEGRADATION OF EXTRACELLULAR DNA BY DNASES

EFFECTS OF GLYCOSAMINOGLYCANS ON DNASE-MEDIATED DEGRADATION OF DNA, DNA-HISTONE COMPLEXES, AND NETS

BY
SAHAR SOHRABIPOUR, BMSc

A Thesis Submitted to the School of Graduate Studies in Partial Fulfilment of the

Requirements for the Degree

Master of Science

McMaster University

McMaster University MASTER OF SCIENCE (2020) Hamilton, Ontario (Medical Sciences)

TITLE: Effects of Glycosaminoglycans on DNase-Mediated Degradation of DNA, DNA-Histone Complexes, and NETs

AUTHOR: Sahar Sohrabipour, BMSc (The University of Western Ontario)

SUPERVISOR: Patricia C. Liaw

NUMBER OF PAGES: xvi, 143

LAY ABSTRACT

Sepsis, a life-threatening condition due to hyperactivation of the immune system in response to infection, results in widespread inflammation and blood clotting. During sepsis, immune cells release sticky strands of DNA that block blood vessels and damage organs. Two different enzymes in the blood (DNase I and DNase1L3) can digest these DNA strands, and may represent a new class of anti-sepsis drugs. Our goal was to determine how heparins, commonly used blood thinners, alter the function of these enzymes. We found that (a) larger-sized heparins improved the activity of DNase I towards DNA-histone complexes and do not require any specific portion of heparin, (b) DNase I is more efficient than DNase1L3 in digesting DNA strands released from immune cells, and (c) levels of DNase I and DNase1L3 are altered in septic patients. Taken together, our studies provide new insights into how these enzymes function.

ABSTRACT

Neutrophil extracellular traps (NETs) are a link between infection and coagulation in sepsis. The major structural component of NETs is nucleosomes, consisting of DNA and histones. NETs not only act as a scaffold to trap platelets, but NET components also promote coagulation and impair fibrinolysis. Thus, removal of extracellular DNA by DNases may be a potential therapeutic strategy for sepsis. Since heparin is used for thromboprophylaxis in sepsis and may also be a potential anti-sepsis therapy, we investigated the mechanisms by which various forms of heparins modulate DNase function.

There are two types of DNases *in vivo*: DNase I (produced by exocrine and endocrine glands) and DNase1L3 (secreted by immune cells). DNase I cleaves free DNA, whereas DNase1L3 preferentially cleaves DNA in complex with proteins such as histones. In this study, we investigated how DNase I and DNase1L3 activities are modulated by the following heparins: unfractionated heparin (UFH), enoxaparin (a low-molecular-weight heparin), Vasoflux (a low-molecular-weight, non-anticoagulant heparin), and fondaparinux (the pentasaccharide unit).

Using agarose gel experiments, we showed that UFH, enoxaparin, and Vasoflux enhance the ability of DNase I to digest DNA-histone complexes (presumably by displacing DNA from histones), whereas fondaparinux does not. These findings are consistent with the K_D values of the binding of heparin variants to histones, with fondaparinux having >1000-fold lower affinity for histones compared to the other heparins. Taken together, our data suggests that the ability of heparin to enhance DNase I-mediated digestion of DNA-histone complexes is size-dependent and independent of the

pentasaccharide region of heparin. With respect to DNase1L3, we observed that it is able to digest histone-bound DNA, and that all heparins, except fondaparinux, inhibited DNase1L3-mediated digestion of histone-bound DNA.

Next, we visualized the degradation of NETs by fluorescence microscopy. DNase I (± heparin variants) completely degraded NETs, presumably by digesting extracellular chromatin at histone-free linker regions, thereby releasing nucleosome units. DNase1L3 also degraded NETs, but not as effectively as DNase I, and was inhibited by all heparins except fondaparinux. Finally, we showed that DNase I levels are decreased and DNase1L3 levels are elevated in septic patients. Taken together, our findings demonstrate that heparin modulates the function of DNases, and that endogenous DNase levels are altered in sepsis pathophysiology.

ACKNOWLEDGEMENTS

I would like to acknowledge the many individuals that have made the completion of this thesis possible, and recognize the invaluable support and assistance that each of you have provided me during my graduate studies.

First and foremost, I wish to express my deepest gratitude and appreciation to my supervisor Dr. Patricia Liaw. Thank you so much for providing me with this wonderful opportunity to pursue a Master's degree. Your exceptional guidance, expertise, and kindness will forever be valued, and I am very lucky to have had you as my mentor. I had the privilege of learning so much from you, and the opportunity to grow as a scientist, a student, and a person. Besides improving academically, I was also able to strengthen many invaluable skills thanks to your mentorship, such as perseverance during difficult times, and teamwork due to the many collaborations and projects I had the opportunity to be a part of in addition to my studies. Graduate school has been such a rewarding experience that would not have been possible without you.

To my supervisory committee members Dr. Colin Kretz and Dr. Jeffrey Weitz, thank you both for your valuable feedback and insights, which have truly helped strengthen my thesis. Both your expertise and wisdom has been very inspiring, and motivates me to constantly challenge myself to achieve excellence in all my future endeavours.

To my parents Mojgan Nikpar and Hamid Sohrabipour, words can never truly express how grateful I am for the lifelong support that you have both provided me. Thank you both from the bottom of my heart.

Thank you to my labmates, both past and present, for being amazing team members! I want to extend my thanks to Dr. Dhruva Dwivedi, our lab manager, for being so helpful and kind. I appreciate your support.

To the wonderful friends that I have met here at TaARI, thank you for enriching my graduate school experience. I am so grateful for the friendships I have made, and it has been a pleasure working with each of you. Special thanks to Kanwal Singh, who has always gone above and beyond, and provided me with endless support! Thank you so much for always being there for me, and for your enthusiastic encouragement every step of the way.

Lastly, I would like to thank the following funding agencies that have financially supported my graduate studies: Ontario Graduate Scholarship (2018 – 2020), CanVECTOR Studentship Award, and McMaster Entrance Scholarship. Thank you to the Canadian Critical Care Translational Biology Group for the Travel Award and the University of British Columbia Centre for Blood Research for the Earl W. Davie Symposium Trainee Travel Award, both of which provided me with opportunities to present my research at national conferences.

Writing this acknowledgement section of my thesis was a heart-warming experience, and I am so grateful to have such an incredible support system filled with wonderful and brilliant individuals.

TABLE OF CONTENTS

LIST OF FIGURES

LIST OF TABLES

LIST OF ABBREVIATIONS

1L3 – 1 like 3
α2AP – Alpha 2-antiplasmin
α2M – Alpha 2-macroglobulin
ADP – Adenosine diphosphate
AT – Antithrombin
ATP – Adenosine triphosphate
ANOVA – Analysis of variance
APACHE II – Acute Physiology And Chronic Health Evaluation II
APC – Activated protein C
BLI – Bio-layer interferometry
Ca^{2+} – Calcium
CRP – C-reactive protein
DNA – Cell-free DNA
DAMPs – Damage-associated molecular patterns
DIC – Disseminated intravascular coagulation
DNA – Deoxyribonucleic acid
DNase – Deoxyribonuclease
DVT – Deep vein thrombosis
EDTA – Ethylenediaminetetraacetic acid
ELISA – Enzyme-linked immunosorbent assay
EPCR – Endothelial cell protein C receptor
F – Factor
FDPs – Fibrin degradation products
GAGs – Glycosaminoglycans
GP – Glycoprotein
GPI – Glycosylphosphatidyl inositol
HALO – Heparin AnticoaguLation to Improve Outcomes in Septic Shock
HMGB1 – High mobility group box 1
HMWK – High-molecular-weight kininogen
HRP – Horseradish peroxidase
IBD – Inflammatory bowel disease
ICU – Intensive care unit
IL – Interleukin
LMWHs – Low-molecular-weight heparin
Mg^{2+} – Magnesium
Mn^{2+} – Manganese
MPO – Myeloperoxidase
NE – Neutrophil elastase
NETs – Neutrophil extracellular traps
PAD4 – Peptidylarginine deiminase 4
PAMPs – Pathogen-associated molecular patterns
PC – Protein C

PE – Pulmonary embolism
PK – Prekallikrein
PKC – Protein kinase C
PLC – Phospholipase C
PMA – Phorbol 12-myristate 13-acetate
PolyP – Polyphosphates
PPP – Platelet-poor plasma
PRRs- Pathogen recognition receptors
PS – Phosphatidylserine
RFU – Relative fluorescence units
RNA – Ribonucleic acid
ROS – Reactive oxygen species
SEM – Standard error of the mean
Serpin – Serine protease inhibitor
SLE – Systemic lupus erythematosus
TAFI – Thrombin activatable fibrinolysis inhibitor
TF – Tissue factor
TFPI – Tissue factor pathway inhibitor
TLRs – Toll-like receptors
TM – Thrombomodulin
TMB – Tetramethylbenzidine
TNF-α – Tissue necrosis factor-alpha
tPA – Tissue plasminogen activator
TXA2 – Thromboxane A2
UFH – Unfractionated heparin
uPA – Urokinase-type plasminogen activator
VTE – Venous thromboembolism
VWF – von Willebrand factor
Zn^{2+} – Zinc

DECLARATION OF ACADEMIC ACHIEVEMENT

Sahar Sohrabipour completed all the experiments, contributed to the conception, ideas, and design of the studies, analyzed and interpreted the results, conducted the statistical analyses, and wrote this thesis.

Dr. Patricia C. Liaw contributed to the conception, ideas, and design of the studies, obtained funding to support the completion of this research, and reviewed the results and thesis.

1.0 Introduction to Sepsis

1.0.1 Sepsis as a global health priority

Sepsis is defined as life-threatening organ dysfunction as a result of a maladaptive host response to an infection, which includes systemic inflammation and coagulation (Singer et al., 2016). The incidence of sepsis is increasing, and this condition is responsible for one in five deaths globally per year (Kempker et al., 2020). In 2017, approximately 49 million people were diagnosed with sepsis, and 11 million people had died from this condition (Kempker et al., 2020). The World Health Organization declared sepsis a global health priority in 2017 (Reinhart et al., 2017). In Canada alone, sepsis affects approximately 30,000 people each year, and $325,000,000 is spent annually on treating this condition (Canadian Sepsis Foundation, 2019). Current existing management strategies involve early administration of broad-spectrum antibiotics, source control, fluid resuscitation, and use of mechanical ventilation (Rhodes et al., 2017). Nonetheless, there is no cure for sepsis (Lakshmikanth et al., 2016). As a result, further research on sepsis must be done to better understand the pathophysiology of this disease, which may translate into novel therapeutic strategies.

1.0.1 The interplay between infection, inflammation, and coagulation

Infection, inflammation, and coagulation are known to be closely linked in sepsis. Many pathogens can lead to sepsis, however bacterial infections are the most common cause (Dolin et al., 2019). In response to an infection, the immune system becomes activated by binding of pathogen-associated molecular patterns (PAMPs) on pathogens to pathogen recognition receptors (PRRs) on innate immune cells, including neutrophils,

macrophages, and monocytes (Gyawali et al., 2019). Consequently, these immune cells can release many proinflammatory cytokines including tissue necrosis factor-alpha (TNF-α), interleukin (IL)-1, and IL-6 (Gyawali et al., 2019). These proinflammatory cytokines can cause endothelial cells to become activated and express E- and P-selectin, which are involved in recruiting leukocytes, thereby exacerbating the immune response (Barthel et al., 2007). Additionally, activated endothelial cells release von Willebrand factor (VWF), a platelet-capturing protein, which further contributes to coagulopathy (Springer., 2014). Moreover, PAMPs can upregulate tissue factor (TF) expression on circulating monocytes, which triggers the extrinsic pathway of the coagulation cascade, and leads to a state of hypercoagulability in septic patients (Remick., 2007). In addition to an increase in procoagulant effects, an impairment in natural anticoagulant pathways and a state of hypofibrinolysis also contribute to excessive coagulation in sepsis (Simmons et al., 2015). Eventually, these impairments can lead to disseminated intravascular coagulation (DIC), which is a life-threatening condition characterized by systemic microvascular thrombosis, followed by excessive bleeding due to consumption of coagulation proteins and platelets (Okamoto et al., 2016). DIC is a common complication in sepsis affecting about 35% of patients, and further contributes to organ dysfunction (Iba et al., 2019).

1.1 Hemostasis

1.1.1 Primary Hemostasis

During vascular injury, subendothelial exposure triggers clot formation to limit blood loss through the process of hemostasis (Pryzdial et al., 2018). There are three main components of hemostasis: primary, secondary and tertiary hemostasis (Repetto et al.,

2017). Primary hemostasis involves adhesion, activation, and aggregation of platelets to form a platelet plug, while secondary hemostasis involves formation of a stable fibrin clot (Repetto et al., 2017; Xu et al., 2016). Upon vascular injury, the underlying subendothelial matrix components such as different types of collagen and laminin, become exposed to the circulation (Wang et al., 2016). VWF in circulation binds to the exposed collagen through its A1 and A3 domains (Springer., 2014). Circulating platelets rapidly adhere to the subendothelium at sites of vascular damage through various adhesion molecules or glycoproteins (GP) on their cell surface (Ni et al., 2003). For example, the GPIb-IX-V complex on platelets binds to the A1 domain of VWF, and the platelet receptors GPVI and integrin $\alpha_2\beta_1$ mediates binding with collagen (Ni et al., 2003; Repetto et al., 2017). Once platelets adhere to the subendothelial matrix, they become activated and release many agonists, such as adenosine diphosphate (ADP) and thromboxane A2 (TXA2) (Estevez et al., 2017). Platelets contain granules, including alpha and dense granules, that store and release contents, which are critical to normal platelet function (Blair et al., 2009). Alpha granules are the most abundant granules, and contain many proteins including VWF, P-selectin, and fibrinogen (Blair et al., 2009). Dense granules are smaller than alpha granules, and contain molecules including polyphosphates, ADP, adenosine triphosphate (ATP), and calcium (Ca^{2+}) (Chen et al., 2018). The release of alpha and dense granule contents from platelets causes further platelet activation, as well as aggregation through various signalling mechanisms (Jackson., 2007). The released agonists are able to interact with platelet receptors, which are coupled to G proteins, such as the G_q protein that activates phospholipase C (PLC). Activation of PLC generates second messengers, which lead to

protein kinase C (PKC) activation and increased intracellular Ca^{2+} levels, thereby causing platelet aggregation (Shah et al., 2001). A highly expressed integrin, $\alpha_{IIb}\beta_3$, is also involved in platelet aggregation (Durrant et al., 2017). Fibrinogen binds to $\alpha_{IIb}\beta_3$, and forms bridges between adjacent platelets, thereby causing platelets to aggregate (Ley et al., 2016). As a result, platelet aggregation forms a platelet plug, which temporarily seals an injury in the vessel wall (Durrant et al., 2017; Ley et al., 2016).

1.1.2 The Coagulation Cascade: Secondary Haemostasis

The coagulation cascade consists of sequential activation of zymogens to enzymes, and is divided into the extrinsic, intrinsic, and common pathway (Figure 1.1) (Loof et al., 2014; Versteeg et al., 2013). The coagulation cascade and fibrinolytic system are closely regulated to ensure a delicate balance in blood flow under normal physiological conditions; however, excessive clotting can lead to thrombosis, whereas impaired clot formation, stability, or premature clot degradation can lead to hemorrhaging (Pryzdial et al., 2018).

1.1.3 The Extrinsic Pathway

Many extravascular cell types have been found to express TF, which is an integral membrane protein that plays a key role in the extrinsic pathway (Butenas et al., 2005). Monocytes are intravascular cells that can also upregulate cell surface TF expression in response to infectious or inflammatory stimuli (Ernofsson et al., 1997). The extrinsic pathway (tissue factor pathway) is triggered in response to tissue damage, in which the disrupted endothelium exposes extravascular TF to the blood (Palta et al., 2014). Factor (F) VII circulates in the blood as either its inactive zymogen form (99%) or as free FVIIa (1%) (Giansily-Blaizot et al., 2017). FVII or FVIIa can bind to TF, and the zymogen form

becomes activated by either the TF:FVIIa complex itself, or by thrombin, FIXa, FXa and FXIIa through feedback activation (Giansily-Blaizot et al., 2017). The extrinsic tenase complex forms when phospholipid-bound TF binds to FVIIa (Haynes et al., 2012). This complex can activate FX to FXa in the presence of Ca^{2+} ions (Mackman et al., 2007). Activation of FX is the beginning of the common pathway. Additionally, the extrinsic tenase complex can activate FIX into FIXa, which is part of the intrinsic pathway (Haynes et al., 2012; Mackman et al., 2007).

1.1.4 The Intrinsic Pathway

The intrinsic pathway (contact activation pathway) is activated when blood comes into contact with negatively charged surfaces or molecules, such as deoxyribonucleic acid (DNA), ribonucleic acid (RNA), polyphosphates (polyP), or glass (Palta et al., 2014). This exposure leads to the autocatalytic activation of the zymogen FXII into the serine protease FXIIa (Smith et al., 2015). FXIIa, along with its cofactor high-molecular-weight kininogen (HMWK), activates prekallikrein (PK) to plasma kallikrein (Smith et al., 2015). Plasma kallikrein forms a positive feedback loop by causing further activation of FXII (Müller et al., 2011). Next, FXIIa activates its substrate FXI to FXIa, and FXIa activates FIX to FIXa (Gailani et al., 2007). The intrinsic tenase complex forms on negatively charged phospholipid surfaces and includes FIXa, its cofactor FVIIIa, and Ca^{2+} (Gailani et al., 2007; Zhao et al., 2015). This complex can activate FX to FXa, which is the beginning of the common pathway (Zhao et al., 2015).

1.1.5 The Common Pathway

The intrinsic and extrinsic pathways merge at the common pathway (Palta et al., 2014). The common pathway begins when FX becomes activated to FXa by either the extrinsic or intrinsic tenase complex (Palta et al., 2014; Smith et al., 2015). A prothrombinase complex is formed when FXa associates with its cofactor, FVa, on a phospholipid surface in the presence of Ca^{2+} ions (Lechtenberg et al., 2013). This complex converts prothrombin into thrombin (Smith et al., 2015). Thrombin then converts fibrinogen into fibrin monomers, and activates FXIII to FXIIIa (Standeven et al., 2002). Fibrin monomers polymerize into oligomers that lengthen into protofibrils, which eventually aggregate into fibrin strands (Chernysh et al., 2012). FXIIIa covalently crosslinks the fibrin strands to form a stable and insoluble fibrin clot (Palta et al., 2014; Smith et al., 2015). In addition, thrombin activates FV, FVIII, and FXI, thereby further amplifying thrombin generation (Narayanan., 1999). Thrombin can also activate platelets and endothelial cells (Minami et al., 2004).

1.1.6 Fibrinolysis: Tertiary Haemostasis

Fibrinolysis is a process that occurs to degrade the fibrin clot, and involves conversion of plasminogen to plasmin by tissue plasminogen activator (tPA) or by urokinase-type plasminogen activator (uPA) (Cesarman-Maus et al., 2005). Plasmin is then able to degrade fibrin into soluble fibrin degradation products (FDPs) (Cesarman-Maus et al., 2005). Fibrin is also a cofactor for plasminogen activation by binding to both tPA and plasminogen (Fredenburgh et al., 1992). In addition, plasmin is able to cleave the native form Glu-plasminogen at Lys^{77}–Lys^{78}, causing its conversion to Lys-plasminogen

(Fredenburgh et al., 1992; Hajjar et al., 1988). Compared to Glu-plasminogen, Lys-plasminogen has increased binding affinity for fibrin due to its more open conformation, and is activated more efficiently by tPA and uPA (Hajjar et al., 1988; Zhang et al., 2003). Endothelial cells produce and release tPA, while urinary epithelium, monocytes, and macrophages produce uPA (Chapin et al., 2015). Fibrinolysis is tightly controlled and regulated under normal physiological conditions (Longstaff et al., 2015). The main inhibitor of tPA and uPA is plasminogen activator inhibitor-1 (PAI-1), which is a serine protease inhibitor (serpin) (Pannekoek et al., 1986). To protect the fibrin clot from lysis, thrombin activates thrombin activatable fibrinolysis inhibitor (TAFI) to TAFIa (Bouma et al., 2006). TAFIa is a carboxypeptidase that removes C-terminal lysines from fibrin; consequently, the cofactor activity of fibrin in tPA-mediated plasminogen activation is attenuated, thereby downregulating fibrinolysis (Bajzar., 2000; Bouma et al., 2006). Additionally, FXIII becomes activated by thrombin to FXIIIa, which is a transglutaminase that is able to localize alpha 2-antiplasmin (α2AP) to fibrin, thus inhibiting fibrinolysis (Fraser et al., 2011; Rollins et al., 2016). Furthermore, plasmin that is unbound to fibrin can be inhibited by α2AP, or by alpha-2 macroglobulin (α2M) to a lesser extent (Chapin et al., 2015; Schneider et al., 2004). Mechanisms that inhibit fibrinolysis exist to prevent excessive clot breakdown, which could lead to hemorrhaging; however, fibrinolysis is also crucial in preventing excessive clot formation and thrombosis (Longstaff et al., 2015). In addition to fibrinolysis, natural anticoagulant mechanisms exist to regulate the coagulation cascade and prevent excessive clotting (Chapin et al., 2015).

1.1.7 Natural anticoagulant mechanisms

The coagulation cascade is a crucial process in hemostasis to stop bleeding during vascular injury; however, excessive activation of the coagulation cascade can lead to life-threatening thrombosis (Palta et al., 2014). As a result, natural anticoagulant mechanisms prevent excessive activation of the coagulation cascade and include: antithrombin (AT), tissue factor pathway inhibitor (TFPI), and the protein C (PC) pathway (Dahlback., 2005).

AT is a plasma glycoprotein that belongs to the serine protease inhibitor (serpin) family (Bock et al., 1982). AT possesses two specific active binding sites including a reactive center loop (RCL) and a heparin-binding domain (Perry., 1994). The RCL allows AT to bind and inhibit thrombin, FIXa, FXa, FXIa, FXIIa, and FVIIa, while the heparin-binding domain allows AT to bind to heparin (Perry., 1994). Specifically, the active site of the serine proteases binds and cleaves the RCL of AT, which forms a 1:1 covalent complex that is irreversible and rapidly removed from the circulation within 5 minutes (Perry., 1994). However, this complex forms very slowly (Jin et al., 1997). The binding of heparin or heparan sulfate to AT accelerates the rate at which AT inhibits various coagulation factors by up to 1000-fold (Paschoa., 2016; Yeung et al., 2015). Heparan sulfate is a naturally occurring glycosaminoglycan (GAG) that is expressed on the surface of cells, such as vascular endothelial cells, whereas heparin is a therapeutic GAG (Meneghetti et al., 2015). The major form of AT is alpha-AT (90% in plasma) and has all four glycosylation sites occupied with oligosaccharides, whereas beta-AT (10% in plasma) has three of the four sites occupied (Hepner et al., 2013). As a result, beta-AT has higher affinity towards heparin than alpha-AT (McCoy et al., 2003).

TFPI is a multivalent Kunitz-type serpin and exists in two major isoforms, TFPIα and TFPIβ, due to alternative splicing (Wood et al., 2014). TFPIα has three Kunitz-type inhibitor domains (K1, K2, and K3) and a highly basic C-terminus, while TFPIβ has the K1 and K2 domains and a unique C-terminus that encodes for the attachment of glycosylphosphatidyl inositol (GPI)-anchor (Mast., 2016; Wood et al., 2014). The K1 domain binds FVIIa, and the K2 domain binds FXa, thereby forming a TF-FVIIa-FXa-TFPI quaternary complex (Maroney et al., 2013; Wood et al., 2013). Thus, both TFPI isoforms inhibit the TF:FVIIa complex in a FXa-dependent manner (Mast., 2016). In contrast, only TFPIα inhibits the prothrombinase complex by binding of its basic C-terminal region to the B domain of FV, and its K2 domain to FXa (Wood et al., 2013).

Another major anticoagulant pathway that regulates the coagulation cascade is the PC pathway (Esmon., 2003). There are many important components in this pathway including thrombin, thrombomodulin (TM), the endothelial cell protein C receptor (EPCR), PC, and protein S (Esmon., 2003). The PC pathway is initiated when thrombin binds to TM on endothelial cells (Dahlback., 2005). EPCR binds to the Gla domain of PC and presents PC to the thrombin-TM complex, thereby accelerating the rate of activated protein C (APC) generation (Dahlback., 2005; Esmon., 2003). Next, APC dissociates from EPCR, binds to its cofactor protein S on cell surfaces, and causes proteolytic cleavage of FVa and FVIIIa (Griffin et al., 2007).

1.1.8 Disruption of hemostasis during sepsis

Under normal physiological conditions, there is a delicate balance in blood flow to prevent excessive clotting or bleeding, as mentioned above in section 1.1.2 (Pryzdial et al.,

2018). In sepsis, there is a dysregulation in this balance characterized by excessive activation of the coagulation cascade, suppression of natural anticoagulant mechanisms, and impaired fibrinolysis (Gando., 2013; Gyawali et al., 2019). Taken together, these impairments result in a state of hypercoagulability, which can contribute to DIC or to venous thromboembolism (VTE), which is a life-threatening condition that manifests as deep vein thrombosis (DVT) or pulmonary embolism (PE) (Goldhaber., 2012). Plasma levels of TF are elevated in septic patients, thereby causing increased activation of the coagulation cascade (Simmons et al., 2015). This elevated expression of TF leads to an upregulation of proinflammatory cytokines, such as IL-1 and IL-6, which suppresses natural anticoagulant mechanisms (Simmons et al., 2015). Moreover, there is a decrease in the expression of TFPI in sepsis (Semeraro et al., 2015). AT is another key natural anticoagulant that becomes impaired in sepsis due to increased consumption, increased degradation by neutrophil elastase, and impaired synthesis (Scully et al., 2019). Another natural anticoagulant mechanism that is disrupted in sepsis is the PC pathway (Guitton et al., 2011). Specifically, there is decreased synthesis of PC and protein S, and downregulation of EPCR and TM, resulting in decreased APC levels (Scully et al., 2019; Simmons et al., 2015). Disruptions in these three natural anticoagulant pathways in septic patients contribute to a state of hypercoagulability (Guitton et al., 2011).

In addition to excessive activation of the coagulation cascade and suppression of natural anticoagulant mechanisms, inhibition of fibrinolysis also occurs in septic patients (Levi et al., 2012). The levels of PAI-1 are elevated, which prevents clot lysis (Gando., 2013; Scully et al., 2019). Other mechanisms that lead to a procoagulant and anti-

fibrinolytic state in sepsis include the release of neutrophil extracellular traps by neutrophils, and increased DNA and histone levels, which will be described below.

Figure 1.1. The coagulation cascade and fibrinolytic system. The coagulation cascade consists of sequential activation of zymogens to enzymes, and is divided into the extrinsic, intrinsic, and common pathway (Versteeg et al., 2013). Tissue damage exposes TF, which initiates the extrinsic pathway, while negatively charged surfaces, such as DNA, RNA, and polyP initiate the intrinsic pathway (Swystun et al., 2011). Both pathways lead to the common pathway, which initiates blood clotting and the formation of an insoluble fibrin clot (Healy et al., 2017). Upon the initiation of the coagulation cascade, fibrinolysis is also activated at the same time but acts more slowly to maintain hemostasis (Loof et al., 2014). During fibrinolysis, plasminogen is converted to plasmin by tPA and uPA; afterwards, plasmin degrades the fibrin clot into FDPs (Gando., 2013). DNA is anti-fibrinolytic due to inhibition of plasmin-mediated fibrin degradation (Gould et al., 2015). Histones are also anti-fibrinolytic due to binding fibrin and increasing the thickness of the fibers (Gould et al., 2015). Further, histones are procoagulant by promoting prothrombin autoactivation (Barranco-Medina et al., 2013). Histones bind to PC and prevent the generation of APC (Ammollo et al., 2011). APC is a natural anticoagulant enzyme that inhibits FVa and FVIIIa, and is also a physiological inhibitor of histones (Xu et al., 2009). Both the coagulation cascade and fibrinolytic system are highly regulated under normal physiological conditions (Longstaff et al., 2015; Palta et al., 2014). Figure adapted from: (Loof et al., 2014).

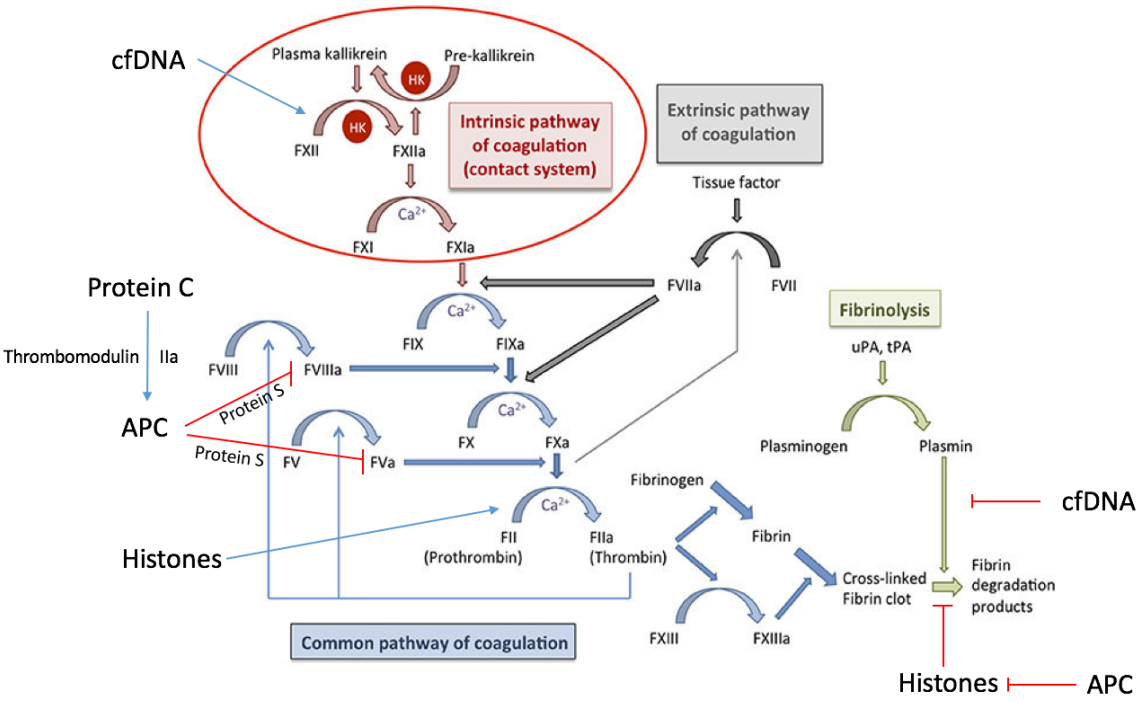
cfDNA
Plasma kallikrein
Pre-kallikrein
HK
HK
FXII
FXIIa
Intrinsic pathway of coagulation (contact system)
Ca2+
FXI
FXIa
Extrinsic pathway of coagulation
Tissue factor
FVIIa
FVII
Protein C
Thrombomodulin
IIa
APC
Protein S
Protein S
FVIII
FVIIIa
FIX
FIXa
Ca2+
FV
FVa
FX
FXa
Ca2+
Fibrinolysis
uPA, tPA
Plasminogen
Plasmin
Histones
FII
(Prothrombin)
FIIa
(Thrombin)
Ca2+
Fibrinogen
Fibrin
FXIII
FXIIIa
Cross-linked Fibrin clot
Fibrin degradation products
cfDNA
Histones
APC
Common pathway of coagulation

1.2 Immunothrombosis

1.2.1 Crosstalk between monocytes, neutrophils, and platelets

Excessive activation of the coagulation cascade or impaired fibrinolysis can lead to thrombosis, as described above in section 1.1; however, another trigger for thrombosis involves the innate immune response, and is termed immunothrombosis (Gaertner et al., 2016). Monocytes and neutrophils are able to respond to an infection by recognizing PAMPs on pathogens, and releasing proinflammatory cytokines, thereby exacerbating inflammation (Gyawali et al., 2019). This proinflammatory phenotype recruits additional leukocytes, mainly neutrophils and monocytes, which trigger fibrin formation by exposure of cell-derived TF (von Brühl et al., 2012). A study by von Brühl and colleagues demonstrated that platelets are able to associate with leukocytes through GPIbα, identifying a crosstalk between platelets, monocytes, and neutrophils in the initiation and amplification of thrombosis (von Brühl et al., 2012). Platelet-leukocyte interactions are important because platelets are able to release proinflammatory cytokines, such as CXC-chemokine ligand 1, which recruit additional leukocytes (Gaertner et al., 2016). Moreover, platelets can stimulate the release of neutrophil extracellular traps (NETs) from neutrophils, which contributes to thrombosis, and serves as another mechanism underlying immunothrombosis (von Brühl et al., 2012).

1.2.2 NETosis

NETosis is a form of programmed cell death in which activated neutrophils release NETs, which consist of DNA, histones, and neutrophil granular enzymes, such as neutrophil elastase (NE) and myeloperoxidase (MPO) (von Brühl et al., 2012). The major

structural component of NETs is nucleosomes, which consist of DNA wrapped around a core histone octamer containing two copies of each histone H2A, H2B, H3, and H4 (von Brühl et al., 2012). The nucleus is the main source of DNA in NETs, however mitochondrial DNA has also been identified as a source (Lood et al., 2016). Many different stimuli are capable of triggering NETosis, such as microorganisms, damage-associated molecular patterns (DAMPs), phorbol 12-myristate 13-acetate (PMA), autoantibodies, and cytokines (Kaplan et al., 2012). These stimuli can bind to various neutrophil receptors, including Toll-like receptors (TLRs), Fc receptors, and complement receptors, which are involved in initiating the intracellular signaling pathways of NETosis (Brinkmann et al., 2004). Binding to receptors increases cytoplasmic Ca^{2+} levels, which activates PKC (Kaplan et al., 2012). Next, PKC is able to activate NADPH oxidase, which leads to the production of reactive oxygen species (ROS) and peptidylarginine deiminase 4 (PAD4) activation (Dekker et al., 2000). The release of NETs requires the decondensation of chromatin by PAD4 (Franck et al., 2018). PAD4 is a nuclear enzyme that converts specific arginine residues to citrulline on histones, thereby reducing the positive charge on histones (Franck et al., 2018). In addition, NE and MPO production and translocation into the nucleus further promotes chromatin decondensation (Papayannopoulos et al., 2010). Next, the nuclear envelope and granular membranes disintegrate, and the chromatin is released into the cytosol, where granular and cytosolic proteins become attached and decorate the chromatin (Fuchs et al., 2007). Finally, the plasma membrane ruptures, the NETs are released into the extracellular space, and the neutrophil dies (Metzler et al., 2014). The intracellular signaling pathway of NETosis is shown in Figure 1.2.

1.2.3 NETosis: a link between infection, inflammation, and coagulation

NETosis has recently emerged as a new mechanism that links infection, inflammation, and coagulation together in sepsis (Yang et al., 2017). The most abundant leukocytes are neutrophils, and they are the first to respond to an infection (Rosales., 2018). Microorganisms are able to activate neutrophils and trigger the release of NETs; conversely, NETs are capable of trapping and neutralizing pathogens, including bacteria, viruses, fungi, and parasites (Clark et al., 2007). In response to an infection, PRRs on innate immune cells recognize PAMPs on pathogens, which results in the release of many proinflammatory cytokines including TNF-α and IL-8 (Gyawali et al., 2019). Both TNF-α and IL-8 have been shown to induce NETosis (Barliya et al., 2017). Conversely, NETs can exert proinflammatory effects by stimulating the production of cytokines, including IL-6 and IL-8, thereby exacerbating the immune response in sepsis (de Bont et al., 2019; Giaglis et al., 2016). In addition, NETs also exert procoagulant effects (Foley et al., 2016). NETs can present TF, which activates the extrinsic pathway of coagulation (Döring et al., 2020). The NET-associated protein NE can cleave TFPI, further contributing to thrombin generation (Massberg et al., 2010). Moreover, activated platelets induce NETosis, and NETs have been shown to amplify platelet activation and aggregation, thereby forming a positive feedback loop (Zucoloto et al., 2019). The individual NET components, DNA and histones, also exert procoagulant and anti-fibrinolytic effects, which will be discussed in section 1.3.

1.2.4 NETs as a double-edged sword

NETs have been described as a double-edged sword of innate immunity due to both their protective and harmful effects within the host (Kaplan et al., 2012). NETosis is a unique form of cell death that is conserved across vertebrates, highlighting the important role that NETs play in the immune response (Tatsiy et al., 2018). Specifically, NETs are web-like structures that are capable of trapping and neutralizing pathogens, including bacteria, fungi, and viruses (Clark et al., 2007). NETs are also composed of many antimicrobial peptides and enzymes including NE, MPO, and cathepsin G, which are involved in eliminating pathogens (Brinkmann et al., 2004; Metzler et al., 2011). Although NETs are part of the innate immune response, they also exert many detrimental effects within the host (Yang et al., 2017). The significantly higher levels of MPO-DNA complexes in septic patients, compared to healthy controls, have been found to contribute to a state of hypercoagulability (Yang et al., 2017). The uncontrolled release of NETs from neutrophils contributes to micro- and macro-vascular thrombosis (McDonald et al., 2017). NETs can capture fibrin, erythrocytes, platelets, and VWF, which forms a physical scaffold that helps with thrombus formation and growth (Martinod et al., 2013; Yu et al., 2019). Additionally, NETs have been shown to excessively activate the complement cascade, which is associated with poor outcomes in septic patients, such as multiple organ damage (Markiewski et al., 2008; Sabbione et al., 2017). Complement proteins such as properdin and C3 can become deposited on NETs, and activated by NET-associated enzymes (e.g. MPO); therefore, NETs are a platform for complement activation (de Bont et al., 2019). Studies have also shown that excessive NET formation and impaired NET clearance results

in autoimmune responses, which can lead to acute or chronic inflammatory disorders (Kaplan et al., 2012). Taken together, targeting NETs may be a valuable therapeutic strategy to prevent or attenuate its deleterious effects in sepsis.

Figure 1.2. Intracellular signalling pathways of NETosis. Different stimuli such as microorganisms, PMA, and DAMPs trigger NETosis (Kaplan et al., 2012). The activation of NADPH oxidase leads to the production of ROS and PAD4 activation (Dekker et al., 2000). PAD4 promotes chromatin decondensation (Franck et al., 2018). Next, NE and MPO are produced and translocated into the nucleus to further promote chromatin decondensation (Papayannopoulos et al., 2010). Afterwards, the chromatin is released into the cytosol, where granular and cytosolic proteins become attached and decorate the chromatin (Fuchs et al., 2007). The plasma membrane is ruptured, the NETs are released, and the neutrophil dies (Metzler et al., 2014). Source: (Jorch et al., 2017)

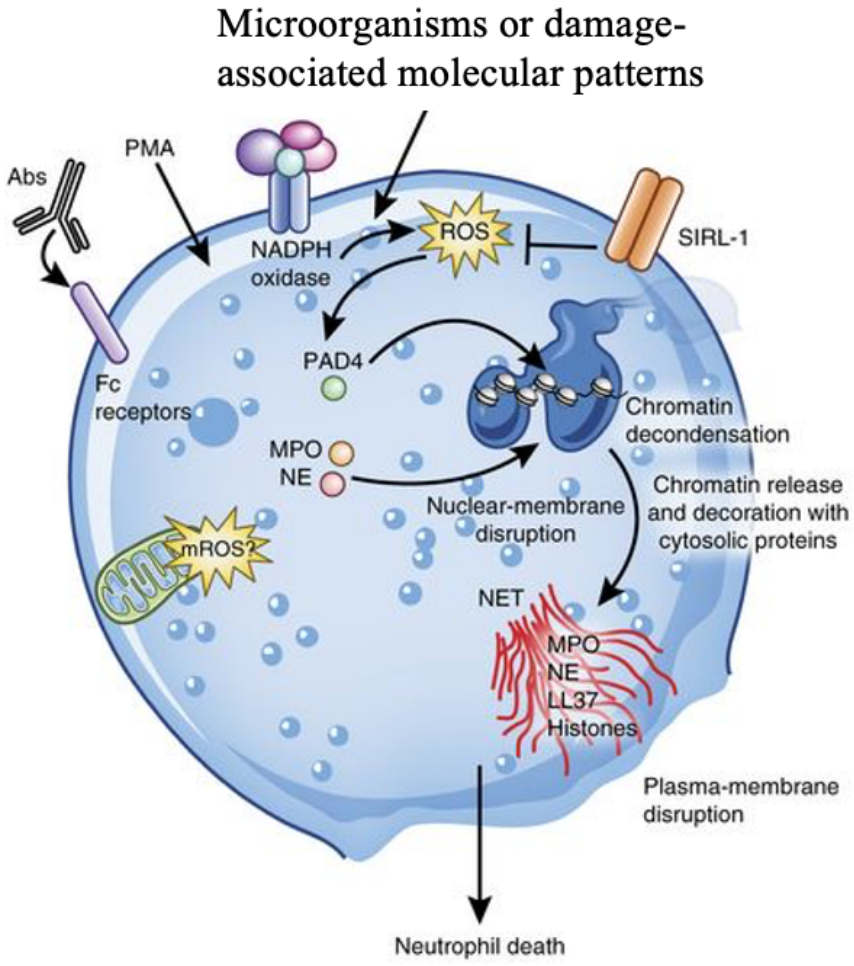

1.3 DNA and Histones

1.3.1 DNA

NETosis is an important source of extracellular DNA as described in section 1.2; however, other processes are also able to release DNA into the circulation, such as necrosis (Stroun et al., 2001). Elevated levels of DNA have been reported in many conditions such as sepsis, cancer, trauma, myocardial infarction, and autoimmune diseases (Bronkhorst et al., 2019; Dwivedi et al., 2012). Our group has previously reported that plasma levels of DNA have a high prognostic value in predicting mortality in patients with severe sepsis (Dwivedi et al., 2012).

With respect to the tissue origin of DNA in septic patients, the largest contributor to elevated DNA in most septic patients were from leukocytes (mainly granulocytes), as determined by Moss and colleagues (Moss et al., 2018). This group used a reference methylation atlas of 25 human tissues and cells to determine the origin of DNA in an unbiased manner in healthy and pathological conditions (Moss et al., 2018). The DNA methylation profiles of 14 septic patients revealed that 13 patients had greater than 20-fold higher leukocyte levels compared to healthy levels (Moss et al., 2018). These findings suggest that neutrophils, the most abundant leukocytes, are a major source of DNA in sepsis. Other cell types that contributed to extracellular DNA release in sepsis patients include: hepatocytes, monocytes, lymphocytes, neurons, vascular endothelial cells, colon epithelial cells, pancreatic acinar cells, and erythrocyte progenitors (Moss et al., 2018).

DNA can trigger the intrinsic pathway of blood coagulation in a FXII- and FXI-dependent manner, thereby contributing to the procoagulant properties of DNA (Gould et

al., 2014; Swystun et al., 2011). Additionally, DNA is anti-fibrinolytic due to the inhibition of plasmin-mediated fibrin degradation (Gould et al., 2015). DNA forms a non-productive ternary complex by binding to both plasmin and fibrin, which impairs fibrinolysis (Gould et al., 2015).

1.3.2 Histones

In addition to DNA, histones are another key component of NETs, and they are able to exert many harmful effects to the host, such as contributing to vascular dysfunction and organ injury in sepsis (Xu et al., 2009). Histones are a highly basic protein family that consist of arginine and lysine amino acids (Mariño-Ramírez et al., 2005). As a result, histones have a positive charge, which allows them to associate with DNA (Mariño-Ramírez et al., 2005). Free histones induce endothelial cell death in a TLR2- and TLR4-dependent mechanism (Xu et al., 2011). Histones can also cause platelet activation and aggregation (Fuchs et al., 2011). Furthermore, histones are procoagulant (by promoting prothrombin autoactivation) and anti-fibrinolytic (by binding to fibrin and increasing the thickness of the fibers), which negatively alters the hemostatic balance and contributes to tissue injury and microvascular thrombosis (Barranco-Medina et al., 2013; Gould et al., 2015). Histones have been shown to upregulate the expression of TF on monocytes and induce phosphatidylserine (PS) exposure on the membrane of red blood cells, thereby further contributing to its procoagulant effects (Gould et al., 2016; Semeraro et al., 2014). Similar to DNA, the mechanisms by which histones are cleared from the circulation are poorly understood. The natural anticoagulant enzyme APC is also a physiological inhibitor of histones (Xu et al., 2009). A study by Xu and colleagues found that APC cleaves

histones, thereby neutralizing the cytotoxic effects of histones on endothelial cells (Xu et al., 2009). In addition, they showed that the co-injection of APC and histones rescued mice from histone-mediated lethality, while mice that were injected with histones alone died within one hour (Xu et al., 2009). Additionally, C-reactive protein (CRP) is an acute-phase protein that can neutralize histones released into the circulation, thereby defending the host against histone toxicity (Abrams et al., 2013). A study by Abrams et al. demonstrated that CRP can rescue mice injected with lethal doses of histones (Abrams et al., 2013). Taken together, targeting extracellular histones in sepsis may be an effective strategy to reduce the aforementioned harmful effects.

1.3.3 DNA-histone complexes

Extracellular DNA and histones both contribute to the pathophysiology of sepsis through various mechanisms as described in sections 1.3.1 and 1.3.2. DNA and histones may also be bound tightly together in a complex, termed nucleosomes (Marsman et al., 2016). Dying or damaged cells release nucleosomes through various processes including necrosis and pyroptosis (Marsman et al., 2016). Whether the extracellular DNA or histones are in a complex or unbound to each other influences the pathological effects that they exert, and their interactions with other molecules in the extracellular space (Silk et al., 2017). For example, mice injected with purified histones died within one hour, however, mice injected with purified nucleosomes did not show any cytotoxic effects (Gauthier et al., 1996; Xu et al., 2009). On the other hand, nucleosomes have been shown to induce necrosis in cultured lymph node cells, however free DNA and histones do not have this effect (Decker et al., 2003). Another source of histone-bound DNA is by NETosis as

described in 1.2.1; however, the DNA and histones are also decorated with granular enzymes, such as MPO and NE (Saffarzadeh et al., 2012). Interestingly, studies have shown that NETs are cytotoxic to endothelial cells *in vitro*, however purified nucleosomes did not display cytotoxic effects to endothelial cells (Neeli et al., 2008). One possible explanation can be attributed to PAD4, which converts arginine to citrulline on histones during NETosis, thereby reducing their positive charge and creating a more open chromatin structure compared to nucleosomes that have not been processed by PAD4 (Neeli et al., 2008). As a result, the histones are more exposed and capable of inducing their cytotoxic effects (Neeli et al., 2008). In sepsis, the levels of circulating nucleosomes have been shown to be a biomarker for predicting organ dysfunction and disease prognosis (Chen et al., 2012). In the literature, nucleosomes and unbound DNA and histones are usually described interchangeably; however, distinguishing between the two forms is important to better understand what exactly is contributing to the pathophysiology of a disease, thereby improving the specificity and efficacy of therapies.

1.4 DNases

1.4.1 DNases

The mechanisms by which DNA is cleared from the circulation are not well understood. The half-life of circulating DNA is approximately 16 minutes in healthy individuals, presumably due to degradation by deoxyribonuclease (DNase) I and DNase 1 like 3 (1L3), which are Ca^{2+}- and magnesium (Mg^{2+})-dependent endonucleases that are capable of degrading DNA (Dennis Lo et al., 1999; Gauthier et al., 1996).

The elevated levels of DNA in septic patients may be due to increased release from cells, impaired clearance, and/or decreased levels of DNase I and DNase1L3 (Gould et al., 2015). Understanding the mechanisms by which DNA is elevated in septic patients can improve therapeutic strategies to mitigate the deleterious effects that DNA exerts.

1.4.2 The structure of DNase I

DNase I is a 29.8 kDa endonuclease that is negatively charged at physiological pH (Shiokawa et al., 2000). DNase I consists of an N-terminal signal peptide that allows for the translocation of this protein into the rough endoplasmic reticulum (Napirei et al., 2005). All nucleases have the same catalytic centre, which consists of two histidine (His) residues at amino acid positions 134 and 252, and their hydrogen-bond residues glutamic acid (Glu) at amino acid position 78 and aspartic acid (Asp) at amino acid position 212 (Jones et al., 1996). Additionally, nucleases contain the following residues that are required for binding to DNA: tyrosine (Tyr)^{76}, arginine (Arg)^{111}, asparagine (Asn)^{170}, Tyr^{175}, and Tyr^{211} (Jones et al., 1996; Napirei et al., 2005). The essential disulfide bond between cysteine (Cys)^{173} and Cys^{209} are also highly conserved (Jones et al., 1996; Pan et al., 1998). Enzymes part of the DNase I family also contain four ion-binding pockets, two for binding to Ca^{2+}, and two for binding to Mg^{2+} (Guéroult et al., 2010). Binding of Ca^{2+} and Mg^{2+} are critical for the proper functioning of DNase I because these cations optimize the electrostatic fit between DNase and negatively charged DNA (Guéroult et al., 2010). With respect to differences, DNase I lacks a C-terminal peptide domain, which is present in DNase1L3 discussed below in section 1.5.1 (Sisirak et al., 2016; Soni et al., 2019). The crystal structure of DNase I is provided in Figure 1.3.

Figure 1.3. Crystal structure of DNase I. Crystal structure of DNase I at 2 Å resolution. The DNA binding site and catalytic centre, which are conserved amongst all nucleases, are shown. Figure adapted from: rcsb.org and (Oefner et al., 1986).

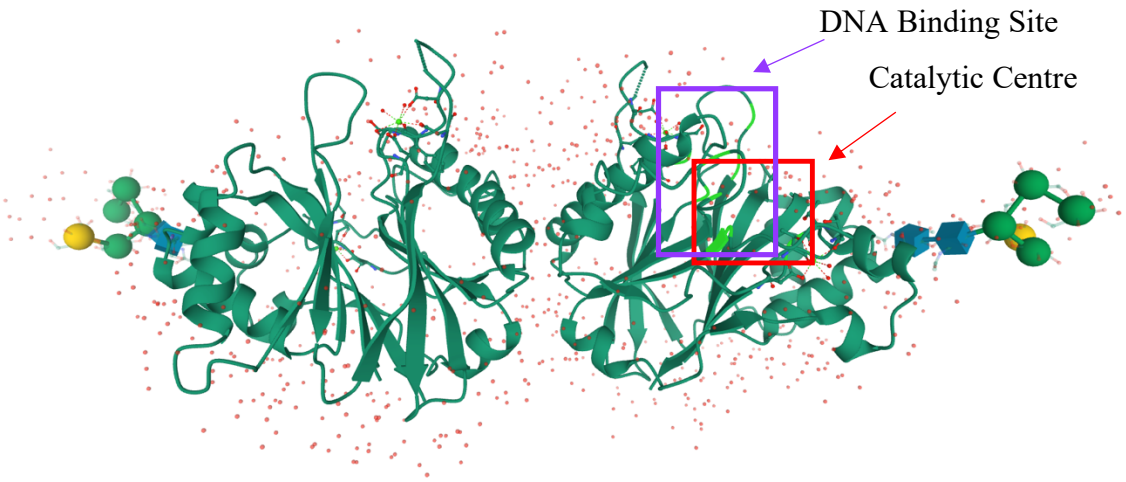

1.4.3 The role of DNase I in normal physiology

DNase I is a secretory endonuclease that plays an important role in maintaining normal physiology (Dennis Lo et al., 1999). A variety of non-hematopoietic endocrine and exocrine glands (especially in the gastrointestinal and urogenital tract) produce DNase I (Napirei et al., 2005). DNase I requires Ca^{2+}, Mg^{2+} or manganese (Mn^{2+}), and a pH of 7.0 for optimal enzymatic activity (Napirei et al., 2005). Monomeric actin, zinc (Zn^{2+}), and bivalent cation chelators are able to inhibit DNase I (Mannherz et al., 1995). Additional biochemical properties of DNase I are provided in Table 1. The main role of DNase I is thought to be involved in the degradation of extracellular DNA that is released by damaged or dying cells through various mechanisms, such as necrosis (Napirei et al., 2000). Degradation of extracellular DNA is important to prevent the pathological effects that DNA can exert to the host as described in section 1.3.1, and to suppress autoimmunity which can arise from the development of autoantibodies against DNA and nucleosomes (Napirei et al., 2000). Although other DNase enzymes are also involved in degrading extracellular DNA, DNase I is the major endonuclease and is responsible for 90% of DNA digestion (Nadano et al., 1993). DNase I preferentially cleaves protein-free DNA, and is unable to cleave the nucleosome regions of chromatin where approximately 150 base pairs of DNA is tightly wrapped around the histone octamers, in the absence of a serine protease (Napirei et al., 2009). The serine proteases, such as thrombin and plasmin, are required to first proteolyze the DNA-bound histones (e.g. histones H1 and H3) (Napirei et al., 2009). Protein-free DNA is then accessible to DNase I, and can be digested (Napirei et al., 2009). The current model depicting the mechanisms by which DNase I degrades DNA is shown

in Figure 1.5. A schematic diagram of our proposed new model depicting the mechanism of DNase I is provided in Figure 1.6.

1.4.4 The role of DNase I in pathophysiology

Changes in the levels or activity of DNase I has been widely reported in many diseases, thereby highlighting the potential for this enzyme to contribute to pathophysiology (Vancevska et al., 2013). Knockout models of DNase I in mice, or mutations in DNase I in humans have been associated with the development of systemic lupus erythematosus (SLE), which is a chronic autoimmune disease characterized by the development of autoantibodies against extracellular DNA, and can cause tissue and organ damage (Keyel., 2017). Additionally, impaired DNase I activity has also been reported in patients with severe inflammatory bowel disease (IBD), and has been suggested to play a role in the development of IBD (Malíčková et al., 2011). Interestingly, the activity of DNase I was found to be significantly decreased in females compared to males in both SLE and IBD, but remained similar in healthy controls (Malíčková et al., 2011). Decreased activity of DNase I has also been found in patients with stomach, colon, and pancreatic cancer (Vancevska et al., 2013). Taken together, normal levels and activity of DNase I is important in preventing pathology. To date, no studies have determined the levels of DNase I in septic patients. Therefore, we measured these values in septic patients admitted to the intensive care unit (ICU) in a longitudinal manner (days 1 – 28). Given that the levels of DNA are persistently elevated in some septic patients, studying this endonuclease in greater detail can shed light on this matter, and on the potential use of DNase I as a therapeutic strategy.

1.4.5 DNase I as a potential therapy for sepsis and vascular diseases

DNase I plays an important role in degrading extracellular DNA, and impairments in the levels or activity of this endonuclease can contribute to pathophysiology; therefore, the use of DNase I as a potential therapy is intriguing. Specifically, diseases with decreased levels or activity of DNase I, and/or increased levels of DNA may demonstrate the most success and promising results with DNase I treatment. Recombinant human DNase I, Pulmozyme (dornase alfa), has been approved for use in patients with cystic fibrosis as an inhalant drug to improve pulmonary function (McCoy et al., 1996). Additionally, a study by Davis and colleagues revealed that intravenous and subcutaneous injections of Pulmozyme in 17 human patients with SLE were well tolerated (Davis et al., 1999). Taken together, Pulmozyme is safe to use in humans, and should be explored as a therapeutic strategy for other diseases as well, such as sepsis.

Given that plasma levels of DNA have a high prognostic value in predicting mortality in patients with severe sepsis, and that DNA levels are persistently elevated in some septic patients, treatment with Pulmozyme may be a beneficial strategy (Dwivedi et al., 2012). Moreover, significantly increased levels of MPO-DNA complexes (a marker for NETosis) have been identified in septic patients, and NETs can exert many pathological effects in the host as described in section 1.2.3 (Denning et al., 2019).

DNase I has been shown to degrade NETs and prevent vascular occlusion and organ damage; however, a study by Farrera and Fadeel demonstrated that physiological concentrations of DNase I (20 ng/mL) were unable to degrade NETs (Farrera et al., 2013; Jiménez-Alcázar et al., 2017). As a result, administrating therapeutic levels of DNase I in

diseases with increased NETosis, such as sepsis, can effectively target and degrade NETs, thereby improving outcomes. However, NETs are also involved in the innate immune response by trapping and neutralizing pathogens, and thus the timing of DNase I administration is important to preserve the protective effects of NETs with respect to clearing pathogens (Mai et al., 2015). Our group has previously determined that administrating DNase I four to six hours after inducing sepsis in mice resulted in decreased DNA levels, proinflammatory cytokines, and fibrin deposition; in contrast, administrating DNase two hours after inducing sepsis resulted in increased inflammation and organ damage (Mai et al., 2015). The use of Pulmozyme shows promising results, and greater research on the dosage, timing, and effects of this drug should be done to achieve optimal results in septic patients.

1.5 DNase1L3

1.5.1 The structure of DNase1L3

DNase1L3 is a 33.1 kDa endonuclease that is positively charged at physiological pH, and preferentially cleaves histone-bound DNA (Napirei et al., 2005). There are many structural similarities between DNase I and DNase1L3, as both endonucleases are part of the DNase I protein family (Napirei et al., 2005). Both enzymes have high homology and similar amino acid sequences (Napirei et al., 2005; Shiokawa et al., 2000). As mentioned in section 1.4.2, the catalytic centre, DNA binding site, essential disulfide bond between Cys^{173} and Cys^{209}, and four ion-binding pockets are highly conserved, and present in DNase1L3 (Guéroult et al., 2010; Jones et al., 1996; Napirei et al., 2005). With respect to differences, DNase1L3 is N-glycosylated at Asn^{283}, whereas DNase I is N-glycosylated at

Asn^{18} and Asn^{106} (Napirei et al., 2005). Additionally, DNase1L3 contains a positively charged C-terminal peptide rich in lysine and arginine, in a stable alpha helix conformation; however, DNase I lacks this C-terminal peptide (Sisirak et al., 2016; Soni et al., 2019). Sisirak et al. suggested that the positive charge and stable alpha helix conformation of the C-terminal peptide gives DNase1L3 its unique ability to digest histone-bound DNA (Sisirak et al., 2016). Moreover, this group demonstrated that DNase1L3 lost its ability to digest histone-bound DNA after deleting the C-terminal peptide (Sisirak et al., 2016). Figure 1.4 provides a crystal structure of DNase1L3, and an image highlighting the presence of a C-terminal peptide in DNase1L3, but not in DNase I.

Figure 1.4. Crystal structure of DNase1L3. Crystal structure of DNase1L3 (A). The catalytic centre and DNA binding site are conserved between DNase I and DNase1L3 (labeled in Figure 1.3). DNase1L3 contains a positively charged C-terminal peptide, whereas DNase I is lacking a C-terminal peptide (B). Source: (McCord et al., 2018; Sisirak et al., 2016).

A.

B.

1.5.2 The role of DNase1L3

Similar to DNase I, DNase1L3 is also a secretory enzyme that plays an important role in maintaining normal physiology (Jiménez-Alcázar et al., 2017). DNase1L3 is expressed independently and has a different origin than DNase I (Jiménez-Alcázar et al., 2017). Immune cells, especially dendritic cells and macrophages, secrete DNase1L3 (Onuora., 2016). DNase1L3 shares many biochemical properties with DNase I, including a dependency on Ca^{2+}, Mg^{2+} or Mn^{2+}, inhibition by Zn^{2+} and bivalent cation chelators, and a pH of 7.0 for optimal enzymatic activity (Napirei et al., 2005).

An important difference to highlight between DNase I and DNase1L3 is their substrate specificity. DNase1L3 has low activity towards digesting protein-free DNA, but can cleave DNA-protein complexes with high activity, which is not the case with DNase I as described in section 1.4.2 (Jiménez-Alcázar et al., 2017; Napirei et al., 2009). Furthermore, PAI-1 and monomeric actin slightly activate DNase1L3, whereas monomeric actin inhibits DNase I (Napirei et al., 2005). Plasmin inhibits DNase1L3 *in vitro* by proteolysis; however, plasmin does not proteolyze DNase I in mice, presumably due to the fact that this endonuclease is N-glycosylated at two sites, while DNase1L3 is not (Napirei et al., 2009). A summary of the biochemical characteristics of DNase1L3 is provided in Table 1, and a schematic diagram that shows the enzymatic activity of this endonuclease is provided in Figure 1.5.

A study by Jiménez-Alcázar and colleagues found that the presence of either DNase I or DNase1L3 was sufficient to degrade NETs in mice during sterile neutrophilia and septicemia; however, the absence of both DNases lead to vascular occlusion and organ

damage (Jiménez-Alcázar et al., 2017). This study highlights the importance of DNase1L3 in preventing pathology. Additionally, loss-of-function mutations in DNase1L3 in humans, as well as DNase1L3-deficiency in mice, have been found to contribute to the development of SLE in two studies (Al-Mayouf et al., 2011; Sisirak et al., 2016). Both studies demonstrated the critical role that DNase1L3 plays in degrading chromatin that gets released from dying cells, thereby preventing the development of autoantibodies to chromatin and DNA (Al-Mayouf et al., 2011; Sisirak et al., 2016).

Further research on DNase1L3 should be done in diseases that are associated with elevated levels of extracellular DNA and chromatin, such as sepsis, which could potentially reveal novel therapeutic strategies and/or expand upon current knowledge regarding the pathophysiology of a disease. We are the first group to measure the levels of DNase1L3 in septic patients admitted to the ICU in a longitudinal manner (days 1 – 28) to determine if these levels are abnormal in sepsis.

Table 1. Comparison between the biochemical characteristics of DNase I and DNase1L3 (Jiménez-Alcázar et al., 2017; Napirei et al., 2009; Sisirak et al., 2016).

	DNase I	**DNase1L3**
Half Life	20 minutes	Not reported
Molecular Weight	29.8 kDa	33.1 kDa
Physiological Concentration	20 ng/mL (0.67 nM)	2 ng/mL (0.06 nM)
Charge at physiological pH	-9.4	+6.7
Mouse K/O Model	Increased risk of developing thrombosis when challenged	Developed autoantibodies to DNA and chromatin, increased monocytes and activated T cells, and kidney damage
Mouse K/O Models of Both DNase I and DNase1L3	• Unable to tolerate chronic neutrophilia or septicemia (rapid death after NETs occluded vessels) • Displayed phenotypes of infection-induced thrombotic microangiopathies (TMAs) and disseminated intravascular coagulation (DIC)	
Inhibitors	Monomeric actin, Zn^{2+}, bivalent cation chelators	Heparin, plasmin (*in vitro*), Zn^{2+}, bivalent cation inhibitors
Requirements	Ca^{2+}, Mg^{2+} or Mn^{2+}, pH of 7.0	
Substrate Specificity	Protein-free DNA, or DNA-protein complexes in the presence of a serine protease	Preference for DNA-protein complexes
Secreted By	Non-hematopoietic endocrine and exocrine cells	Immune cells (mainly macrophages and dendritic cells)
Tissue Source	Gastrointestinal and urogenital tract	Spleen, liver, thymus, lymph node, bone marrow, small intestine, and kidney

Figure 1.5. Current model depicting the mechanism of action of DNases. DNase I completely degrades DNA (A), but is unable to degrade DNA-histone complexes on its own (B). The presence of either unfractionated heparin (UFH) or serine proteases can displace histones from the DNA, which allows DNase I to gain access to DNA-cleavage sites and degrade the DNA (C). In contrast, DNase1L3 is able to bind to and degrade DNA-histone complexes (D). Source: biorender.com

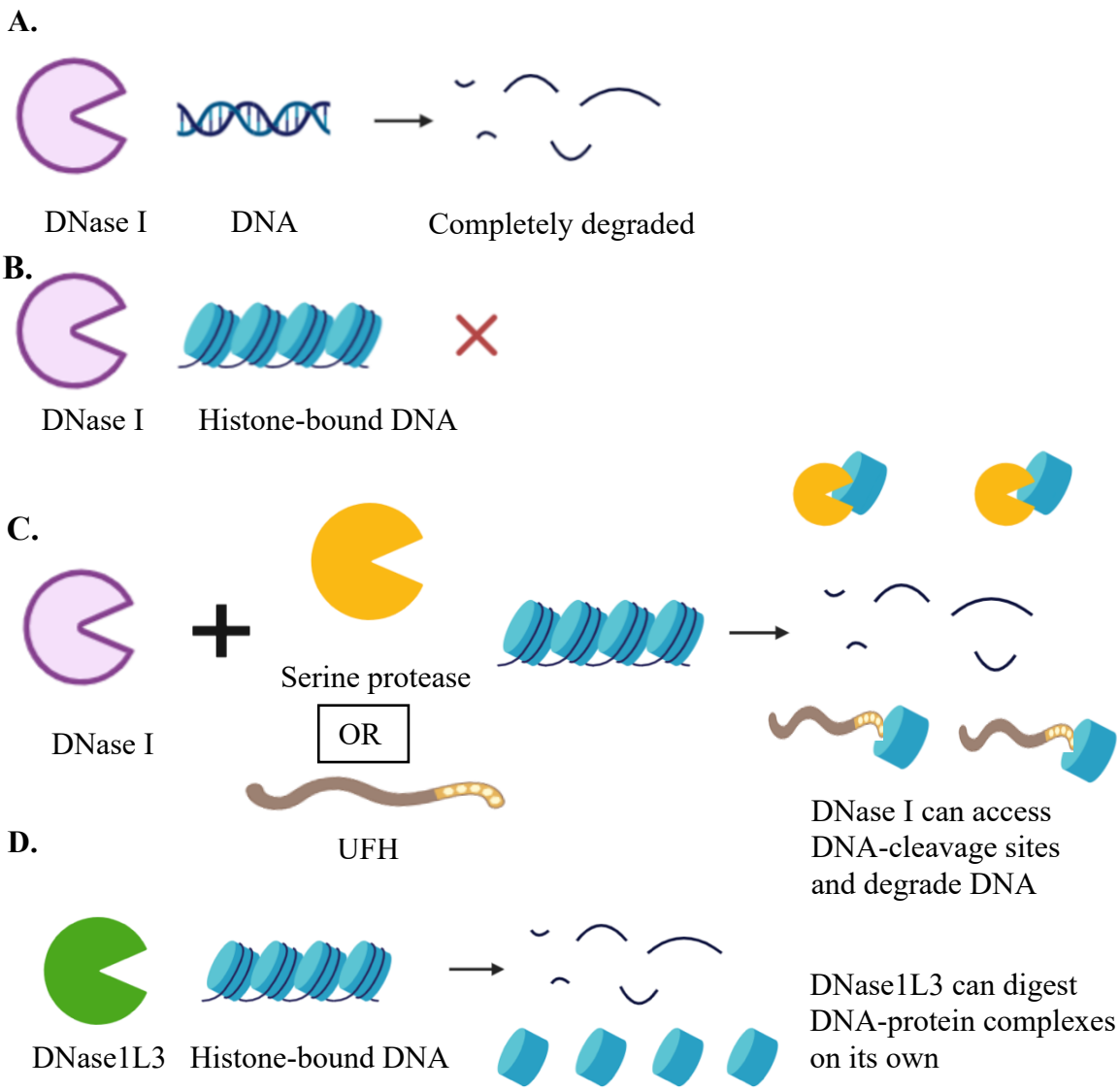

Figure 1.6. Our proposed model depicting the mechanism of DNase I. DNase I can digest DNA-histone complexes in the presence of UFH, enoxaparin, or Vasoflux (A), but not fondaparinux (B). This suggests that the ability of GAGs to enhance DNase I-mediated digestion of histone-bound DNA is size-dependent, and independent of the AT-binding pentasaccharide of heparins. On the other hand, DNase I is able to degrade NETs down to individual nucleosomes (C). This may be due to the histone citrullination that occurs during NETosis by PAD4, which is a process that causes chromatin decondensation, and weakens DNA-histone interactions by reducing the positive charge on histones.

Source: biorender.com

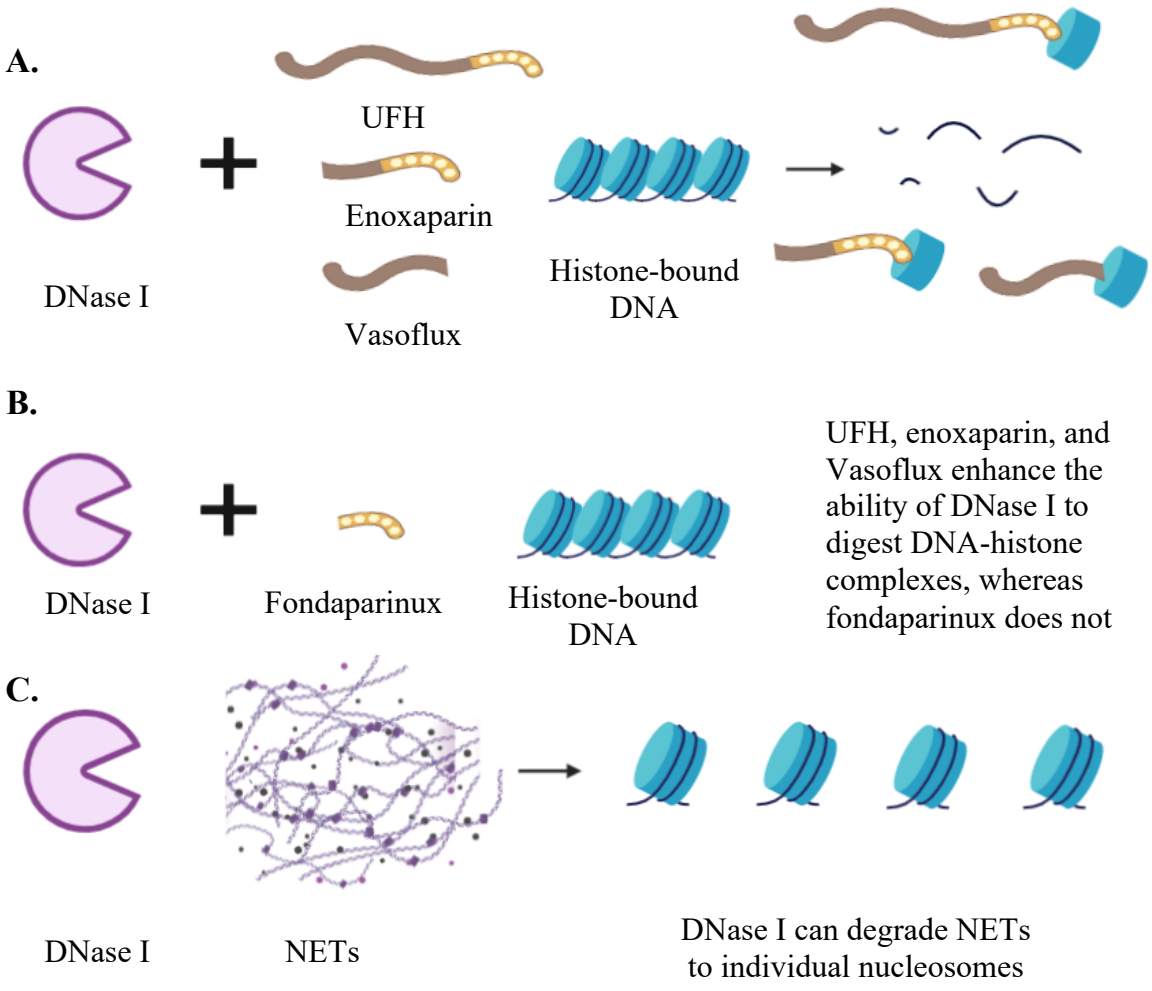

1.6 Heparins

1.6.1 Heparins

Although host DNases are capable of degrading the DNA component of NETs and DNA-histone complexes, targeting the remaining histones is also crucial given the cytotoxic effects they exert within the host, as described in section 1.3.2. Heparins have been shown to bind and neutralize histones (Iba et al., 2015). Heparins are classified as glycosaminoglycans (GAGs) and have anticoagulant properties due to their ability to bind to the serpin AT with high affinity, thereby accelerating the rate at which AT inhibits various coagulation factors by up to 1000-fold (Paschoa., 2016; Yeung et al., 2015). A unique pentasaccharide sequence is required for heparins to bind to AT (Choay et al., 1981). The different molecular weights of the heparins determine which coagulation factors are inhibited by AT (thrombin, FIXa, FXa, FXIa, or FXIIa) (Paschoa., 2016). Figure 1.7 shows the chemical structures of the four heparins that will be discussed below.

1.6.2 Unfractionated Heparin (UFH)

Unfractionated heparin (UFH) is a heterogenous mixture of linear polysaccharides, and is the largest form of heparin with an average molecular weight of 15 kDa (ranging from 5 to 30 kDa) (Bounameaux., 1998). UFH causes a conformational change in AT upon binding, which catalyzes the inhibition of thrombin, FIXa, FXa, FXIa, and FXIIa (Paschoa., 2016). Inhibition of thrombin requires a ternary complex to be formed between UFH, AT, and thrombin (Hirsh et al., 1992). The formation of this complex occurs because UFH is at least 18 oligosaccharides in length, which allows it to serve as a template to bind both thrombin and AT to form the complex (Hirsh et al., 1992). In contrast, UFH can bind to

AT and inhibit FXa without the requirement of forming a ternary complex (Conners et al., 2002).

1.6.3 Low-molecular-weight heparins (LMWHs)

Low-molecular-weight heparins (LMWHs) are prepared by enzymatic or chemical depolymerization of UFH, which results in an average molecular weight of 5 kDa (Canales et al., 2008). For example, enoxaparin is a commonly used LMWH and has an average molecular weight of 4.5 kDa (Walker et al., 2017). LMWHs bind to AT and promote a conformational change, which catalyzes the inhibition of FXa (Ibbotson et al., 2002). Compared to UFH, LMWHs have lower activity against thrombin due to their shorter chain lengths, which reduces their ability to form a ternary complex with thrombin and AT (Canales et al., 2008).

1.6.4 Fondaparinux

Fondaparinux is a synthetic pentasaccharide that selectively binds to AT with high affinity (Yusuf et al., 2006). Fondaparinux causes a conformational change in AT, thereby accelerating the rate at which FXa is inhibited (Paolucci et al., 2002). Upon binding to FXa, AT releases fondaparinux, which allows it to bind to other AT molecules (Paolucci et al., 2002). Fondaparinux has an average molecular weight of 1.7 kDa, and is therefore unable to cause AT-mediated inhibition of thrombin due to its small molecular size (Dager et al., 2004).

1.6.5 Vasoflux

Vasoflux is a LMWH that has been chemically modified through periodate oxidation by Dr. Weitz and colleagues to reduce its affinity for AT (Weitz et al., 1999).

Vasoflux is able to inhibit FIXa activation of FX, and catalyze the inactivation of fibrin-bound thrombin by heparin cofactor II, making this anticoagulant more effective for clot-bound thrombin than UFH and the other LMWHs (Weitz et al., 1999).

1.6.6 The cofactor activity of heparins

A study by Napirei et al. found that UFH can act in a similar manner as serine proteases with respect to enhancing the ability of DNase I to cleave chromosomal DNA (Napirei et al., 2009). However, it is unclear if UFH enhances the activity of DNase I by displacing histones, thereby making DNA-cleavage sites more accessible. Alternatively, it is possible that UFH indirectly enhances the activity of DNase I by hyperactivating the plasminogen system (Napirei et al., 2005). Heparin is able to accelerate the rate at which tPA converts plasminogen to plasmin. Plasmin then proteolyzes DNA-bound proteins, which would allow DNase I to have greater accessibility to DNA-cleavage sites.

In contrast, UFH inhibits DNase1L3 by directly binding to this endonuclease (Napirei et al., 2009). DNase1L3 has a charge of +6.7 at physiological pH, which can explain why UFH, which is a negatively charged molecule, binds to this endonuclease (Napirei et al., 2009). Unlike DNase1L3, DNase I has a charge of -9.4 at physiological pH, which may explain why DNase I is not inhibited by UFH (Napirei et al., 2009).

To date, no studies have looked at the effects of the other forms of GAGs including enoxaparin, fondaparinux, and Vasoflux on the ability to activate or inhibit DNase I and DNase1L3. Studying the interactions of these heparins with both DNase I and DNase1L3 can provide an explanation as to why UFH enhances the activity of DNase I but inhibits DNase1L3. These endonucleases are important in maintaining normal physiology as

mentioned in sections 1.4.1 and 1.5.1; therefore, it is crucial to understand how potential therapies, such as anticoagulants, interact with DNases. Additionally, since histone-bound DNA is a major component of NETs, understanding what exactly helps DNase I cleave these complexes and what inhibits DNase1L3 is important. We studied the cofactor activity of GAGs to better understand their mechanism of action with respect to improving DNase-mediated degradation of procoagulant molecules. Further, we determined if the cofactor activity of GAGs is size-dependent and/or requires the pentasaccharide sequence.

1.6.7 The use of heparins in sepsis

The use of UFH, LMWH, and fondaparinux are indicated for thromboprophylaxis and treating VTE (Mulloy et al., 2015). With respect to sepsis, there have been many clinical trials and studies looking at the efficacy of using heparins as a potential treatment (Li et al., 2017). As mentioned in section 1.1.8, increased activation of the coagulation cascade, hypofibrinolysis, and impairments in natural anticoagulant pathways promote a state of hypercoagulability in sepsis; therefore, treatment with anticoagulants, such as heparins, may be an effective strategy to prevent and mitigate these effects. A systematic review and meta-analysis of a few randomized controlled trials revealed that the use of UFH in sepsis, septic shock, and DIC resulted in decreased mortality (Zarychanski et al., 2015). An ongoing phase 2 clinical trial, Heparin AnticoaguLation to Improve Outcomes in Septic Shock (HALO), is testing the efficacy of UFH in treating patients with septic shock (Houston et al., 2015). With respect to the use of LMWH in sepsis, a meta-analysis of randomized controlled trials found that patients receiving LMWH had significantly decreased 28-day mortality and Acute Physiology and Chronic Health Evaluation II

(APACHE II) scores; however, the incidence of bleeding events were significantly increased (Fan et al., 2016). A recent study by Keshari et al. found that fondaparinux treatment in a baboon model of sepsis inhibited coagulation, reduced inflammation and organ damage, and promoted survival (Keshari et al., 2020). Interestingly, UFH, LMWH, and fondaparinux all possess anti-inflammatory properties, which provides additional benefits as a therapy for sepsis due to the systemic inflammatory response that occurs (Downing et al., 1998; Frank et al., 2005; Young., 2008).

Taken together, the use of heparins in sepsis shows promising results due to their anticoagulant and anti-inflammatory properties, and should be further studied. However, anticoagulants also carry the risk of hemorrhaging due to their ability to inhibit clot formation (Mulloy et al., 2015). In the event of an adverse effect, reversal agents are extremely important. Protamine sulfate, cryoprecipitate, or fresh frozen plasma are reversal agents for UFH and LMWH, and prothrombin complex concentrate can be used for fondaparinux (Harter et al., 2015). Interestingly, a study by Wildhagen et al. found that a 15 kDa non-anticoagulant heparin (AT affinity-depleted heparin), can prevent histone-mediated cytotoxicity *in vitro*, and reduce mortality in septic mice without increasing the risk of bleeding (Wildhagen et al., 2014).

In addition to anticoagulant and anti-inflammatory properties, heparins are also able to bind and neutralize extracellular histones, which is important because free histones in circulation exert deleterious effects within the host (Iba et al., 2015). NETs have been found to contribute to a state of hypercoagulability in sepsis; thus, targeting these procoagulant molecules may improve outcomes (Yang et al., 2017). However, dismantling NETs with

DNases may have adverse effects because histones will become released from DNA and be free to exert damage (Xu et al., 2009). Therefore, using a combination of both heparins and DNases in sepsis may be a more beneficial therapeutic strategy in order to effectively degrade both the DNA and histone components of NETs, as well as serve as a cofactor for DNase I-mediated degradation of histone-bound DNA.

Figure 1.7. Chemical structures of heparins. UFH is a heterogenous mixture of linear polysaccharides with an average molecular weight of 15 kDa, and includes the AT-binding pentasaccharide (A). LMWHs are prepared by enzymatic or chemical depolymerization of UFH, which results in an average molecular weight of 5 kDa, and includes the AT-binding pentasaccharide (B). The structure of fondaparinux is a synthetic AT-binding pentasaccharide (C). Vasoflux is a LMWH that has been chemically modified through periodate oxidation to reduce its affinity for AT (D). Source: (Guan et al., 2016; Weitz et al., 1999).

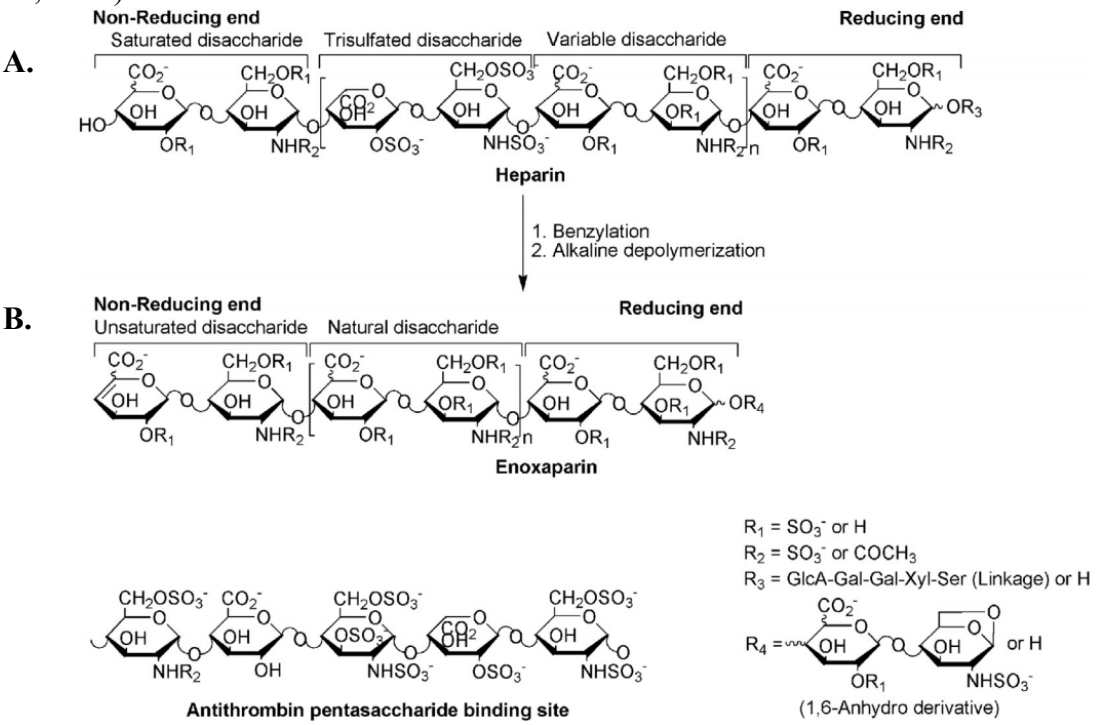

C.

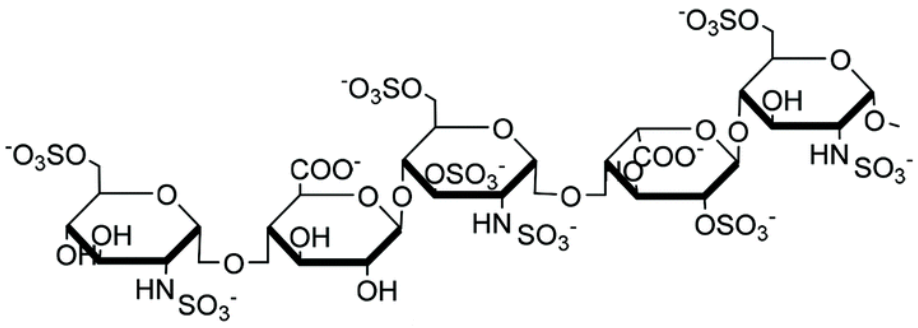

AT-binding pentasaccharide

D.

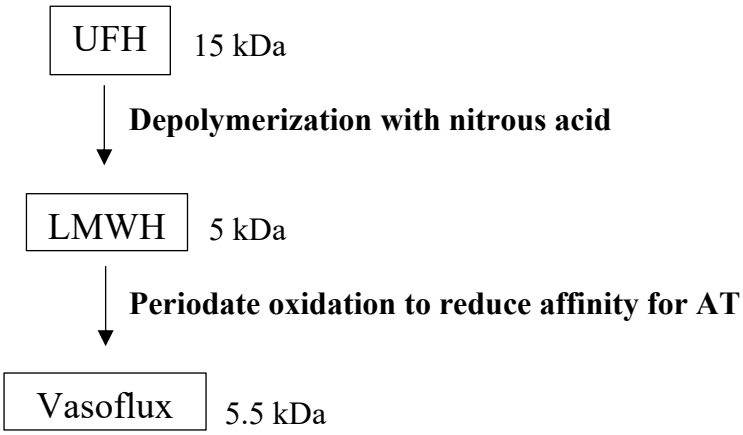

1.7 Hypotheses and Specific Aims

1.7.1 Hypotheses

1. The ability of GAGs to enhance DNase I-mediated digestion of DNA-histone complexes is size-dependent, and independent of the AT-binding pentasaccharide of GAGs.
2. The ability of GAGs to inhibit DNase1L3-mediated digestion of DNA-histone complexes is size-dependent, and independent of the AT-binding pentasaccharide of GAGs.
3. Septic patients have decreased plasma levels of DNase I and DNase1L3 compared to healthy controls.

1.7.2 Specific Aims

1. To determine the mechanisms by which GAGs enhance DNase I-mediated degradation of DNA-histone complexes, and inhibit the activity of DNase1L3.
2. To compare the degradation of NETs by DNase I and DNase1L3 in the presence and absence of GAGs.
3. To measure the plasma levels of DNase I and DNase1L3 in septic patients longitudinally (days 1 to 28) to better understand why the levels of DNA are persistently elevated in some septic patients.

2.0 Materials and Methods

2.0.1 Materials

Recombinant human DNase I (Pulmozyme® dornase alfa) was purchased from Roche Canada (Mississauga, ON, Canada). SpectraMax plate reader was from Molecular Devices (Sunnyvale, CA, USA). Phorbol 12-myristate 13-acetate (PMA) was purchased form Sigma-Aldrich (St. Louis, MO, USA). Unfractionated heparin (UFH) was purchased from LEO® Pharma (Thornhill, ON, Canada), Lovenox (enoxaparin) was from Hamilton General Hospital Pharmacy (Hamilton, ON, Canada), and Arixtra (fondaparinux) was purchased from GlaxoSmithKline (Mississauga, ON, Canada). Vasoflux was prepared by depolymerizing UFH to LMWH, followed by oxidation with sodium periodate, which reduces its AT affinity. Dr. Jeffrey Weitz (TaARI, ON, Canada) kindly provided Vasoflux. Plasmin was from Haematologic Technologies Inc (Essex, VT, USA). APC was purchased from Enzyme Research Laboratories (South Bend, IN, USA). Highly APC-specific monoclonal antibody (HAPC 1555) was kindly provided by Dr. Charles Esmon. Roche cOmplete Protease Inhibitor Cocktail (EDTA-free) was from MilliporeSigma (Burlington, MA, USA). Unfractionated bovine histones were purchased from Worthington Biochemical Corporation (Lakewood, NJ, USA). SYTOX Green and DAPI were purchased from Invitrogen (Burlington, ON, Canada). The two different DNase I monoclonal antibodies were purchased from Santa Cruz Biotechnology (Dallas, TX, USA). The DNase1L3 ELISA kit was purchased from abbexa (Cambridge, United Kingdom). The BLITz system was from FortéBio (Fremont, CA, USA). Individual human histones H2A, H2B, H3, and H4 were purchased from New England Biolabs (Ipswich, MA, USA).

Heparinized microhematocrit capillary tubes and heparinized BD microtainer tubes were purchased from VWR (Mississauga, ON, Canada).

2.0.2 Preparation of Platelet-Poor Plasma (PPP)

From healthy volunteers, peripheral venous blood was collected via venipuncture into either 3.2% trisodium citrate or 3.2% trisodium citrate and benzamidine HCl (20 mmol L^{-1}) (Sigma- Aldrich, MO, USA). Benzamidine HCl is a reversible inhibitor of APC and was added to some tubes to block plasma protease inhibitors from irreversibly inhibiting APC. After blood collection, the whole blood was centrifuged at 1500 x g for 10 minutes at 20°C. The plasma layer was collected, aliquoted, and stored for each healthy volunteer at -80°C.

From septic patients enrolled in our DYNAMICS study, blood was collected from existing arterial or venous lines via venipuncture into Becton Dickinson buffered sodium citrate vacutainer tubes (0.105 M trisodium citrate) (Liaw et al., 2019). Benzamidine HCl was added to some tubes to block plasma protease inhibitors from irreversibly inhibiting APC. After blood collection, the whole blood was centrifuged at 1700 x g for 10 minutes at 20°C. The plasma layer was collected, aliquoted, and stored at -80°C.

2.0.3 Isolation of Genomic DNA from Whole Blood via PAXgene

Human genomic DNA was isolated as per the manufacturer's instructions (QIAGEN, Mississauga, ON). PAXgene Blood DNA tubes (QIAGEN, Mississauga, ON) were used to collect whole blood from healthy adult volunteers via venipuncture. To isolate DNA, blood was transferred to processing tubes, which contains lysis buffer. The tubes were centrifuged to pellet the cell nuclei and mitochondria, which were then washed and

suspended in digestion buffer. Next, a protease was added to remove protein contaminants. DNA was precipitated in isopropanol, washed in 70% ethanol, dried, and resuspended in resuspension buffer (10 mM Tris-Cl, 0.5 mM EDTA, pH 9.0). NanoDrop One (ThermoFisher Scientific, Mississauga, ON) was used to determine the concentration of isolated DNA by the absorbance at 260 nm. Purity was confirmed by calculating the ratio of absorbance of 260 nm/280 nm. PAXgene DNA was kindly isolated by Erblin Cani and Sarah Medeiros.

2.0.4 DNA-Histone Complexes Degradation Assay

PAXgene-purified genomic DNA and unfractionated bovine histones were incubated for 1 hour at 37°C to form DNA-histone complexes. Next, either DNase I or DNase1L3 alone or in combination with one of UFH, enoxaparin, fondaparinux, Vasoflux, plasmin, or APC were added to different tubes at 37°C for various time points to digest the DNA-histone complexes. $CaCl_2$ (10 mM) and $MgCl_2$ (10 mM) were added to each condition containing DNase I or DNase1L3. Ethylenediaminetetraacetic acid (EDTA) (50 mM) was used to stop reactions at various time points. The samples were added to an agarose gel to visualize the DNA.

2.0.5 Gel Electrophoresis

Samples containing DNA were mixed with DNA Gel Loading Dye (6x) (Thermo Fisher Scientific, Waltham, MA) and 20 μL of each sample was loaded on a 1.8% agarose gel for electrophoresis at 100 V or 110 V for 1 hour. Gels were stained with RedSafe (Froggabio, North York, ON) or ethidium bromide (Thermo Fisher Scientific, Waltham,

MA), and visualized using UV transillumination. Agarose gels were quantified using densitometry analysis on the Image Lab 5.2.1 software.

2.0.6 Neutrophil Isolation from Whole Blood

Whole blood was collected from healthy individuals into citrated tubes. Next, 6% dextran solution (Sigma-Aldrich St. Louis, MO) was added and the tube was incubated for 45 minutes at room temperature to allow for plasma separation. The plasma was collected, slowly layered on top of Histopaque 1077 solution (Sigma-Aldrich St. Louis, MO), and centrifuged at 1200 RPM for 20 minutes at 25°C. The supernatant was discarded, the pellet was resuspended with a red blood cell lysis buffer, and HBSS was added. The tube was centrifuged at 1200 RPM for 5 minutes at 4°C. The supernatant was discarded, and the remaining neutrophil-rich pellet was resuspended with RPMI.

2.0.7 Formation of NETs and Visualization using Fluorescence Microscopy

To visualize the isolated human neutrophils and NETs, neutrophils were added to glass coverslips (500,000 cells/coverslip) either with the addition of 100 nM of PMA (to visualize NETs) or without 100 nM PMA (to visualize neutrophils). Coverslips were incubated for 4 hours at 37°C and 5% CO_2. After 4 hours, DNase I or DNase1L3 were added either alone or in combination with UFH, enoxaparin, fondaparinux, Vasoflux, or APC to the PMA-containing coverslips to degrade NETs. Coverslips were incubated for 5, 15, or 30 minutes at 37°C and 5% CO_2 to allow for the degradation of NETs. Reactions were stopped with 50 mM EDTA. Next, the coverslips were stained with 5 μM DAPI to visualize intracellular DNA or 167 nM SYTOX Green to stain extracellular DNA. Olympus

BX41 fluorescence microscope was used to visualize the neutrophils and NETs, and an Olympus DP72 camera (Olympus Corporation) was used to capture images.

2.0.8 Quantification of Neutrophils and NETs using a Fluorometric Assay

Isolated human neutrophils (2 x 10^5/200 μL) were added to a Costar 96-well black polystyrene plate. The neutrophils were stimulated with 100 nM of PMA and incubated at 37°C with 5% CO_2 for 4 hours to allow for NETosis. After 4 hours, DNase I or DNase IL3 were added either alone or in combination with UFH, enoxaparin, fondaparinux, Vasoflux, or APC to the wells to degrade NETs for 30 minutes. Afterwards, 5 μM of SYTOX Green was added to each well for 10 minutes. The samples were analyzed using a SpectraMax plate reader on fluorescent top read, with a wavelength combination of excitation at 485 nm and emission at 538 nm. The values were expressed in relative fluorescence units (RFU).

2.0.9 Patients and Inclusion Criteria

The septic patients were recruited from a prospective, multi-centre observational study of 392 septic ICU patients (the DYNAMICS Study, Clinical Trials.gov Identifier:NCT01355042). The study was approved by the Research Ethics Boards of all participating centers. Written informed consent was obtained from the patient or substitute decision-maker prior to enrolment into the study. When *a priori* consent was not feasible, a deferred consent approach was used. All septic events were adjudicated by at least 2 experienced ICU physicians. The inclusion criteria were a modification of those defined by (Bernard et al., 2001). Patients must have a confirmed or suspected infection on the basis of clinical data at the time of screening, at least one dysfunctional organ system, ≥ 3 signs

of systemic inflammatory response syndrome (SIRS), and were expected to remain in the ICU for ≥ 72 hours. The presence of organ dysfunction are: (1) SBP ≤ 90 mm Hg or MAP ≤ 70 mm Hg or SBP < 40 mm Hg for at least 1 hour despite fluid resuscitation, adequate intravascular volume status, or use of vasopressor in attempt to maintain systolic BP ≥ 90 or MAP ≥ 70 mm Hg, (2) P/F Ratio ≤ 250 in the presence of other dysfunctional organs or systems, or ≤ 200 if lung is the only dysfunctional organ, (3) acute rise in creatinine > 171 mM or urine output <0.5 ml/kg body weight for 1 hour despite adequate fluid resuscitation, (4) unexplained metabolic acidosis (pH ≤ 7.30 or base deficit ≥ 5 with lactate > 1.5 times the upper limit of normal, and (5) platelet count < 50,000 or a 50% drop over the 3 days prior to ICU admission. The inclusion criteria for septic shock are the same as those for sepsis except that patients must be on vasopressors within the previous 24 hours. Patients were excluded if they were < 18 years old, pregnant or breastfeeding, or were receiving palliative care. Deferred informed consent was obtained for enrolment in 64.8% of the patients and *a priori* consent was obtained for 34.2% of the patients.

2.0.10 Quantification of Human DNase I and DNase1L3

Development of an in-house sandwich enzyme-linked immunosorbent assay (ELISA): A mouse monoclonal capture antibody against human DNase I was diluted in 50 mM carbonate buffer, coated on a 96-well clear bottom plate, and incubated overnight at 4°C. The next day, blocking buffer was added to each well to block non-specific protein-binding sites and incubated for 2 hours at room temperature. The blocking buffer was aspirated and the plate was washed 3 times with wash buffer. Plasma from septic patients collected as part of our DYNAMICS study (patients and inclusion criteria provided above)

were diluted with blocking buffer, added to a 96-well clear bottom plate, and incubated for 2 hours at room temperature. Recombinant human DNase I was also diluted and added to generate a standard curve. The liquid was aspirated and the plate was washed 3 times with wash buffer. Next, a mouse monoclonal detector antibody against human DNase I and conjugated to horseradish peroxidase (HRP) was diluted with blocking buffer, added to each well, and incubated for 2 hours at room temperature. The liquid was aspirated and the plate was washed 3 times with wash buffer. Tetramethylbenzidine (TMB) substrate (Thermo Fisher Scientific, Waltham, MA) was added. After 30 minutes, 2 M sulphuric acid was added to stop the reaction. The absorbance was measured at 450 nm in end-point mode using a SpectraMax plate reader to determine the concentrations of DNase I in the septic plasma.

Sandwich ELISA (complete kit including all reagents were purchased from abbexa, Cambridge, UK): A monoclonal capture antibody against DNase1L3 was coated on a 96-well clear bottom plate and incubated overnight at 4°C. A blocking buffer was next added to each well to block non-specific protein-binding sites and incubated overnight at 4°C. Serially diluted DNase1L3 standards and plasma collected from septic patients as part of our DYNAMICS study were added and incubated at 37°C for 2 hours. The liquid was aspirated and a biotinylated DNase1L3 detector antibody was added to each well and incubated at 37°C for 1 hour. The liquid was discarded and the plate was washed 3 times with wash buffer. Next a 1x avidin-HRP conjugate was added to each well and incubated at 37°C for 1 hour. The liquid was aspirated and the plate was washed 5 times with wash buffer. TMB substrate was added. After 5 minutes, 2 M sulphuric acid was added to stop

the reaction. The absorbance was measured at 450 nm in end-point mode using a SpectraMax plate reader to determine the concentrations of DNase1L3 in the plasma of septic patients.

2.0.11 APC Enzyme Capture Assay

This APC enzyme capture assay was developed by Dr. Patricia Liaw. The HAPC 1555 antibody was diluted in coating buffer and added to a 96-well clear bottom plate for incubation overnight at 4°C. The next day, the solution was aspirated, blocking buffer was added, and the plate was incubated for 1 hour at room temperature. APC diluted to create a standard curve and plasma collected from septic patients as part of our DYNAMICS study were added to the plate and incubated at room temperature for 30 minutes. The plate was then washed twice with wash buffer. Next, CS-21(66) Chromogenic Substrate (Enzyme Research Laboratories, South Bend, IN) was added. The absorbance was measured at 405 nm using a SpectraMax plate reader at 0 hours, 1 hour, 3 hours, and overnight to quantify the levels of APC in the septic plasma. To detect levels of APC equal or less than 0.5 ng/mL, a time point greater than 19 hours is required for colour development.

2.0.12 Measuring Binding Affinities between Histones and Heparins using Bio-Layer Interferometry (BLI)

The BLITz system (FortéBio, Fremont, CA) was used to measure the biomolecular interactions between human histones H2A, H2B, H3, and H4 with UFH, enoxaparin, fondaparinux, and Vasoflux. The BILTz system uses Bio-Layer Interferometry (BLI) technology, which is an analytical technique that measures the interference pattern of white light reflected from two surfaces. One surface consists of the biosensor tip, which had the

different biotinylated histones immobilized via a streptavidin-biotinylation interaction. The second surface consists of an internal reference layer. A wavelength shift occurs when the histones bind to an analyte in solution (either UFH, enoxaparin, fondaparinux, or Vasoflux), as this causes an increase in optical thickness at the biosensor tip. Binding interactions are measured and recorded in real time.

2.0.13 Retro-orbital Blood Collection

Blood was collected from healthy male and female C57BL/JC mice retro-orbitally every 2 weeks from alternating orbits to allow for a minimum recovery period of one month. A maximum of 2 retro-orbital bleeds from each eye were collected in this study. The mice ranged from 6 weeks old (at the beginning of the study) to 93 weeks old (by the end of the study). Under general gaseous anesthesia (isoflurane SOP GEN727), 110 – 140 µL (up to 10% of the animal's total blood volume) was collected from the retro-orbital sinus of each mouse using a sterile heparinized capillary tube. Blood was collected into heparinized microtainer blood collection tubes. The mice were injected with 1 mL of subcutaneous fluid (saline) after blood collection to replace the lost blood volume. The mice were transferred back to their housing rooms after ensuring hemostasis. All studies were approved by the Animal Research Ethics Board at McMaster University (Hamilton, ON, Canada) and all mice were treated humanely according to the Canadian Council on Animal Care guidelines. The whole blood was centrifuged twice at 5000 g for 10 minutes. The plasma was collected and stored at -80°C until used.

2.0.14 Inferior Vena Cava Blood Collection

Under general gaseous anesthesia (isoflurane SOP GEN727), 1 mL of blood was collected from the inferior vena cava into heparinized microtainer blood collection tubes. The whole blood was centrifuged twice at 5000 g for 10 minutes. The plasma was collected and stored in aliquots at -80°C until used.

2.0.15 PicoGreen dsDNA Quantitation Assay

The PicoGreen dsDNA Quantitation Assay was used to measure DNA levels in mouse plasmas due to the small volumes obtained from mice. DNA was diluted with 1x TE Buffer (Invitrogen, ON, Canada) to prepare a standard curve (ranging from 0 to 50,000 pg/mL). Mouse plasma samples were diluted 50-fold with 1x TE Buffer and added to each well on a Costar 96-well black polystyrene plate. Next, the Quant-iT PicoGreen reagent (Invitrogen, ON, Canada) was diluted 200-fold with 1x TE buffer and 100 µL was added to each well. The plate was incubated for 5 minutes on a shaker at 180 RPM in the dark. The plate was read using a SpectraMax plate reader on fluorescent top read, with excitation of 490 nm, and emission of 525 nm.

2.0.16 Statistical Analyses

Statistical analyses were performed using GraphPad Prism software (La Jolla, CA, USA). Values are expressed as mean ± standard error of mean (SEM) and p-values < 0.05 were considered significant. Significant differences between groups were determined using a one-way analysis of variance (ANOVA) followed by Tukey's multiple comparisons test. Correlations were calculated using the Pearson's correlation coefficient.

3.0 Results

3.0.1 Determining the affinity between histones and UFH, enoxaparin, fondaparinux, and Vasoflux

To determine if GAGs can bind to histones and displace them from DNA-histone complexes, binding affinities were determined between human histones and UFH, enoxaparin, Vasoflux, and fondaparinux. The binding interactions between histones H2A, H2B, H3, and H4 with either UFH, enoxaparin, fondaparinux, or Vasoflux were determined by BLI technology using the BLITz System. As shown in Table 2, UFH, enoxaparin, and Vasoflux bind histones H2A, H2B, H3, and H4 with high affinities (K_D ranging from < 1 nM to 85.50 nM). Our preliminary results also show that fondaparinux has a very low binding affinity towards histones (8533 nM), which suggests that the binding of GAGs to histones is size-dependent. Raw binding curves of our BLITz data is provided in the Appendix (Figure 7.1).

Table 2. Determining the different dissociation constant values (K_D) between histones H2A, H2B, H3, and H4 with UFH, enoxaparin, fondaparinux, and Vasoflux. Results were obtained with the BLITz System and representative of n = 2 experiments. Values are expressed as mean ± SEM.

GAGs	Histones	K_D (nM) ± SEM
Unfractionated Heparin	H2A	< 1
	H2B	1.15 ± 0.81
	H3	< 1
	H4	< 1
Enoxaparin	H2A	< 1
	H2B	< 1
	H3	< 1
	H4	3.10 ± 2.19
Vasoflux	H2A	< 1
	H2B	85.50 ± 60.47
	H3	< 1
	H4	< 1
Fondaparinux	H2A	8533

3.0.2 Effects of UFH on DNase I activity in a purified system

To determine the effects of the different GAGs on enhancing DNase I activity, DNase I was added to preformed DNA-histone complexes in the absence or presence of various concentrations of UFH, which is the largest form of heparin (average molecular weight of 15 kDa). As shown in Figure 3.1 (Lane 4), the molecular weight of human genomic DNA isolated from healthy adults via PAXgene is around 10 kb. The addition of unfractionated bovine histones to the DNA results in complexes that remain in the wells of the agarose gel (Lane 7). The addition of DNase I alone (Lane 8) was unable to completely degrade the DNA-histone complex due to its low activity towards histone-bound DNA, which supports the findings of previous studies (Jiménez-Alcázar et al., 2017; Napirei et al., 2009). The addition of UFH allowed DNase I to cleave the histone-bound DNA in a dose-response manner, as shown by the disappearance of the DNA-histone complexes in the agarose gel (A, Lanes 11, 12) and densitometry graph (B). A minimum concentration of 7 μM (100 μg/mL) of UFH was required for DNase I to completely degrade the DNA in the DNA-histone complex (A, Lane 11) (B). When UFH alone was added to the DNA-histone complexes, a band of DNA was shown beneath the well, indicating that the presence of UFH displaced the DNA from histones (Lane 13).

Figure 3.1. Effects of UFH on DNase I activity in a purified system. DNA (3 nM) and histones (3 μM) were incubated for 1 hour at 37˚C to form DNA-histone complexes (Lane 7). DNase I (0.5 μM) was added to the complexes either alone (Lane 8) or in combination with increasing concentrations of UFH (Lanes 9, 10, 11, 12) for 30 minutes at 37˚C. The samples were run on a 1.8% agarose gel stained with RedSafe for 1 hour at 110 V (A). Figure is representative of n = 3 gels. Gels were quantified using densitometry, and the percent DNA in the wells are reported as mean ± SEM (n = 3) (B). Significant differences were determined using a one-way ANOVA, and compared to the DNA and histones control (white bar). P-values < 0.05 were considered significant. *p < 0.05, ** p < 0.01, *** p < 0.001, **** p < 0.0001.

A.

UFH (μM)	1 kb ladder	7	-	-	-	-	-	-	0.07	0.7	7	13	7
DNase I (0.5 μM)		-	+	-	-	+	-	+	+	+	+	+	-
DNA (3 nM)		-	-	+	-	+	+	+	+	+	+	+	+
Histones (3 μM)		-	-	-	+	-	+	+	+	+	+	+	+
Lane Number	1	2	3	4	5	6	7	8	9	10	11	12	13

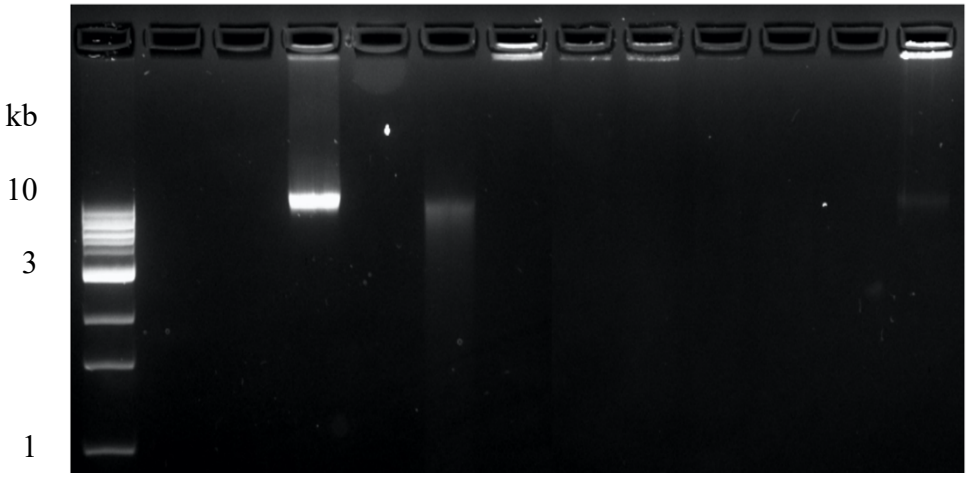

B.

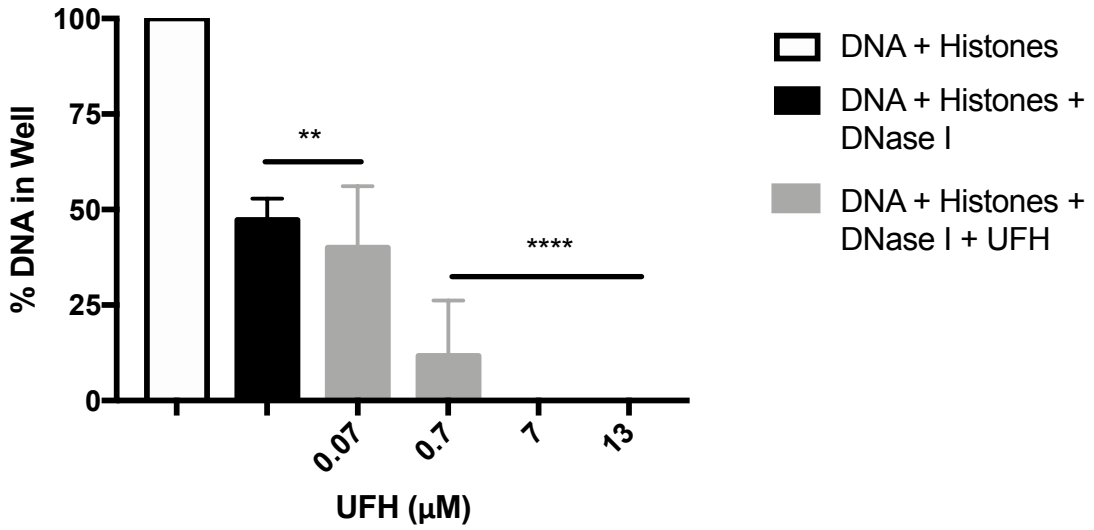
100
75
50
25
0
% DNA in Well
**
****
0.07
0.7
7
13
UFH (μM)
DNA + Histones
DNA + Histones + DNase I
DNA + Histones + DNase I + UFH

3.0.3 Effects of enoxaparin on DNase I activity in a purified system

Previous studies have determined that UFH is able to enhance the activity of DNase I towards DNA-histone complexes, as mentioned above in section 3.0.2; however, no studies have looked at the effects of the other forms of GAGs including enoxaparin, fondaparinux, and Vasoflux on their ability to activate DNase I. As a result, we tested these interactions to better understand the mechanisms by which DNase I degrades histone-bound DNA. First, we looked at the interactions between enoxaparin and DNase I to determine if the cofactor ability of GAGs is size-dependent (Figure 3.2). Enoxaparin is a LMWH and has an average molecular weight of 4.5 kDa. Similar to the experiments done with UFH, the presence of enoxaparin allowed DNase I to degrade the DNA-histone complexes in a dose-response manner (A, Lanes 9, 10, 11, 12) (B). A minimum concentration of 20 μM (100 μg/mL) of enoxaparin was required for DNase I to completely degrade the DNA in the DNA-histone complexes (A, Lane 11) (B). Treating the complexes with only enoxaparin caused the most amount of DNA to dissociate from the DNA-histone complexes, as compared to the other conditions (A, Lane 13).

Figure 3.2. Effects of enoxaparin on DNase I activity in a purified system. DNA (3 nM) and histones (3 μM) were incubated for 1 hour at 37°C to form DNA-histone complexes (Lane 7). DNase I (0.5 μM) was added to the complexes either alone (Lane 8) or in combination with increasing concentrations of enoxaparin (Lanes 9, 10, 11, 12) for 30 minutes at 37°C. The samples were run on a 1.8% agarose gel stained with RedSafe for 1 hour at 110 V. Figure is representative of n = 3 gels. Gels were quantified using densitometry, and the percent DNA in the wells are reported as mean ± SEM (n = 3) (B). Significant differences were determined using a one-way ANOVA, and compared to the DNA and histones control (white bar). P-values < 0.05 were considered significant. *p < 0.05, ** p < 0.01, *** p < 0.001, **** p < 0.0001.

A.

Enoxaparin (μM)	1 kb ladder	20	-	-	-	-	-	-	0.2	2	20	40	20
DNase I (0.5 μM)		-	+	-	-	+	-	+	+	+	+	+	-
DNA (3 nM)		-	-	+	-	+	+	+	+	+	+	+	+
Histones (3 μM)		-	-	-	+	-	+	+	+	+	+	+	+
Lane Number	1	2	3	4	5	6	7	8	9	10	11	12	13

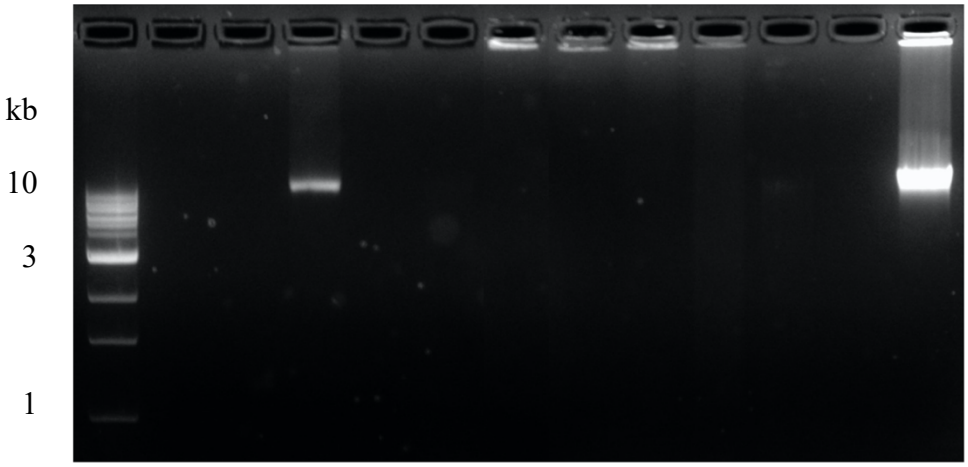

B.

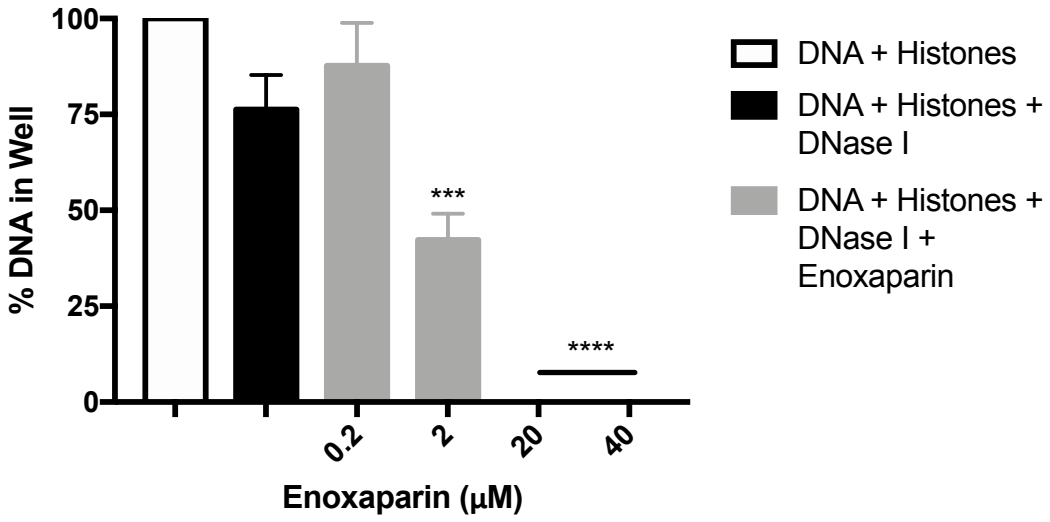
100
75
50
25
0
% DNA in Well
***
****
0.2
2
20
40
Enoxaparin (μM)
DNA + Histones
DNA + Histones + DNase I
DNA + Histones + DNase I + Enoxaparin

3.0.4 Effects of fondaparinux on DNase I activity in a purified system

Next, the effects of fondaparinux on DNase I-mediated degradation of DNA-histone complexes were determined (Figure 3.3). Fondaparinux is the smallest form of heparin, existing as a synthetic pentasaccharide with an average molecular weight of 1.7 kDa. Unlike UFH and enoxaparin, the addition of fondaparinux was unable to accelerate DNase I-mediated degradation of DNA-histone complexes, even at higher concentrations of 120 μM (200 μg/mL) (A, Lane 12) (B). Moreover, when fondaparinux was added to the DNA-histone complexes in the absence of DNase I, no band of DNA migrated into the gel (A, Lane 13). These findings suggest that fondaparinux is unable to displace DNA from histones, and that the cofactor activity of GAGs is size-dependent.

Figure 3.3. Effects of fondaparinux on DNase I activity in a purified system. DNA (3 nM) and histones (3 μM) were incubated for 1 hour at 37˚C to form DNA-histone complexes (Lane 7). DNase I (0.5 μM) was added to the complexes either alone (Lane 8) or in combination with increasing concentrations of fondaparinux (Lanes 9, 10, 11, 12) for 30 minutes at 37˚C. The samples were run on a 1.8% agarose gel stained with RedSafe for 1 hour at 110 V. Figure is representative of n = 3 gels. Gels were quantified using densitometry, and the percent DNA in the wells are reported as mean ± SEM (n = 3) (B). Significant differences were determined using a one-way ANOVA, and compared to the DNA and histones control (white bar). P-values < 0.05 were considered significant. *p < 0.05, ** p < 0.01, *** p < 0.001, **** p < 0.0001.

A.

Fondaparinux (μM)	1 kb ladder	60	-	-	-	-	-	-	0.6	6	60	120	60
DNase I (0.5 μM)		-	+	-	-	+	-	+	+	+	+	+	-
DNA (3 nM)		-	-	+	-	+	+	+	+	+	+	+	+
Histones (3 μM)		-	-	-	+	-	+	+	+	+	+	+	+
Lane Number	1	2	3	4	5	6	7	8	9	10	11	12	13

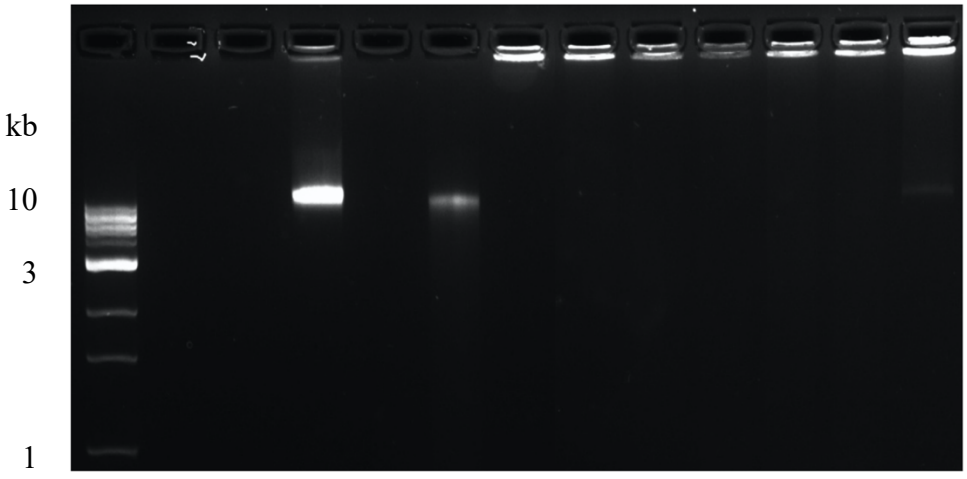

B.

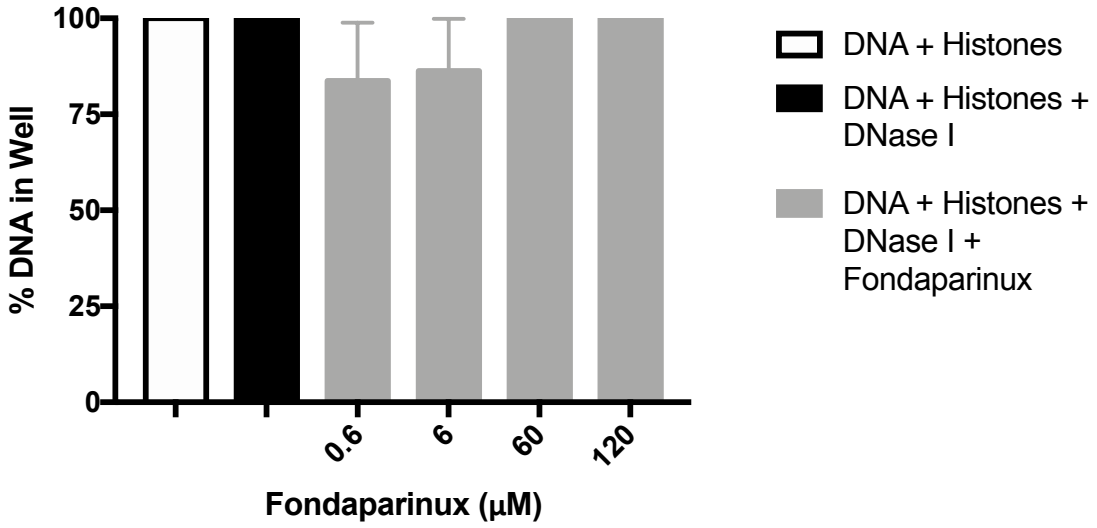
100
75
50
25
0
% DNA in Well
0.6
6
60
120
Fondaparinux (μM)
DNA + Histones
DNA + Histones + DNase I
DNA + Histones + DNase I + Fondaparinux

3.0.5 Effects of Vasoflux on DNase I activity in a purified system

Next, we wanted to determine if the cofactor activity of GAGs requires the AT-binding region (Figure 3.4). Vasoflux is a LMWH that has been chemically modified through periodate oxidation to reduce its affinity for AT by Dr. Weitz and colleagues (Weitz et al., 1999). Similar to the experiments done with UFH and enoxaparin, the presence of Vasoflux allowed DNase I to degrade the DNA-histone complexes in a dose-response manner (A, Lane 9, 10, 11, 12) (B). A minimum concentration of 20 μM (100 μg/mL) of Vasoflux was required for DNase I to completely degrade the DNA in the DNA-histone complexes (A, Lane 11) (B). Interestingly, a minimum concentration of 20 μM (100 μg/mL) of enoxaparin was also required for DNase I to completely degrade the DNA in the DNA-histone complexes (Figure 3.3, Lane 11). These results suggest that the cofactor activity of GAGs in enhancing DNase I-mediated degradation of DNA-protein complexes does not require the AT-binding region, but is size-dependent.

Figure 3.4. Effects of Vasoflux on DNase I activity in a purified system. DNA (3 nM) and histones (3 μM) were incubated for 1 hour at 37°C to form DNA-histone complexes (Lane 7). DNase I (0.5 μM) was added to the complexes either alone (Lane 8) or in combination with increasing concentrations of Vasoflux (Lanes 9, 10, 11, 12) for 30 minutes at 37°C. The samples were run on a 1.8% agarose gel stained with RedSafe for 1 hour at 110 V. Figure is representative of n = 3 gels. Gels were quantified using densitometry, and the percent DNA in the wells are reported as mean ± SEM (n = 3) (B). Significant differences were determined using a one-way ANOVA, and compared to the DNA and histones control (white bar). P-values < 0.05 were considered significant. *p < 0.05, ** p < 0.01, *** p < 0.001, **** p < 0.0001.

A.

Vasoflux (μM)	1 kb ladder	20	-	-	-	-	-	-	0.2	2	20	40	20
DNase I (0.5 μM)		-	+	-	-	+	-	+	+	+	+	+	-
DNA (3 nM)		-	-	+	-	+	+	+	+	+	+	+	+
Histones (3 μM)		-	-	-	+	-	+	+	+	+	+	+	+
Lane Number	1	2	3	4	5	6	7	8	9	10	11	12	13

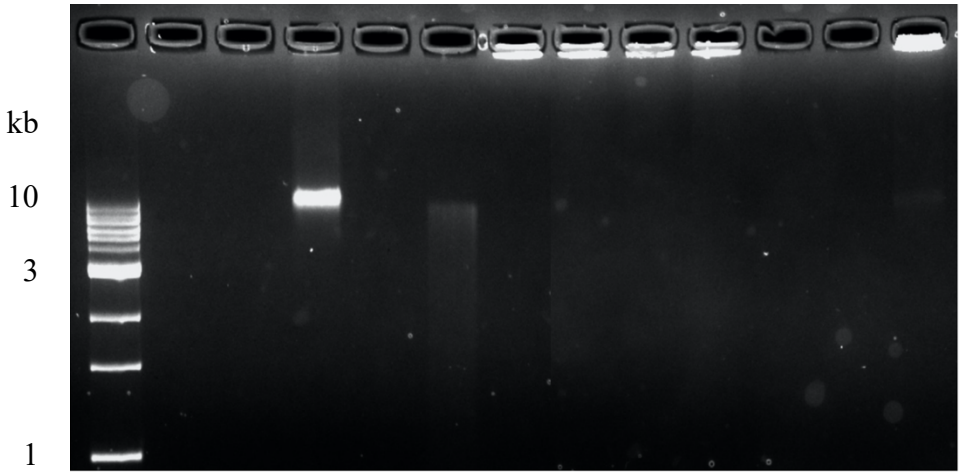

B.

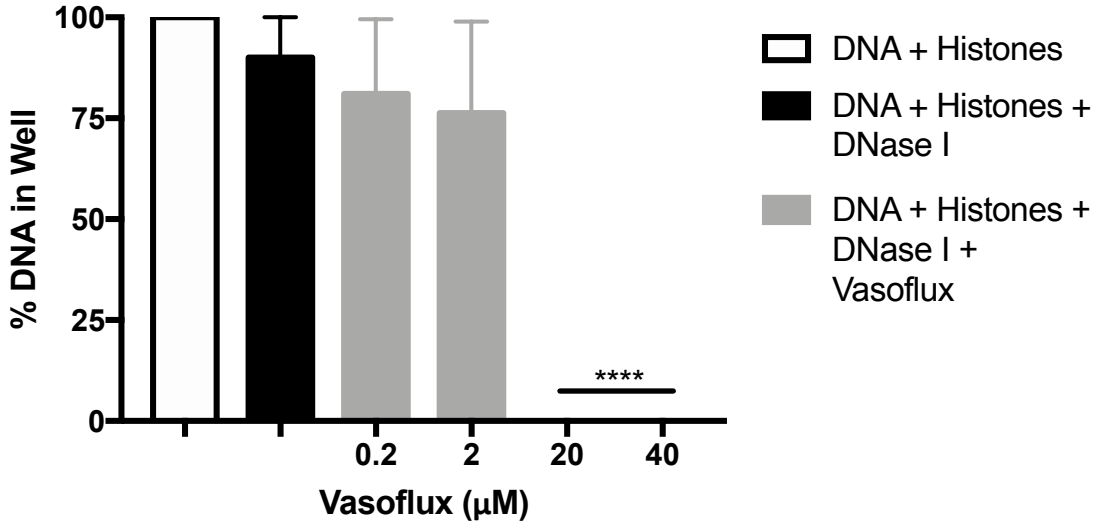
100
75
50
25
0
% DNA in Well
****
0.2
2
20
40
Vasoflux (μM)
DNA + Histones
DNA + Histones + DNase I
DNA + Histones + DNase I + Vasoflux

3.0.6 Effects of DNase I titration on DNA-histone complexes in a time course study

Our previous experiments demonstrated that DNase I (0.5 μM) is able to degrade the DNA component of DNA-histone complexes in the presence of either UFH, enoxaparin, or Vasoflux when incubated for 30 minutes. At these conditions, we observed complete degradation of DNA on the agarose gels. As a result, we tested the same concentration of DNase I (0.5 μM) and lower concentrations (2.5 nM and 0.5 nM) in a time course study (5, 10, 15, 30 minutes incubation) to see an intermediate pattern of DNA degradation. In our previous experiments in section 3.0.2, we determined that a concentration of approximately 0.7 μM of UFH was required to displace the histones from the DNA-histone complexes, and allow for DNase I to significantly degrade the DNA ($p < 0.0001$). Therefore, we used 0.5 μM of UFH in these experiments. A concentration of 0.5 nM of DNase I resulted in no degradation of DNA, even after 30 minutes (Figure 3.5A). A concentration of 2.5 nM of DNase I resulted in a smear pattern of degradation, with all the DNA entering the agarose gel from the wells at 10 minutes (Figure 3.5B, Lane 6). The concentration of DNase I similar to our previous experiments (0.5 μM) resulted in complete degradation of DNA, even at 5 minutes (Figure 3.5C, Lane 5).

Figure 3.5. Effects of DNase I titration on DNA-histone complexes in a time course study. DNA (3 nM) and histones (3 μM) were incubated for 1 hour at 37°C to form DNA-histone complexes (Lane 3). DNase I was added to the complexes at various concentrations: 0.5 nM (A), 2.5 nM (B), or 0.5 μM (C) in the presence of UFH (0.5 μM). In each figure, DNase I was added to the complexes on its own (Lane 4). Reactions were stopped after 5 minutes (Lane 5), 10 minutes (Lane 6), 15 minutes (Lane 7), or 30 minutes (Lane 8) with 50 mM EDTA. The samples were run on a 1.8% agarose gel stained with ethidium bromide for 1 hour at 100 V.

A.

Reaction (minutes):		-	-	-	5	10	15	30
DNase I (0.5 nM)	1 kb ladder	-	-	+	+	+	+	+
UFH (0.5 μM)		-	-	-	+	+	+	+
DNA (3 nM)		+	+	+	+	+	+	+
Histones (3 μM)		-	+	+	+	+	+	+
Lane Number	1	2	3	4	5	6	7	8

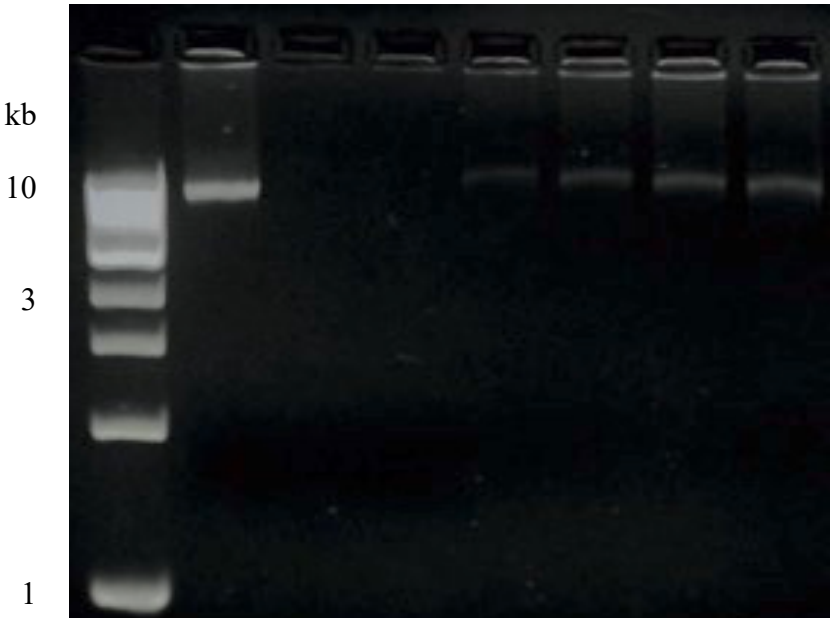

B.

Reaction (minutes):		-	-	-	5	10	15	30
DNase I (2.5 nM)	1 kb ladder	-	-	+	+	+	+	+
UFH (0.5 μM)		-	-	-	+	+	+	+
DNA (3 nM)		+	+	+	+	+	+	+
Histones (3 μM)		-	+	+	+	+	+	+
Lane Number	1	2	3	4	5	6	7	8

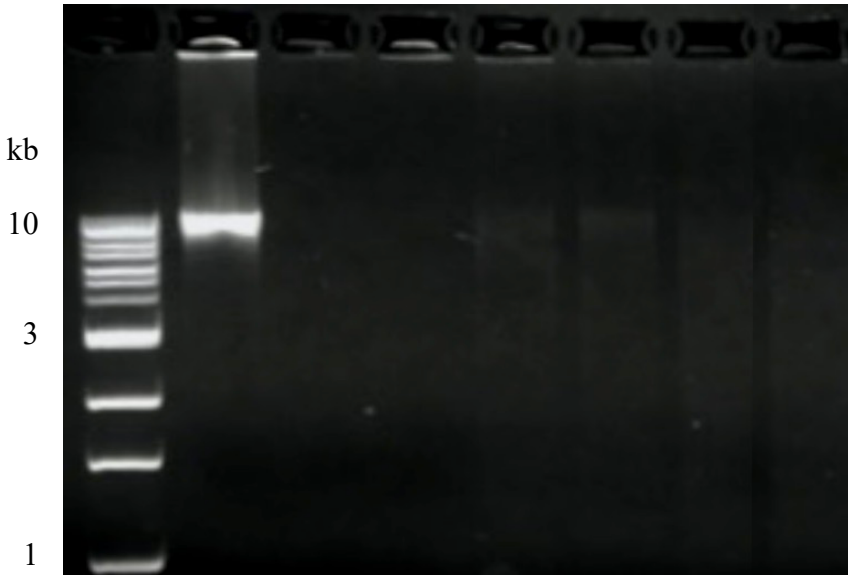

C.

Reaction (minutes):		-	-	-	5	10	15	30
DNase I (0.5 μM)	1 kb ladder	-	-	+	+	+	+	+
UFH (0.5 μM)		-	-	-	+	+	+	+
DNA (3 nM)		+	+	+	+	+	+	+
Histones (3 μM)		-	+	+	+	+	+	+
Lane Number	1	2	3	4	5	6	7	8

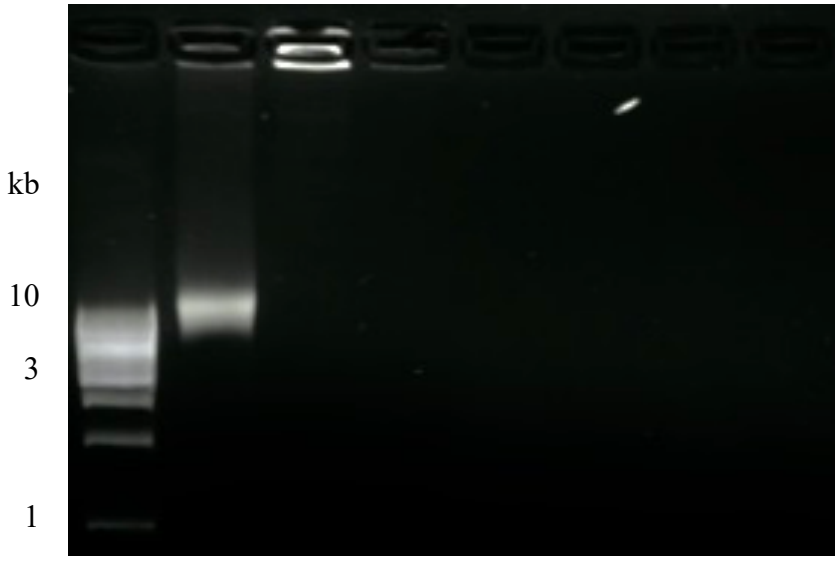

3.0.7 Effects of immediate or overnight GAG treatment on DNA-histone complexes in the absence of DNase I

Next, we treated the preformed DNA-histone complexes with either UFH, enoxaparin, fondaparinux, or Vasoflux to better understand the mechanism by which GAGs enhance the activity of DNase I towards cleaving histone-bound DNA (Figure 3.6). DNA-histone complexes were treated with increasing concentrations of GAGs (1 μM, 5 μM, 10 μM, 25 μM, 50 μM, 100 μM) to determine if GAGs can displace histones from DNA. Reactions were run on an agarose gel immediately (Lanes 4, 5, 6, 7, 8, 9) or after an overnight incubation with GAGs (Lanes 10, 11, 12, 13, 14, 15). DNA-histone complexes that were not treated with GAGs remained in the wells of the agarose gel (Lane 3).

UFH was able to displace histones from DNA in a dose-response manner as shown by the increasing amounts of DNA that migrated into the agarose gel, which continued to increase after an overnight incubation with UFH (A, B). An overnight incubation with 100 μM of UFH resulted in the same amount of DNA migrating into the agarose gel as the DNA only control, as determined by densitometry analysis (B).

Enoxaparin also displaced histones from DNA in a dose-response manner (C, D). Overnight incubation with enoxaparin increased the amount of DNA that migrated into the gel compared to the equivalent concentrations in the immediate conditions. However, overnight treatment with enoxaparin at 100 μM did not show a significant difference compared to the equivalent concentration in the immediate condition. Incubation with 100 μM of enoxaparin in the immediate condition, and overnight incubation with 25 μM of

enoxaparin or greater resulted in the same amount of DNA migrating into the agarose gel as the DNA only control, as determined by densitometry analysis (D).

Fondaparinux was unable to displace histones from DNA, even at the highest concentration (100 μM) with an overnight incubation (E, F).

Treatment with Vasoflux displaced histones and allowed DNA to migrate into the gel in a dose-response manner in the immediate conditions (G, H). Overnight treatment of the DNA-histone complexes with Vasoflux increased the amount of DNA that migrated into the agarose gel. Overnight incubation with 25 μM of Vasoflux or greater resulted in the same amount of DNA migrating into the agarose gel as the DNA only control, as determined by densitometry analysis (H).

Taken together, these results suggest that the cofactor activity of GAGs is size-dependent and does not require the AT-binding region. UFH, enoxaparin, and Vasoflux are able to bind and displace histones from DNA, thereby allowing DNase I to access the DNA-cleavage sites.

Figure 3.6. Effects of increasing concentrations of GAGs on DNA-histone complexes in the absence of DNase I. DNA (3 nM) and histones (3 μM) were incubated for 1 hour at 37°C to form DNA-histone complexes. Increasing concentrations (1 μM, 5 μM, 10 μM, 25 μM, 50 μM, 100 μM) of either UFH (A), enoxaparin (C), fondaparinux (E), or Vasoflux (G) were added to preformed DNA-histone complexes. Samples were run immediately (Lanes 4, 5, 6, 7, 8, 9) or after an overnight incubation with GAGs (Lanes 10, 11, 12, 13, 14, 15) on a 1.8% agarose gel stained with ethidium bromide for 1 hour at 100 V. Each figure is representative of n = 3 gels. Gels were quantified using densitometry, and the percent free DNA values are reported as mean ± SEM (n = 3) (B, D, F, H). Significant differences were determined using a one-way ANOVA, and compared to the DNA only control (white bar). P-values < 0.05 were considered significant. *$p < 0.05$, ** $p < 0.01$, *** $p < 0.001$, **** $p < 0.0001$.

A.

				Immediate						Overnight					
UFH (μM)	1 kb ladder	-	-	1	5	10	25	50	100	1	5	10	25	50	100
DNA (3 nM)		+	+	+	+	+	+	+	+	+	+	+	+	+	+
Histones (3 μM)		-	+	+	+	+	+	+	+	+	+	+	+	+	+
Lane Number	1	2	3	4	5	6	7	8	9	10	11	12	13	14	15

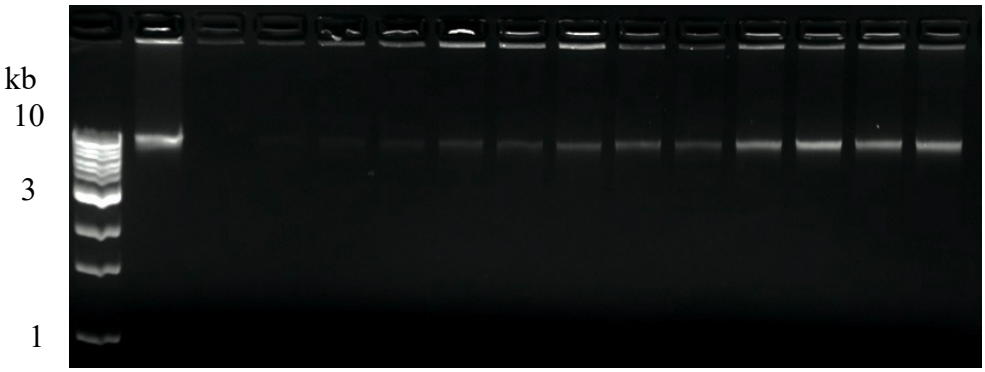

B.

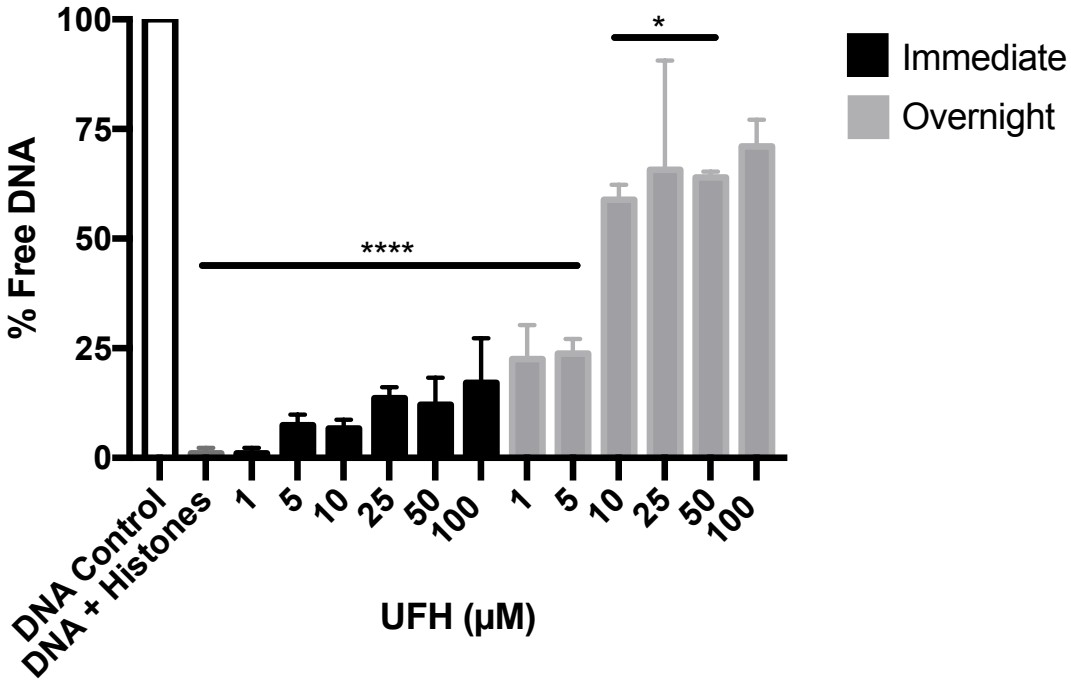

C.

				Immediate						Overnight					
Enoxaparin(μM)	1 kb ladder	-	-	1	5	10	25	50	100	1	5	10	25	50	100
DNA (3 nM)		+	+	+	+	+	+	+	+	+	+	+	+	+	+
Histones (3 μM)		-	+	+	+	+	+	+	+	+	+	+	+	+	+
Lane Number	1	2	3	4	5	6	7	8	9	10	11	12	13	14	15

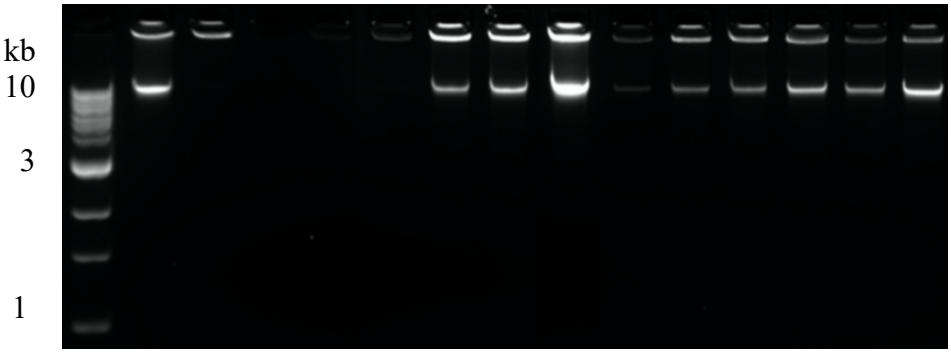

D.

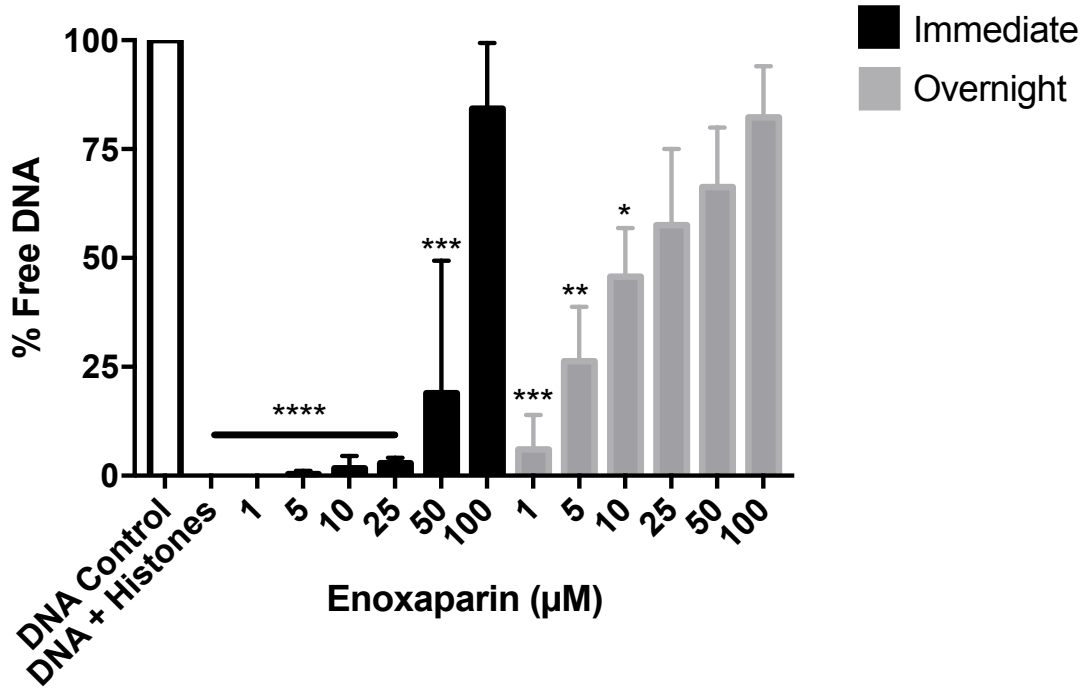

E.

				Immediate						Overnight					
Fondaparinux(μM)	1 kb ladder	-	-	1	5	10	25	50	100	1	5	10	25	50	100
DNA (3 nM)		+	+	+	+	+	+	+	+	+	+	+	+	+	+
Histones (3 μM)		-	+	+	+	+	+	+	+	+	+	+	+	+	+
Lane Number	1	2	3	4	5	6	7	8	9	10	11	12	13	14	15

F.

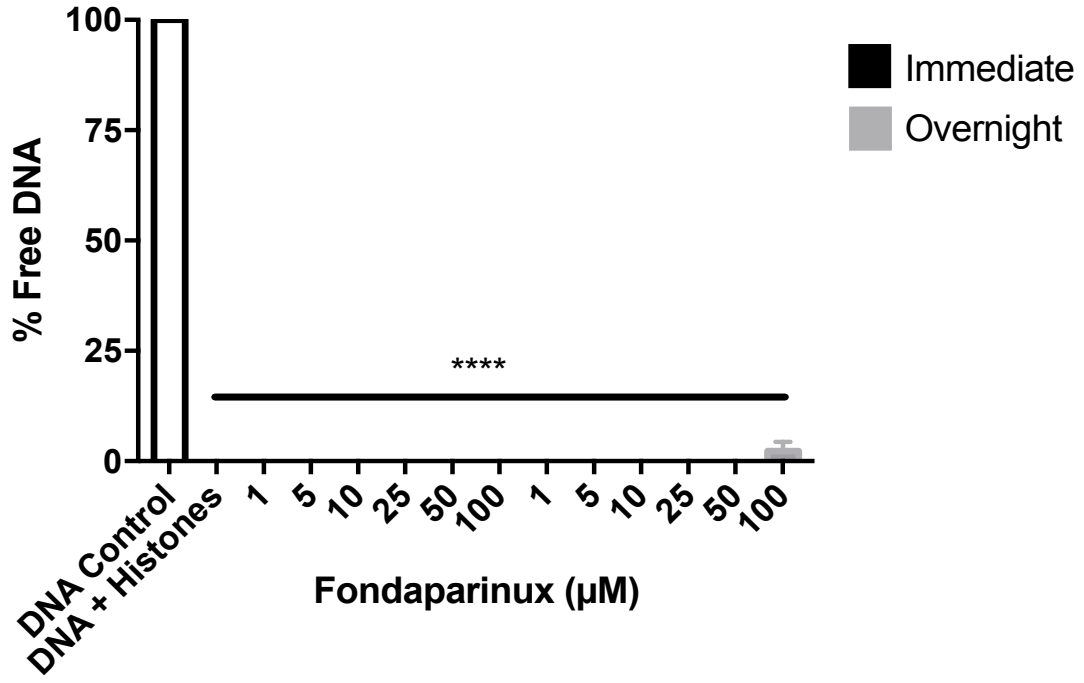

G.

				Immediate						Overnight					
Vasoflux (μM)	1 kb ladder	-	-	1	5	10	25	50	100	1	5	10	25	50	100
DNA (3 nM)		+	+	+	+	+	+	+	+	+	+	+	+	+	+
Histones (3 μM)		-	+	+	+	+	+	+	+	+	+	+	+	+	+
Lane Number	1	2	3	4	5	6	7	8	9	10	11	12	13	14	15

H.

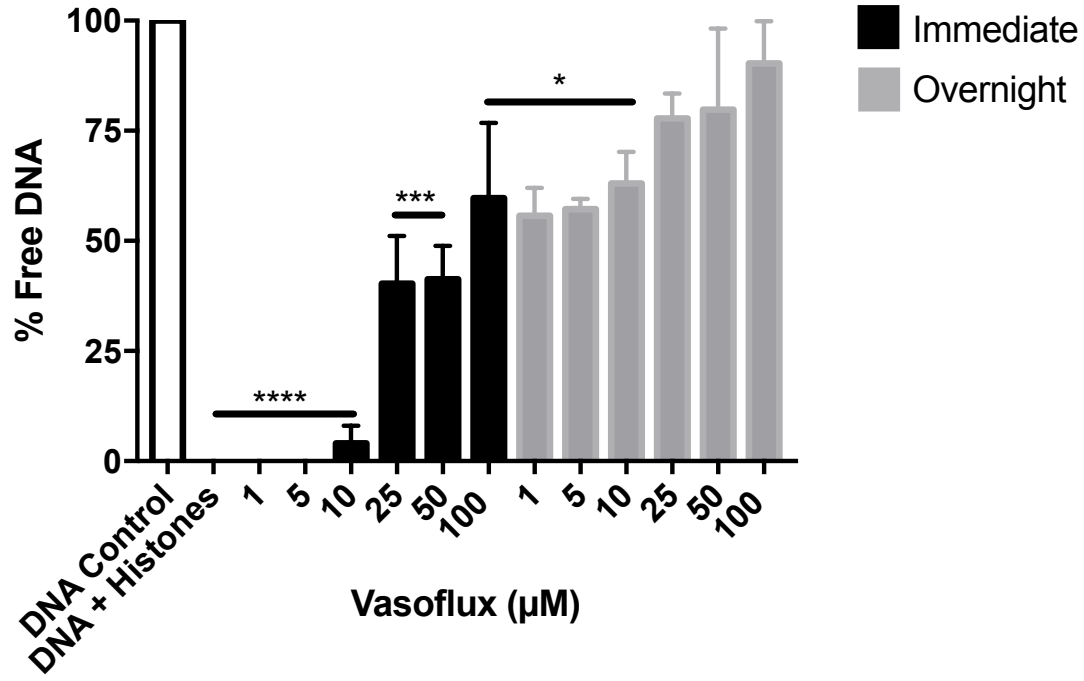

3.0.8 Digestion of DNA-histone complexes with DNase1L3 in the presence of GAGs

Next, we repeated our DNA-histone complex degradation assay using DNase1L3 in the presence or absence of GAGs (Figure 3.7). In literature, DNase1L3 has been reported to have high activity towards digesting histone-bound DNA, and low activity towards digesting protein-free DNA (Napirei et al., 2005, 2009; Sisirak et al., 2016). Our results are consistent with literature (Figure 3.7). The addition of DNase1L3 (0.5 μM) to protein-free DNA (Lane 3) resulted in a lower intensity band compared to DNA alone (Lane 2), and was unable to completely degrade the DNA, thereby confirming that DNase1L3 has low activity towards digesting protein-free DNA. Conversely, the addition of DNase1L3 (0.5 μM) to DNA-histone complexes resulted in complete degradation (Figure 3.7A, Lane 5, Figure 3.7B), which confirms that DNase1L3 has high activity towards digesting histone-bound DNA. UFH has previously been reported to inhibit the activity of DNase1L3, which we also showed in Lane 6, evident by the DNA-histone complex remaining in the well. Interestingly, our studies revealed that enoxaparin (Lane 7) and Vasoflux (Lane 8) also inhibited the activity of DNase1L3, but fondaparinux (Lane 9) did not (A, B). Taken together, our results suggest that the ability of GAGs to inhibit DNase1L3-mediated digestion of DNA-histone complexes is size-dependent, and independent of the AT-binding region.

Figure 3.7. Digestion of DNA-histone complexes with DNase1L3 in the presence of GAGs. DNA (3 nM) was added to the agarose gel (Lane 2). DNase1L3 (0.5 μM) was added to the DNA for 30 minutes at 37˚C (Lane 3). DNA (3 nM) and histones (3 μM) were incubated for 1 hour at 37˚C to form DNA-histone complexes (Lane 4). DNase1L3 (0.5 μM) was added to the complexes either alone (Lane 5) or in combination with 5 μM of: UFH (Lane 6), enoxaparin (Lane 7), Vasoflux (Lane 8), or fondaparinux (Lane 9). The samples were run on a 1.8% agarose gel stained with ethidium bromide for 1 hour at 100 V. Figure is representative of n = 3 gels (A). Gels were quantified using densitometry, and the percent DNA in the wells are reported as mean ± SEM (n = 3) (B). Significant differences were determined using a one-way ANOVA, and compared to the DNA and histones control (white bar). P-values < 0.05 were considered significant. *p < 0.05, ** p < 0.01, *** p < 0.001, **** p < 0.0001.

A.

DNase1L3 (0.5 μM)	1 kb ladder	-	+	-	+	+	+	+	+
GAG (5 μM)		-	-	-	-	+	+	+	+
DNA (3 nM)		+	+	+	+	+	+	+	+
Histones (3 μM)		-	-	+	+	+	+	+	+
Lane Number	1	2	3	4	5	6	7	8	9

B.

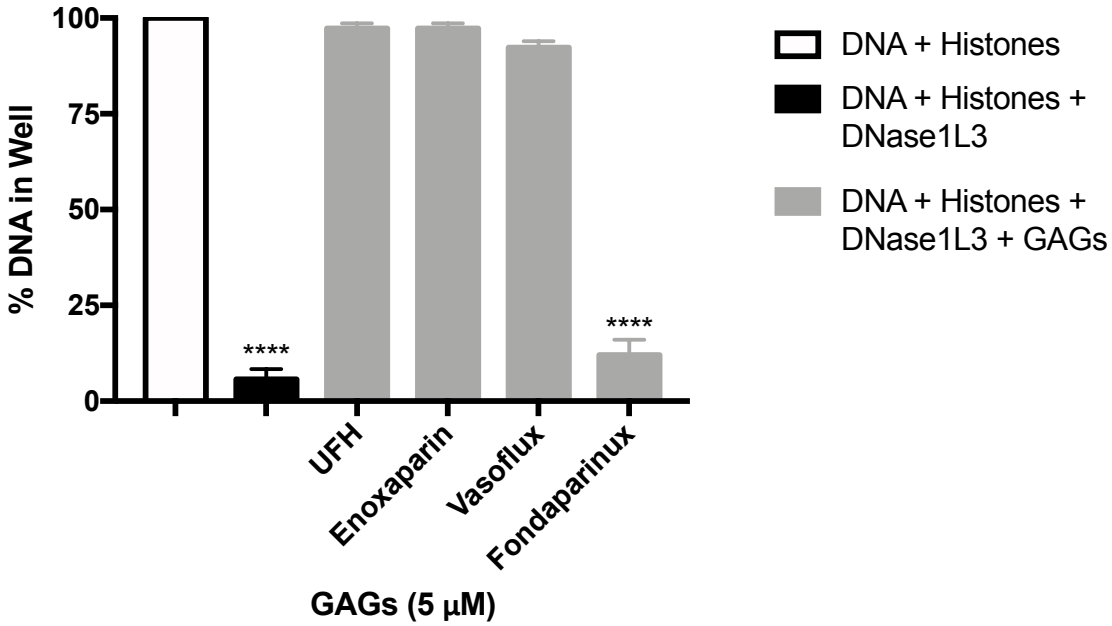
100
75
50
25
0
% DNA in Well
****
****
UFH
Enoxaparin
Vasoflux
Fondaparinux
GAGs (5 µM)
DNA + Histones
DNA + Histones + DNase1L3
DNA + Histones + DNase1L3 + GAGs

3.0.9 Degradation of NETs with DNase I in combination with GAGs

In parallel with the agarose gel studies, we generated NETs *in vitro* and visualized their degradation with DNase I alone or in combination with either UFH, enoxaparin, fondaparinux, or Vasoflux (Figure 3.8). Neutrophils were isolated from whole blood as described above in section 2.0.7, and stained with DAPI to visualize intracellular DNA (A). Next, 100 nM PMA was added to the neutrophils to stimulate NETosis, thereby forming NETs as visualized by SYTOX Green, which stains extracellular DNA and dead cells (C). NETs were also stained with DAPI (B). The addition of DNase I (0.5 μM) alone was effective in degrading the DNA component of NETs, presumably by digesting extracellular chromatin at histone-free linker regions (D). The combination of DNase I with either UFH (E), enoxaparin (F), fondaparinux (G), or Vasoflux (H) showed similar results to that of DNase I alone. We also quantified the degradation of NETs using a plate-reader based fluorometric assay (I). The addition of DNase I significantly reduced the RFU compared to the PMA-stimulated condition (NETs). The addition of GAGs did not further increase the DNase I-mediated NETs degradation compared to DNase I alone.

Figure 3.8. Formation and degradation of NETs with DNase I and GAGs. Neutrophils were isolated from healthy human whole blood, added to coverslips, and stained with 5 μM DAPI (A). Next, 100 nM PMA was added to the neutrophils and incubated for 4 hours at 37°C and 5% CO_2 to allow for NETosis, and stained by DAPI (B), or SYTOX Green (C). DNase I (0.5 μM) was added to the NETs either on its own (D), or in combination with UFH (13 μM) (E), enoxaparin (40 μM) (F), fondaparinux (120 μM) (G), or Vasoflux (40 μM) (H). Images were obtained using a fluorescence microscope. Each image is representative of n = 3 experiments with three different blood donors. In addition, isolated neutrophils were added to a Costar 96-well black polystyrene plate (unstimulated). Next, 100 nM PMA was added to the neutrophils and incubated for 4 hours at 37°C and 5% CO_2 to allow for NETosis as visualized by SYTOX Green. DNase I (0.5 μM) was added to the NETs either on its own, or in combination with UFH (13 μM), enoxaparin (40 μM), Vasoflux (40 μM), or fondaparinux (120 μM), The values are reported as RFU, and expressed as mean ± SEM (I). Significant differences between groups were determined using a one-way ANOVA. Results are representative of n = 4 experiments with four different blood donors. P-values < 0.05 were considered significant. *$p < 0.05$, ** $p < 0.01$, *** $p < 0.001$, **** $p < 0.0001$.

A. Neutrophils (DAPI)

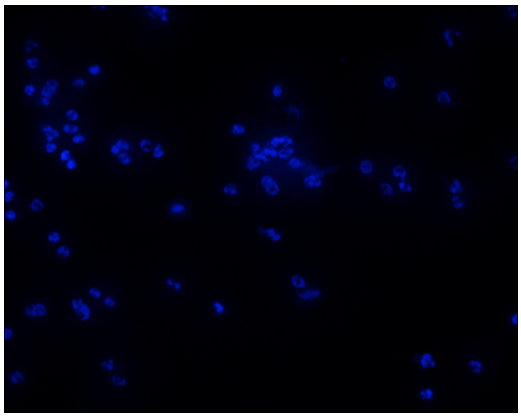

B. NETs (DAPI)

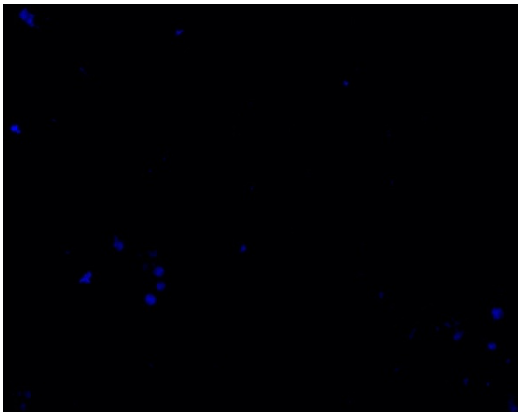

C. NETs (SYTOX)

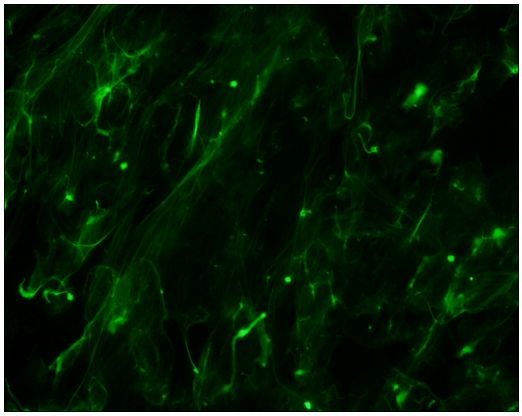

D. NETs + DNase I (0.5 μM)

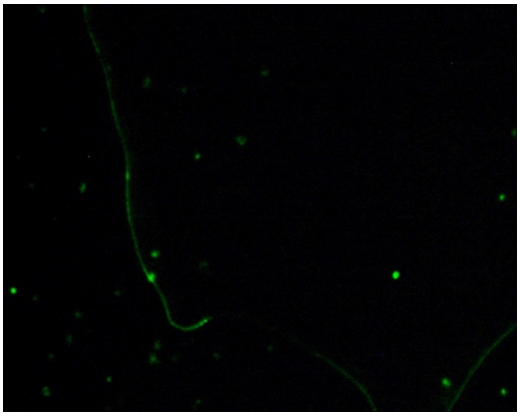

E. NETs + DNase I + UFH (13 μM)

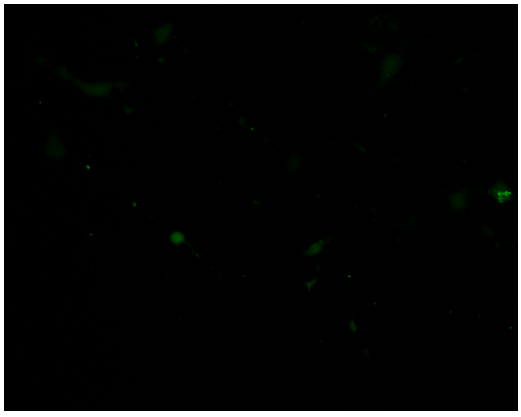

F. NETs + DNase I + Enoxaparin (40 μM)

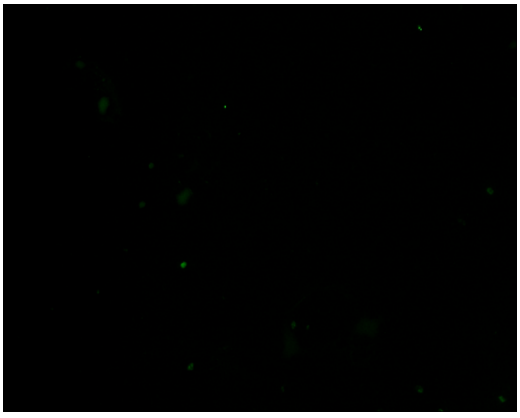

G. NETs + DNase I + Fondaparinux (120 μM)

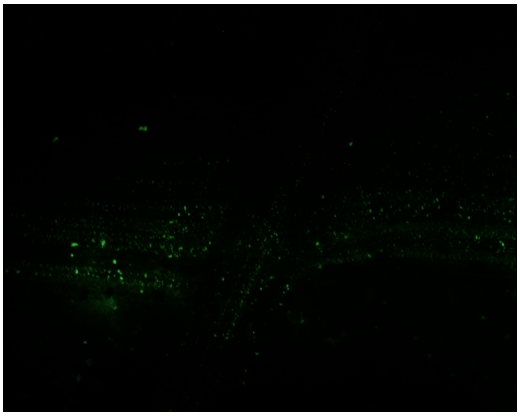

H. NETs + DNase I + Vasoflux (40 μM)

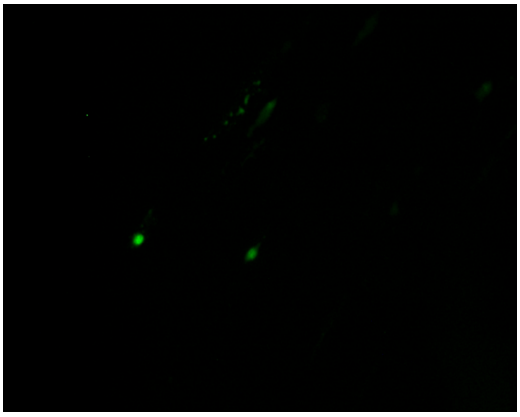

I.

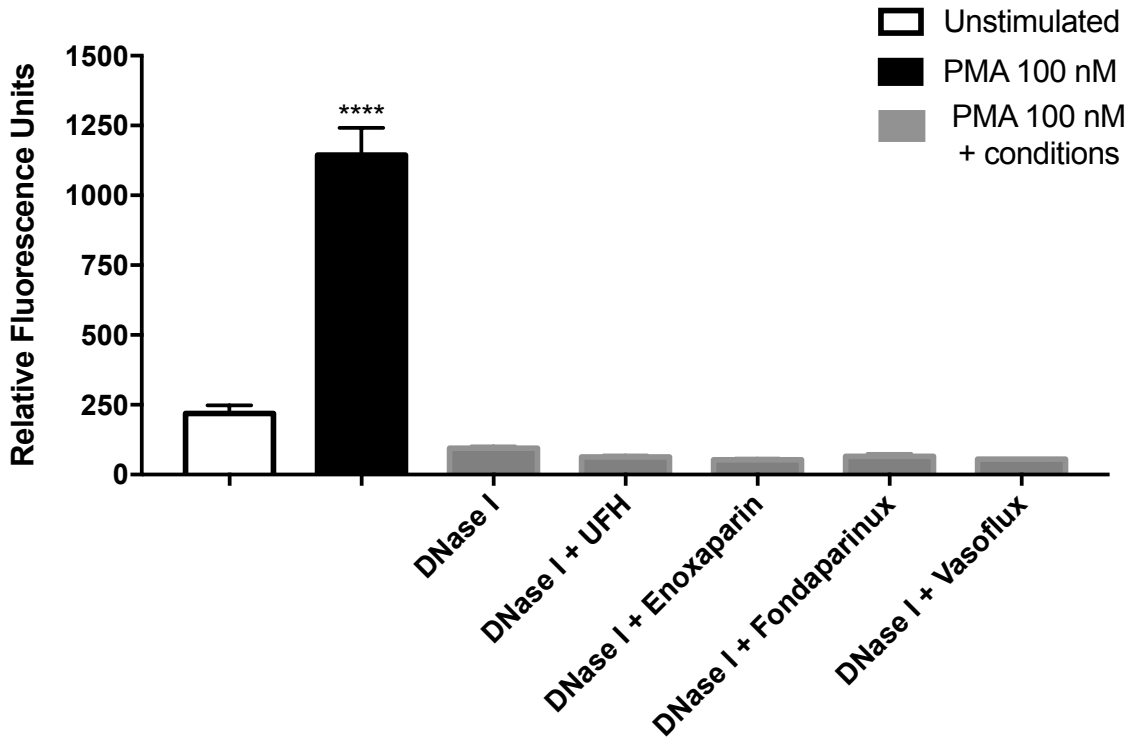

3.0.10 Degradation of NETs with DNase1L3 in combination with GAGs

We next treated NETs with DNase1L3 alone or in combination with UFH, enoxaparin, fondaparinux, or Vasoflux for 30 minutes (Figure 3.9). We visualized the DNA component of NETs with SYTOX Green, and quantified the RFU using a fluorometric assay (F). Treatment with DNase1L3 alone or in combination with fondaparinux was the most effective at degrading the NETs (A, E). Incubation of NETs with DNase1L3 (16 nM) for longer time periods showed no significant differences in RFU values compared to the 30 minute incubation (data not shown).

Treatment with DNase1L3 in combination with either UFH, enoxaparin, or Vasoflux reduced DNase1L3-mediated degradation of NETs (B, C, D). UFH has previously been shown to be an inhibitor of DNase1L3, and our results suggest that enoxaparin and Vasoflux may also be novel inhibitors of DNase1L3. The inhibition of DNase1L3 by GAGs appears to be size-dependent as the larger GAGs reduced the activity of DNase1L3, whereas fondaparinux did not. Further, our results suggest that the AT-binding region is not required for GAGs to inhibit DNase1L3 because Vasoflux also reduced the activity of DNase1L3.

Figure 3.9. Formation and degradation of NETs with DNase1L3 and GAGs. Neutrophils were isolated from healthy human whole blood and added to coverslips. Next, 100 nM PMA was added to the neutrophils and incubated for 4 hours at 37˚C and 5% CO_2 to allow for NETosis as visualized by SYTOX Green, which stains extracellular DNA and dead cells. DNase1L3 (16 nM) was added to the NETs on its own (A), or in combination with UFH (13 μM) (B), enoxaparin (40 μM) (C), Vasoflux (40 μM) (D), or fondaparinux (120 μM) (E). Images were obtained using a fluorescence microscope. Each image is representative of n = 3 experiments with three different blood donors. In addition, isolated neutrophils were added to a Costar 96-well black polystyrene plate (unstimulated). Next, 100 nM PMA was added to the neutrophils and incubated for 4 hours at 37˚C and 5% CO_2 to allow for NETosis as visualized by SYTOX Green. DNase1L3 (16 nM) was added to the NETs either on its own, or in combination with UFH (13 μM), enoxaparin (40 μM), Vasoflux (40 μM), or fondaparinux (120 μM). The values are reported as RFU, and expressed as mean ± SEM (F). Significant differences between groups were determined using a one-way ANOVA. Results are representative of n = 4 experiments with four different blood donors. P-values < 0.05 were considered significant. *$p < 0.05$, ** $p < 0.01$, *** $p < 0.001$, **** $p < 0.0001$.

A. NETs + DNase1L3 (16 nM)

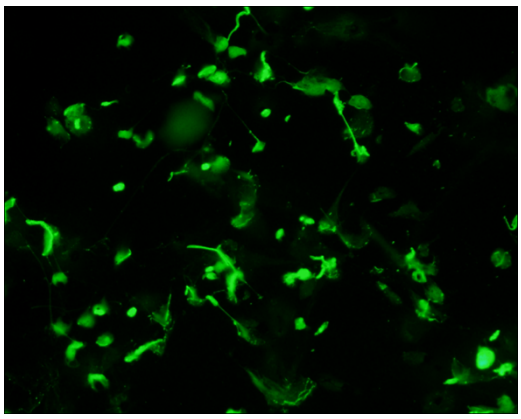

B. NETs + DNase1L3 + UFH (13 μM)

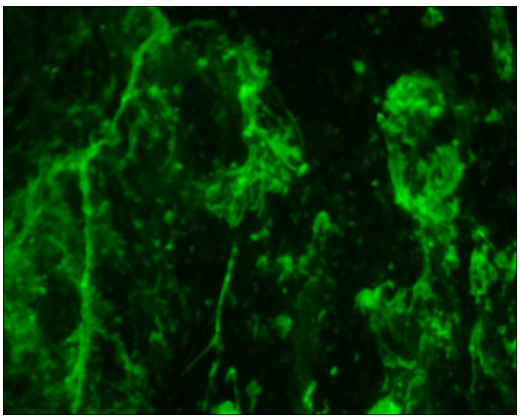

C. NETs+DNase1L3+Enoxaparin (40 μM)

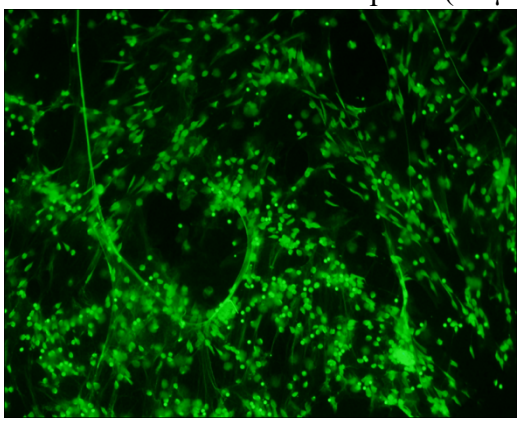

D. NETs + DNase1L3 + Vasoflux (40 μM)

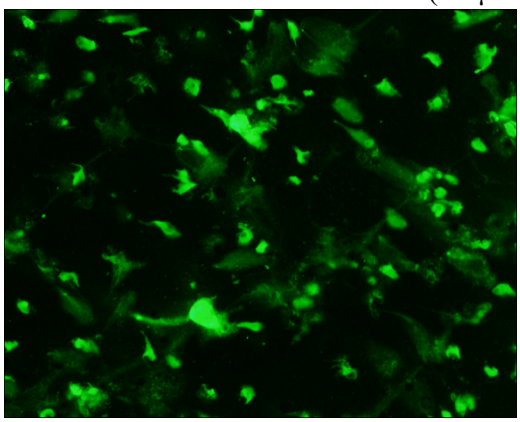

E. NETs + DNase1L3 + Fondaparinux (120 μM)

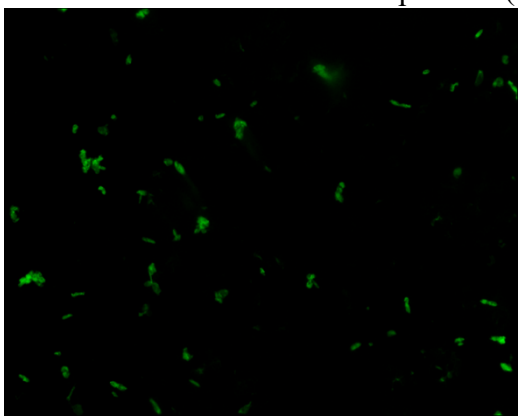

F.

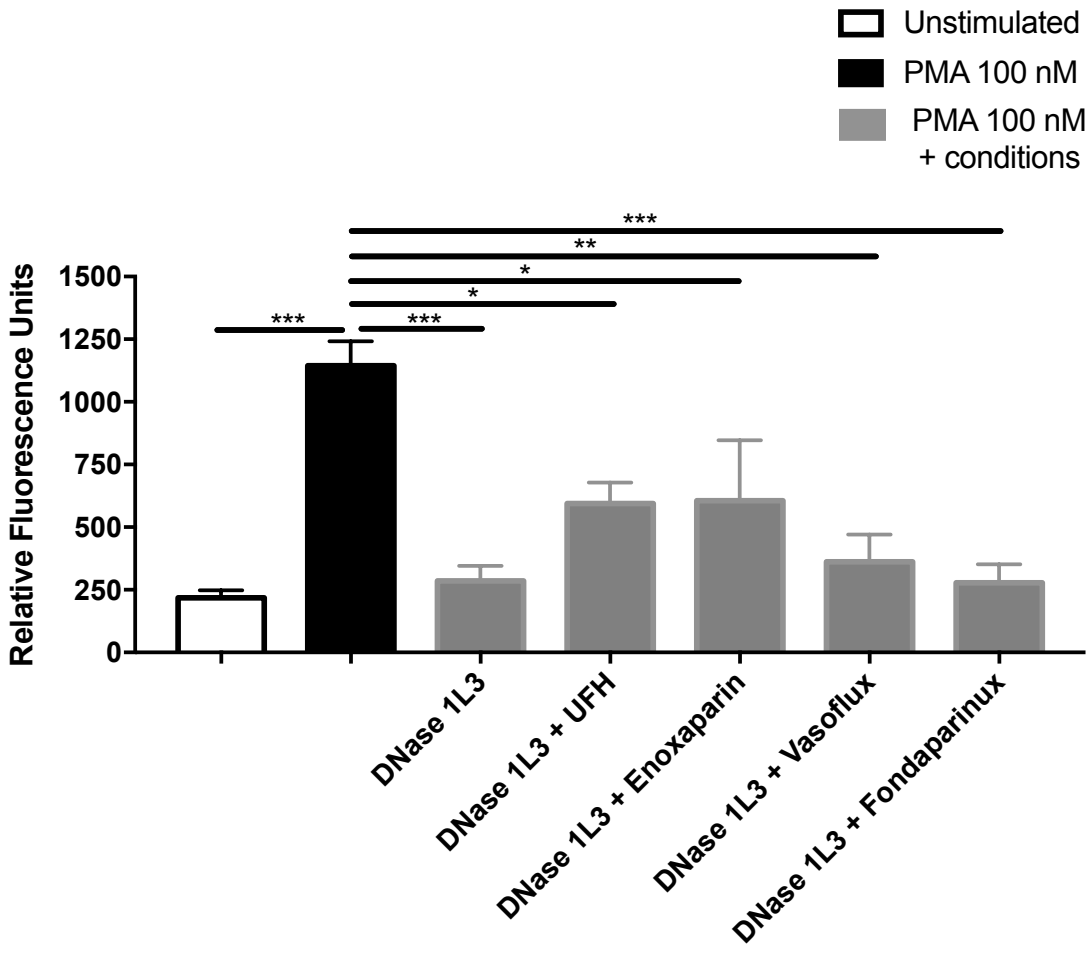
Unstimulated
PMA 100 nM
PMA 100 nM + conditions
Relative Fluorescence Units
1500
1250
1000
750
500
250
0
***
**
*
*
***
***
DNase 1L3
DNase 1L3 + UFH
DNase 1L3 + Enoxaparin
DNase 1L3 + Vasoflux
DNase 1L3 + Fondaparinux

3.0.11 Effects of DNase I titration on NET degradation in a time course study

Our previous NET degradation experiments demonstrated that DNase I (0.5 μM) is able to completely degrade the DNA component of NETs on its own when incubated for 30 minutes (Figure 3.8). Consequently, we tested the same concentration of DNase I (0.5 μM) and lower concentrations (50 nM and 10 nM) in a time course study (5, 15, 30 minutes incubation) to see an intermediate pattern of NET degradation. Neutrophils were isolated from whole blood as described above in section 2.0.7, and stained with DAPI to visualize intracellular DNA (A). Next, 100 nM PMA was added to the neutrophils to stimulate NETosis, thereby forming NETs as visualized by SYTOX Green, which stains extracellular DNA and dead cells (B). An intermediate pattern of degradation was observed when NETs were incubated with 10 nM of DNase I for 5 or 15 minutes (C, D). Complete degradation of NETs was observed at 30 minutes with 10 nM of DNase I (E). Interestingly, we treated NETs with a higher concentration of DNase1L3 (16 nM) compared to DNase I (10 nM), but DNase I was significantly more effective at degrading the DNA component of NETs at 30 minutes (Figure 3.9A, Figure 3.10E), despite the preference of DNase1L3 for degrading histone-bound DNA. This finding suggests that the enzymatic activity of DNase I is greater than the enzymatic activity of DNase1L3. Treatment with 50 nM of DNase I was able to degrade the NETs more effectively than 10 nM of DNase I (F, G, H). There was no difference in the amount of NET degradation when comparing a 5 minute and 30 minute incubation with 50 nM of DNase I. The concentration of DNase I used in our previous experiments (0.5 μM) resulted in complete degradation of NETs, even at 5 minutes (I, J, K).

Additionally, we added DNase I (0.5 μM) with a protease inhibitor cocktail to determine if other neutrophil-derived proteases, such as neutrophil elastase and cathepsin G, act as cofactors in DNase I-mediated degradation of NETs (L). The presence of the protease inhibitor cocktail did not affect the activity of DNase I, as the NETs were still fully degraded (L). Therefore, the other NETs components do not act as cofactors in DNase I-mediated NET degradation.

Figure 3.10. Effects of DNase I titration on NET degradation in a time course study. Neutrophils were isolated from healthy human whole blood, added to coverslips, and stained with DAPI (A). Next, 100 nM PMA was added to the neutrophils and incubated for 4 hours at 37˚C and 5% CO_2 to allow for NETosis, and stained with SYTOX Green (B). DNase I was added to the NETs at increasing concentrations (10 nM, 50 nM, or 0.5 μM) for either 5 minutes, 15 minutes, or 30 minutes to allow for degradation. Reactions were stopped with 50 mM EDTA. NETs were also treated with DNase I (0.5 μM) in the presence of a protease inhibitor cocktail for 30 minutes (L). Coverslips were stained with SYTOX Green. Images were obtained using a fluorescence microscope.

A. Neutrophils (DAPI)

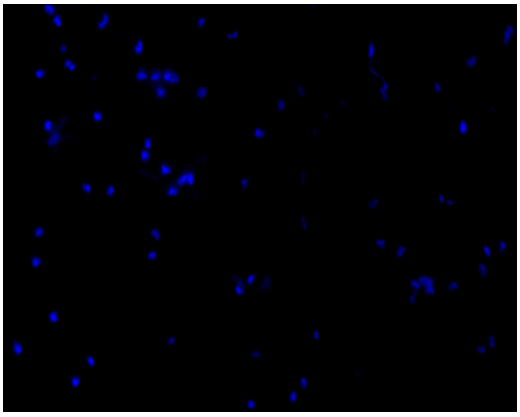

B. NETs (SYTOX)

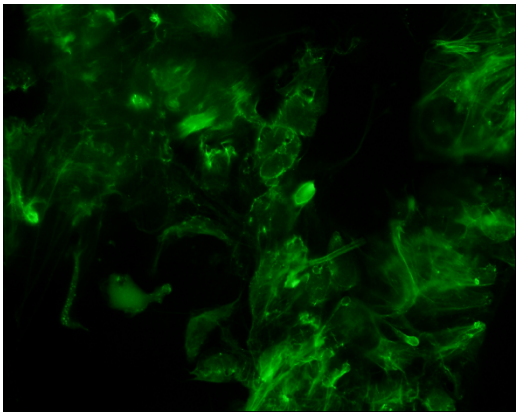

C. NETs + DNase I (10 nM)- 5 minutes

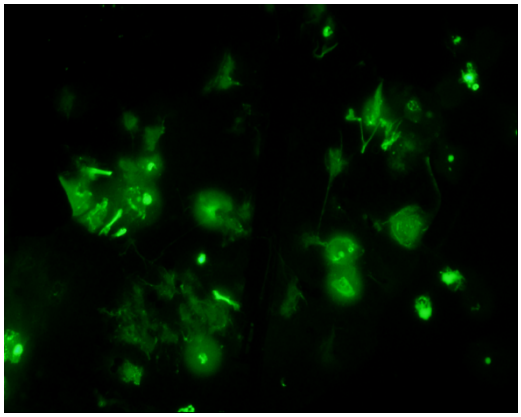

D. NETs + DNase I (10 nM)- 15 minutes

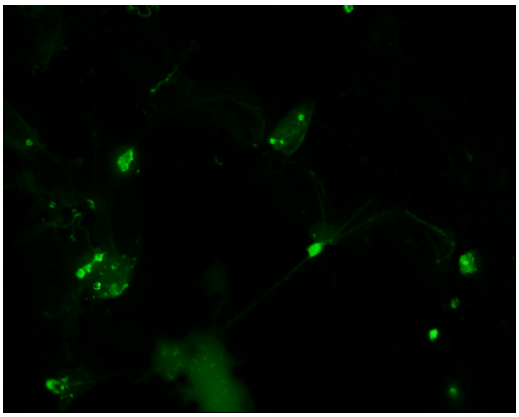

E. NETs + DNase I (10 nM)- 30 minutes

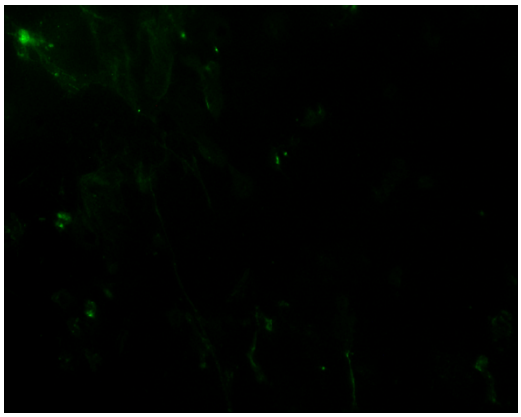

F. NETs + DNase I (50 nM)- 5 minutes

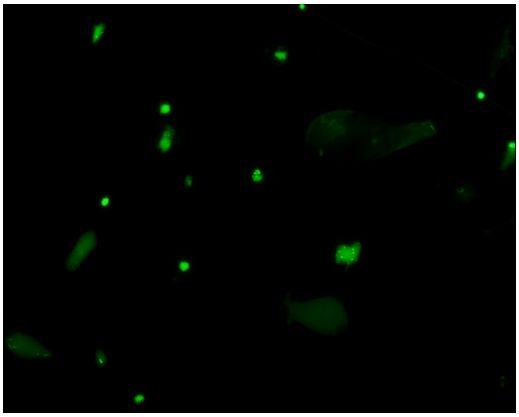

G. NETs + DNase I (50 nM)- 15 minutes

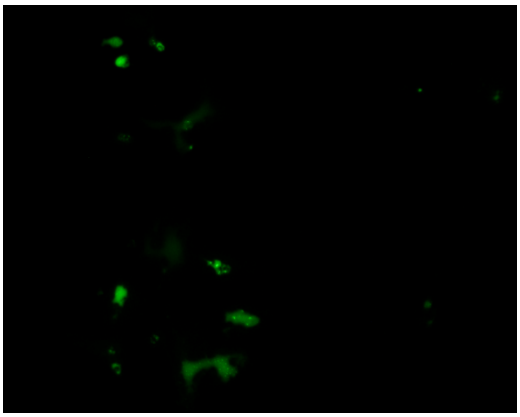

H. NETs + DNase I (50 nM)- 30 minutes

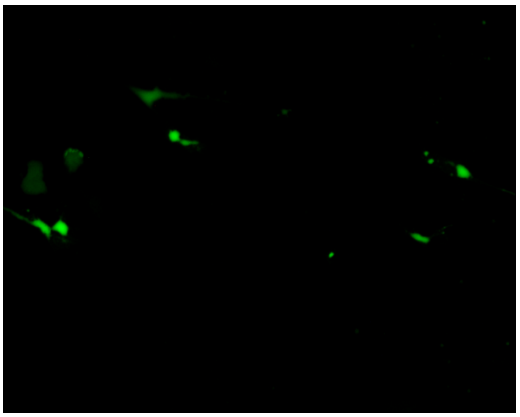

I. NETs + DNase I (0.5 μM)- 5 minutes

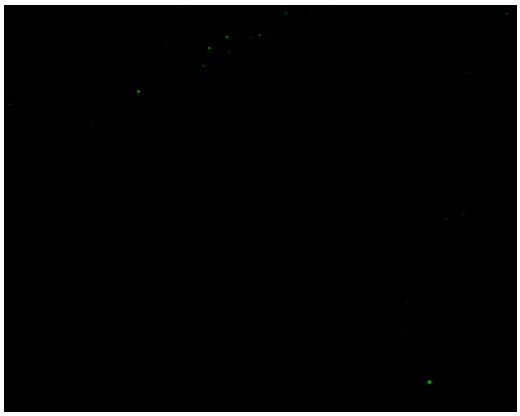

J. NETs + DNase I (0.5 μM)- 15 minutes

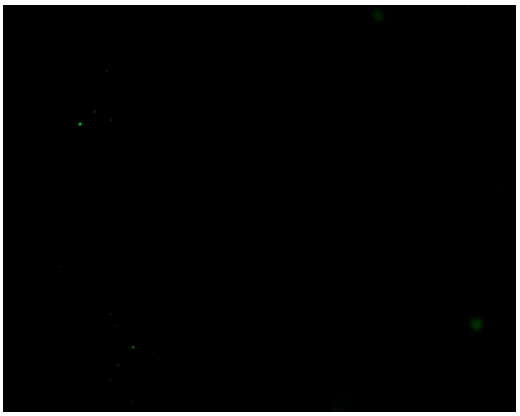

K. NETs + DNase I (0.5 μM)- 30 minutes

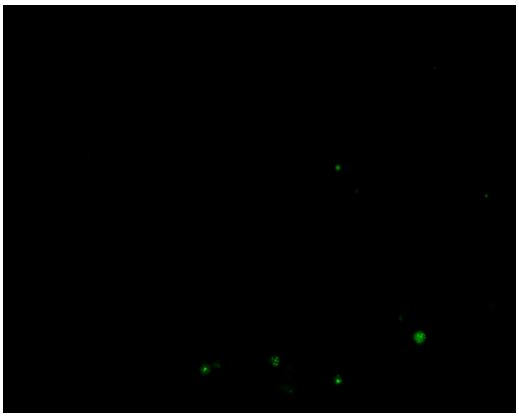

L. NETs + DNase I (0.5 μM) + Protease Inhibitor Cocktail- 30 minutes

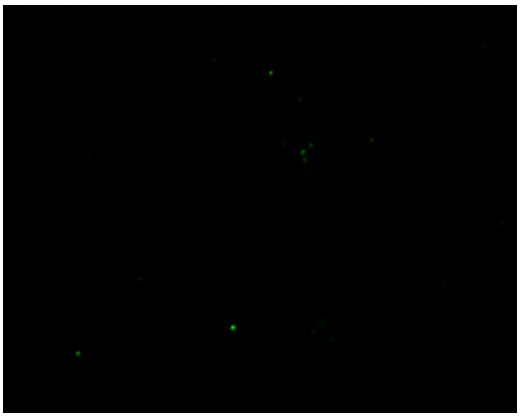

3.0.12 Treating NETs with GAGs in the absence of DNase I and DNase1L3

In addition to treating NETs with DNase I or DNase1L3 in the absence or presence of GAGs, we also treated NETs with either UFH (13 μM) (A), enoxaparin (40 μM) (B), fondaparinux (120 μM) (C), or Vasoflux (40 μM) (D) in the absence of DNase I or DNase1L3 (Figure 3.11). We visualized the DNA component of NETs with SYTOX Green, and quantified the RFU using a fluorometric assay, as described above in section 3.0.8. As expected, treatment with GAGs in the absence of DNase I or DNase1L3 did not decrease the amount of extracellular DNA compared to the no treatment group (Figure 3.11).

Figure 3.11. Treating NETs with UFH, enoxaparin, fondaparinux, or Vasoflux. Neutrophils were isolated from healthy human whole blood and added to coverslips. Next, 100 nM PMA was added to the neutrophils and incubated for 4 hours at 37°C and 5% CO_2 to allow for NETosis as visualized by SYTOX Green, which stains extracellular DNA and dead cells. NETs were treated with either UFH (13 μM) (A), enoxaparin (40 μM) (B), fondaparinux (120 μM) (C), or Vasoflux (40 μM) (D). Images were obtained using a fluorescence microscope. In addition, isolated neutrophils were added to a Costar 96-well black polystyrene plate (unstimulated). Next, 100 nM PMA was added to the neutrophils and incubated for 4 hours at 37°C and 5% CO_2 to allow for NETosis as visualized by SYTOX Green. NETs were treated with either UFH (13 μM), enoxaparin (40 μM), fondaparinux (120 μM), or Vasoflux (40 μM). The values are reported as RFU, and expressed as mean ± SEM (E). Significant differences between groups were determined using a one-way ANOVA. P-values < 0.05 were considered significant. *$p < 0.05$, ** $p < 0.01$, *** $p < 0.001$, **** $p < 0.0001$.

A. NETs + UFH (13 μM)

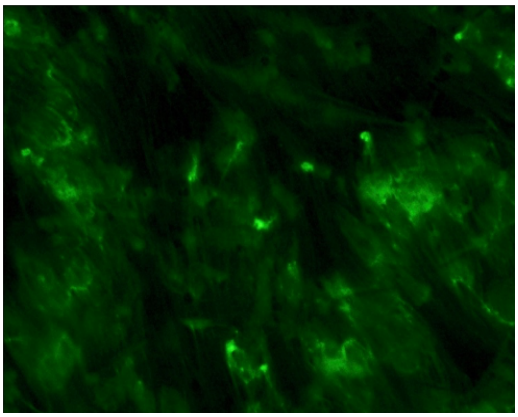

B. NETs + Enoxaparin (40 μM)

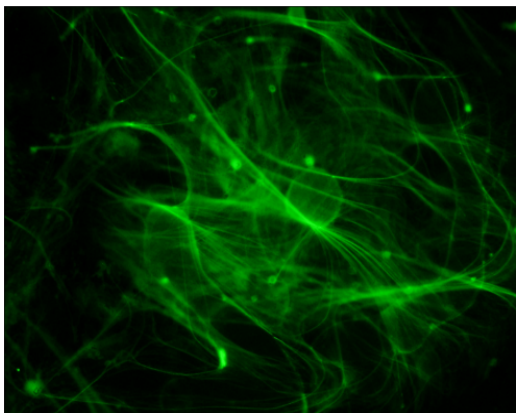

C. NETs + Fondaparinux (120 μM)

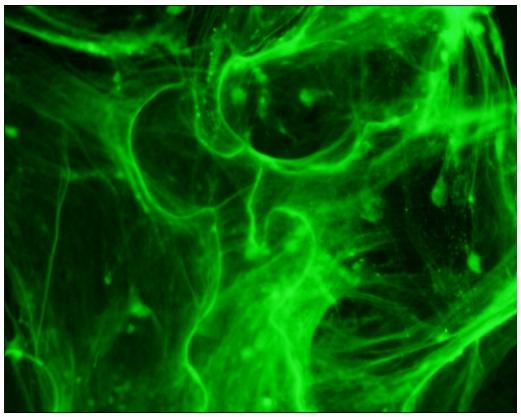

D. NETs + Vasoflux (40 μM)

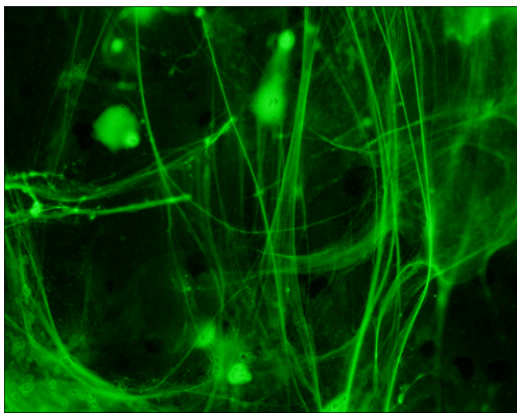

E.

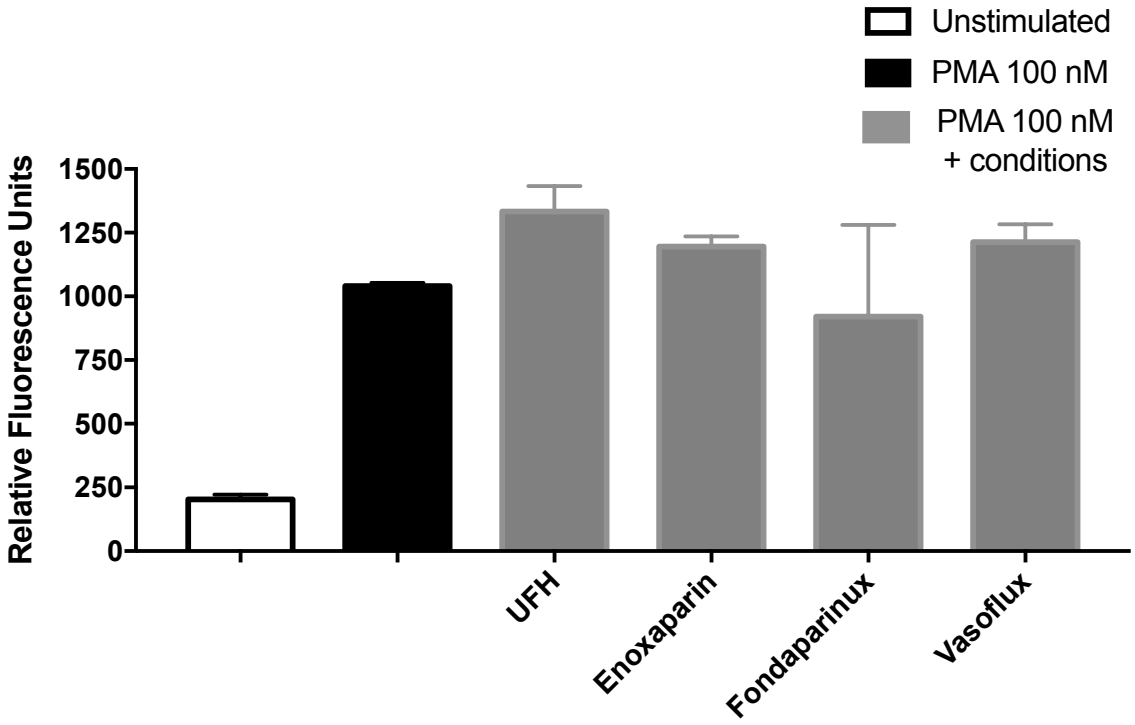

3.0.13 Determining plasma levels of DNase I and DNase1L3 in septic patients

We previously reported that high plasma levels of DNA is a biomarker of poor outcome in septic patients (Dwivedi et al., 2012). Non-survivor patients had persistently elevated levels of DNA compared with survivors. To investigate time-dependent changes in levels of DNase I and DNase1L3 in septic patients, we measured plasma levels of these endonucleases longitudinally (on days 1, 3, 7, 14, 21, 28). DNase I levels were measured in healthy controls (n = 13), septic survivors (n = 9 – 23), and non-survivors (n = 6 – 16) using an in-house sandwich ELISA. DNase1L3 levels were measured in healthy controls (n = 10), septic survivors (n = 5 – 22), and non-survivors (n = 4 – 10) using a commercial ELISA kit. As shown in Figure 3.12A, the levels of DNase I were significantly lower in septic patients compared to healthy controls, and remained low over time (days 1 to 28). Conversely, the levels of DNase1L3 were significantly higher in septic patients compared to healthy controls, and remained elevated over time (days 1 to 28) (Figure 3.12B). Notably, the levels of DNase I and DNase1L3 were not statistically significant between septic patients who survived or did not survive (A, B).

Figure 3.12. Plasma DNase I and DNase1L3 levels in septic patients (days 1 to 28). DNase I levels were measured in healthy controls (n = 13), septic survivors (n = 9 – 23), and non-survivors (n = 6 – 16) longitudinally (on days 1, 3, 7, 14, 21, 28) using an in-house sandwich ELISA (A). DNase1L3 levels were measured in healthy controls (n = 10), septic survivors (n = 5 – 22), and non-survivors (n = 4 – 10) longitudinally (on days 1, 3, 7, 14, 21, 28) using a commercial sandwich ELISA kit (B). Significant differences between groups were determined using a one-way ANOVA and p-values < 0.05 were considered significant. *p < 0.05, ** p < 0.01, *** p < 0.001.

A.

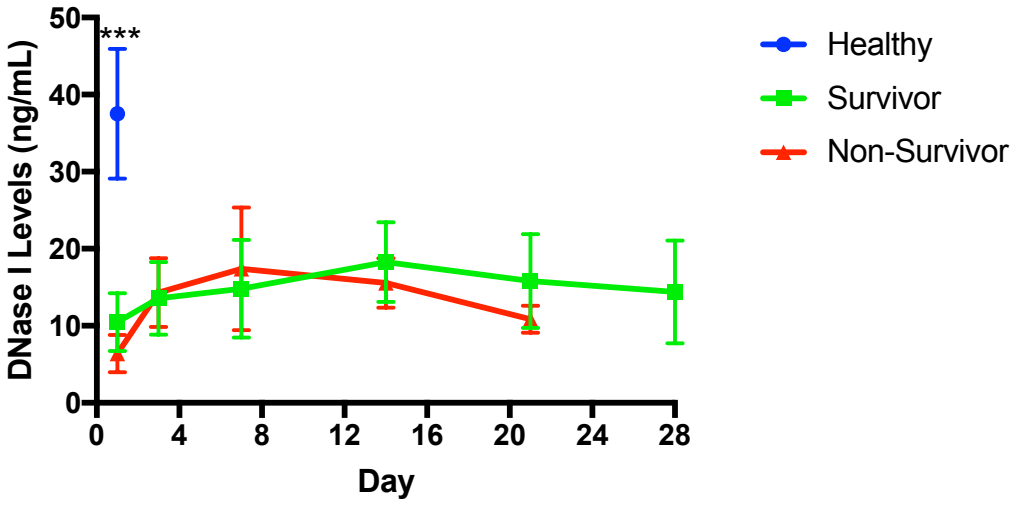

B.

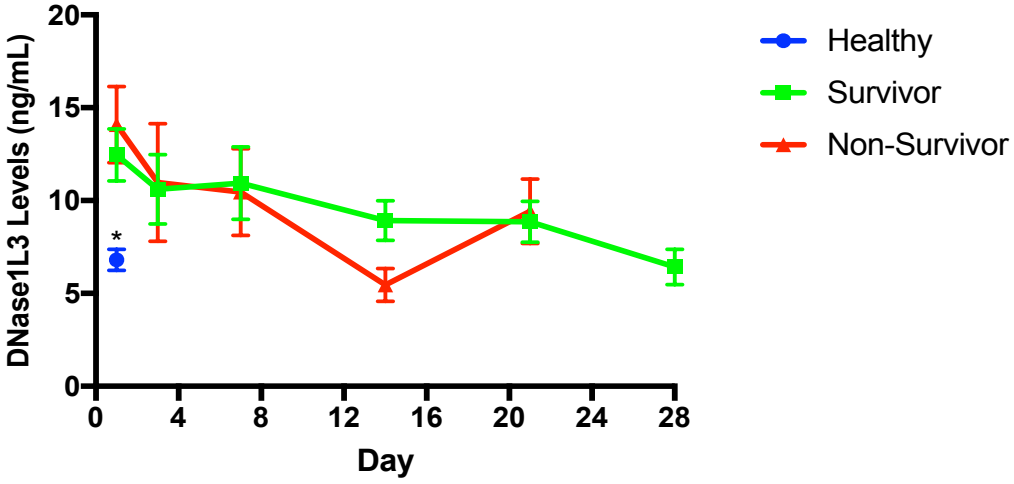

3.0.14 Correlations between DNA and DNase I/DNase1L3 levels in septic patients

Elevated levels of DNA have been reported in patients with sepsis (Dwivedi et al., 2012). This elevation may be due to increased release of DNA from cells, impaired clearance, and/or decreased levels of DNase I and DNase1L3 (Gould et al., 2015). To better understand the mechanism(s) by which DNA levels are elevated, we determined the correlation between the levels of DNA with both DNase I and DNase1L3 in the septic patients in a longitudinal manner (days 1, 3, 7, 14, 21, 28) (Figure 3.13). The correlation between DNA and DNase I showed a negative trend (A – F), while the correlation between DNA and DNase1L3 showed a positive trend (G – L). However, these correlations were not statistically significant.

Figure 3.13. Correlations between DNA levels and DNase I/DNase1L3 levels in septic patients. Correlations were made between DNA and DNase I levels longitudinally on days 1 (A), 3 (B), 7 (C), 14 (D), 21 (E), and 28 (F) using Pearson's correlation coefficient. Correlations were made between DNA and DNase1L3 levels longitudinally on days 1 (G), 3 (H), 7 (I), 14 (J), 21 (K), and 28 (L) using Pearson's correlation coefficient.

A.

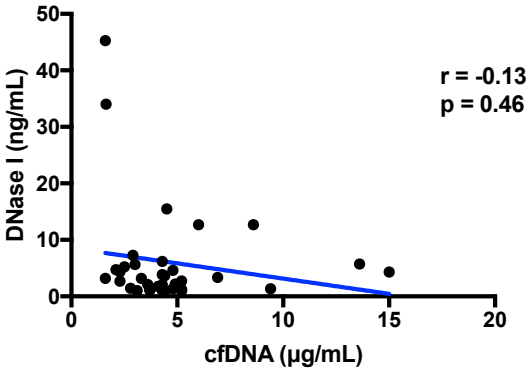
Day 1
DNase I (ng/mL)
cfDNA (µg/mL)
r = -0.13
p = 0.46

B.

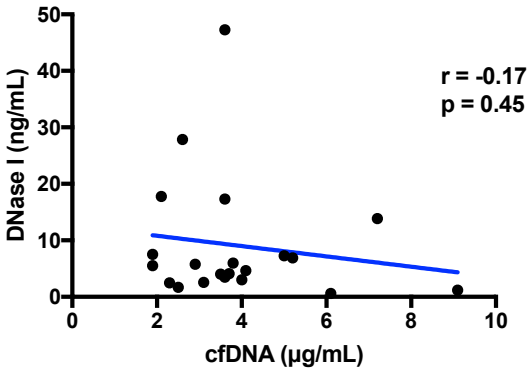
Day 3
DNase I (ng/mL)
cfDNA (µg/mL)
r = -0.17
p = 0.45

C.

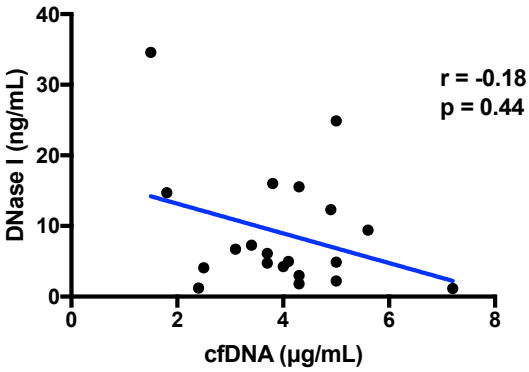
Day 7
DNase I (ng/mL)
cfDNA (µg/mL)
r = -0.18
p = 0.44

D.

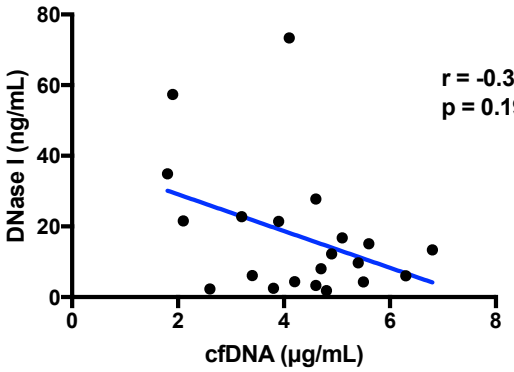
Day 14
DNase I (ng/mL)
cfDNA (µg/mL)
r = -0.30
p = 0.19

E.

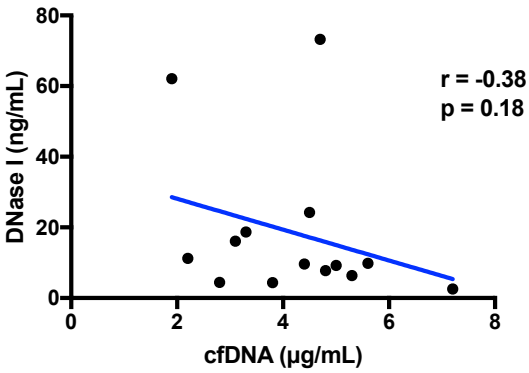
Day 21
DNase I (ng/mL)
cfDNA (µg/mL)
r = -0.38
p = 0.18

F.

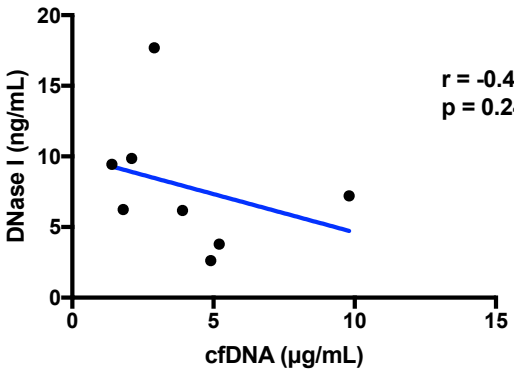
Day 28
DNase I (ng/mL)
cfDNA (µg/mL)
r = -0.48
p = 0.24

G.

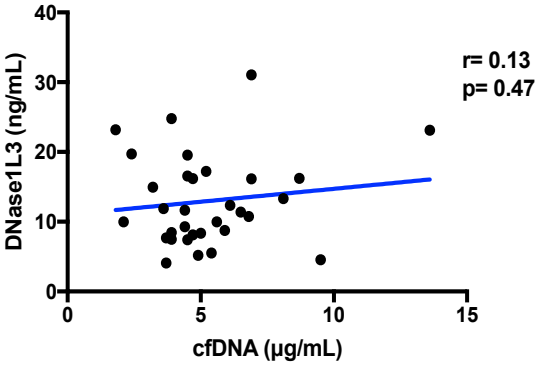
Day 1
DNase1L3 (ng/mL)
cfDNA (µg/mL)
r= 0.13
p= 0.47

H.

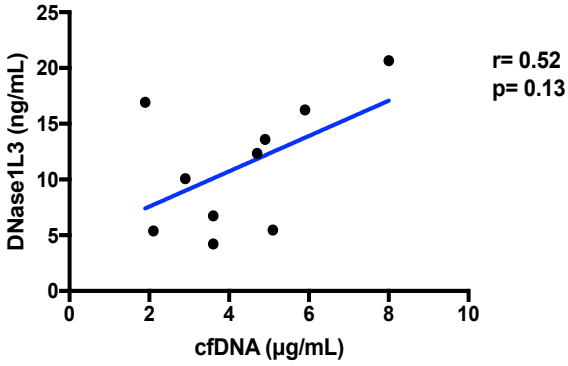
Day 3
DNase1L3 (ng/mL)
cfDNA (µg/mL)
r= 0.52
p= 0.13

I.

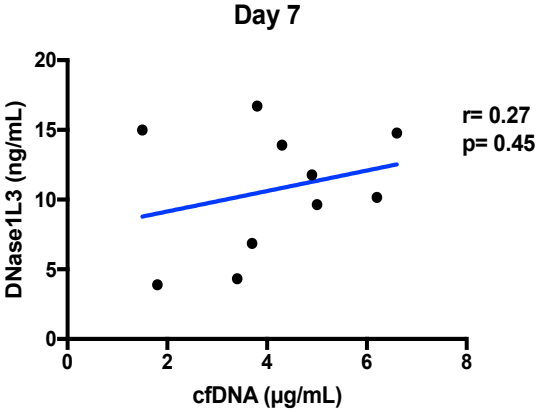
Day 7
DNase1L3 (ng/mL)
cfDNA (µg/mL)
r= 0.27
p= 0.45

J.

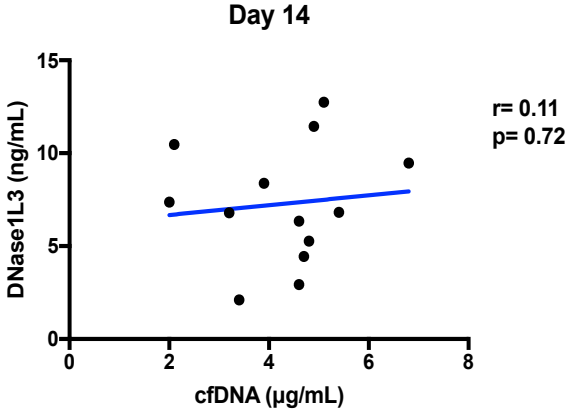
Day 14
DNase1L3 (ng/mL)
cfDNA (µg/mL)
r= 0.11
p= 0.72

K.

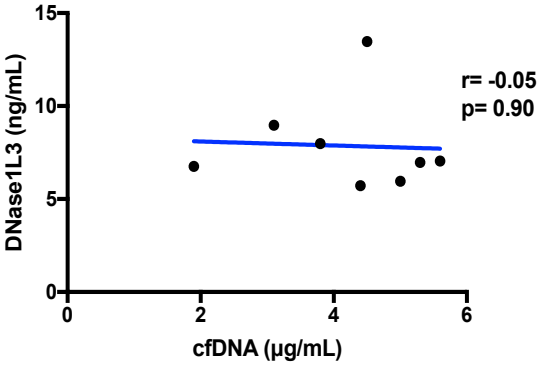
Day 21
DNase1L3 (ng/mL)
cfDNA (µg/mL)
r= -0.05
p= 0.90

L.

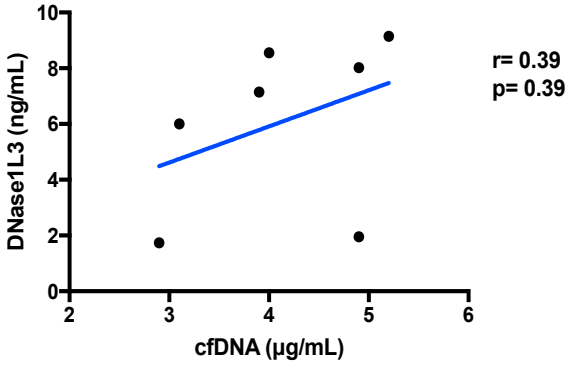
Day 28
DNase1L3 (ng/mL)
cfDNA (µg/mL)
r= 0.39
p= 0.39

3.0.15 Correlations between DNase I and DNase1L3 levels in septic patients

Next, we determined the correlation between the levels of DNase I and DNase1L3. in the septic patients in a longitudinal manner (days 1, 3, 7, 14, 21, 28) to better understand how these host endonucleases are dysregulated in sepsis, and to determine if the reduced DNase I levels that we found in septic patients are compensated by increased DNase1L3 levels (Figure 3.14). There was a significant positive correlation between DNase I and DNase1L3 levels on days 14 and 21 (D, E). There were no significant correlations between these two endonucleases on the remaining days.

Figure 3.14. Correlations between DNase I and DNase1L3 in septic patients. Correlations were made between DNase I and DNase1L3 levels longitudinally on days 1 (A), 3 (B), 7 (C), 14 (D), 21 (E), and 28 (F) using Pearson's correlation coefficient. P-values < 0.05 were considered significant.

A.

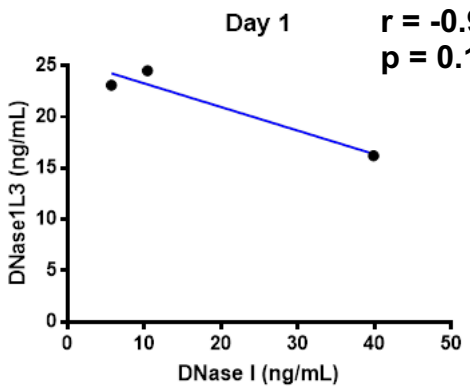
Day 1
r = -0.96
p = 0.18
DNase1L3 (ng/mL)
DNase I (ng/mL)

B.

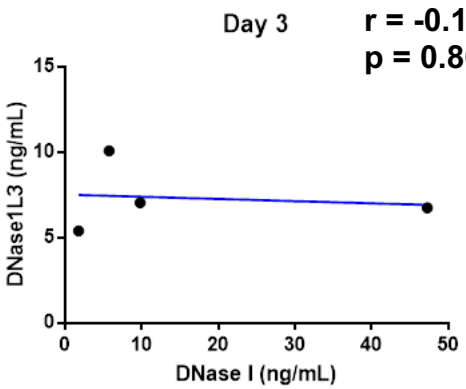
Day 3
r = -0.14
p = 0.86
DNase1L3 (ng/mL)
DNase I (ng/mL)

C.

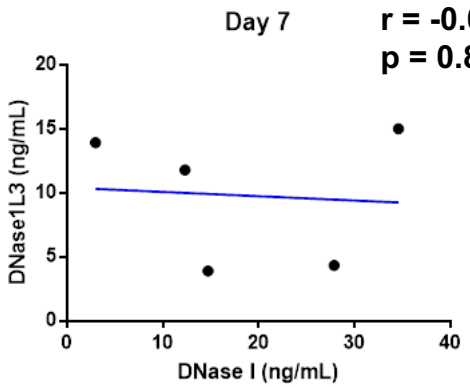
Day 7
r = -0.08
p = 0.89
DNase1L3 (ng/mL)
DNase I (ng/mL)

D.

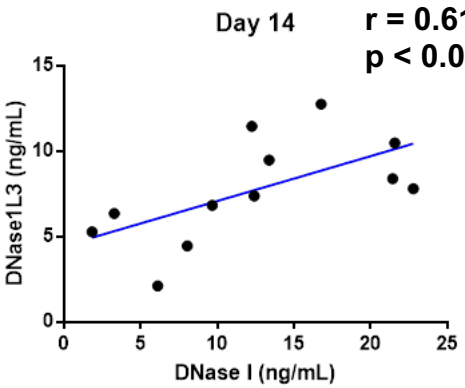
Day 14
r = 0.61
p < 0.05
DNase1L3 (ng/mL)
DNase I (ng/mL)

E.

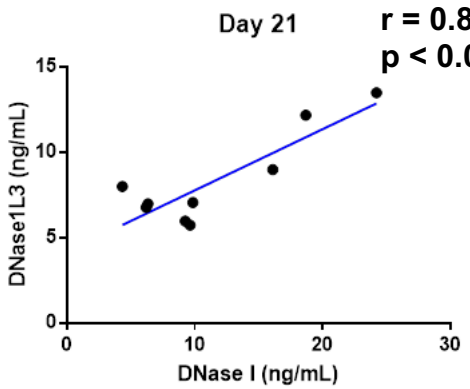
Day 21
r = 0.87
p < 0.01
DNase1L3 (ng/mL)
DNase I (ng/mL)

F.

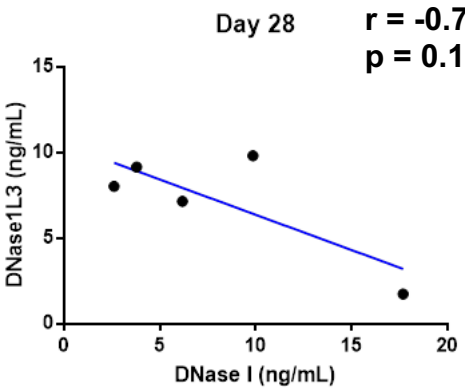
Day 28
r = -0.78
p = 0.12
DNase1L3 (ng/mL)
DNase I (ng/mL)

4.0 Discussion

DNase I is an endonuclease that has therapeutic potential in diseases associated with excessive NET formation. We previously reported that administration of intraperitoneal recombinant DNase I reduces organ damage and improves outcomes in septic mice (Mai et al., 2015). A paper by Lauková and colleagues reported that septic mice (induced with intraperitoneal injection of Escherichia coli) that received intravenous DNase I had a 60% increase in survival and decreased inflammatory markers compared to untreated mice (Lauková et al., 2017). A recent study demonstrated that DNase I and DNase1L3 provide additive protection against harmful effects of intravascular NETs (Jiménez-Alcázar et al., 2017). Given that thromboprophylaxis with heparin (either UFH or LMWH) is recommended for septic patients, it is important to investigate the mechanisms by which GAGs modulate the activities of DNase I and DNase1L3.

We determined the binding affinities between individual human histones and UFH, enoxaparin, Vasoflux, and fondaparinux by BLI technology using the BLITz system. We found that UFH, enoxaparin, and Vasoflux have high affinity for histones, while fondaparinux has low affinity (Table 2). Our results suggest that the ability of GAGs to bind to histones is size-dependent, and that the AT-binding region of heparins is not necessary for histone-heparin interactions. Additionally, UFH, enoxaparin, and Vasoflux bind the four histones with high affinities, which suggests that they would be effective in helping DNase I digest DNA-protein complexes by displacing the histones. This would render the DNA-cleavage sites accessible to DNase I. Our results are consistent with a previous study by Longstaff et al., which found that UFH and enoxaparin have high

affinities towards calf thymus histones using surface plasmon resonance (Longstaff et al., 2016). However, we are the first to determine the binding affinity for each of the individual human histones, as well as the binding affinity for Vasoflux and fondaparinux. We are also the first to determine heparin-histone interactions using BLI technology.

Next, we looked at the potential for GAGs to act as a co-factor for DNase I-mediated degradation of DNA-protein complexes in a purified system. DNase I on its own was unable to degrade the DNA-protein complexes, which is consistent with previous studies (Jiménez-Alcázar et al., 2017; Napirei et al., 2009). Of all the GAGs we studied in our agarose gel experiments, we found that fondaparinux was unable to enhance the activity of DNase I towards cleaving the DNA-protein complexes (Figure 3.3). This LMWH is the smallest form of heparin, existing only as a synthetic pentasaccharide structure, which we believe is the reason why it is ineffective at binding to histones. On the other hand, UFH, enoxaparin, and Vasoflux were able to enhance the ability of DNase I to degrade the DNA-histone complexes (Figures 3.1, 3.2, 3.4). When UFH, enoxaparin, or Vasoflux were added to the complexes in the absence of DNase I, the DNA migrated into the gel, suggesting that these heparins displace histones from DNA (Figure 3.6). These heparins enhance the ability of DNase I to digest DNA-histone complexes by increasing the accessibility of DNase I towards DNA-cleavage sites. Treating the DNA-histone complexes overnight with the highest concentration of fondaparinux (120 μM) still did not displace the histones from the DNA (Figure 3.6). Our agarose gel experiments are consistent with our binding affinity data from the BLITz with respect to UFH, enoxaparin, and Vasoflux being able to bind to

histones, whereas fondaparinux cannot. Taken together, our findings reveal that the GAG-cofactor activity is size-dependent, and does not require the AT-binding region.

Napirei et al. suggested that UFH can indirectly enhance the ability of DNase I by accelerating tPA-mediated activation of plasminogen to plasmin (Napirei et al., 2005). However, since we carried out our experiments in the absence of plasma and therefore plasminogen, this explanation is not supported by our studies.

Next, we wanted to test our findings from the purified system in the context of degrading NETs produced *in vitro*. DNase1L3 has recently gained attention in the literature as an important endonuclease, of which a loss-of-function variant in this gene causes a familial form of systemic lupus erythematosus (Al-Mayouf et al., 2011). Further, in DNase I knock-out mice, the presence of DNase1L3 prevents vascular occlusion by NETs (Jiménez-Alcázar et al., 2017). As a result, we looked at the effects of GAGs on DNase I- and DNase1L3-mediated degradation of NETs. Although DNase I required either a serine protease, UFH, enoxaparin, or Vasoflux to degrade DNA-protein complexes in the purified system, treating NETs with DNase I (0.5 μM) alone resulted in complete degradation of the extracellular DNA, presumably by digesting chromatin at histone-free linker regions, thereby releasing individual nucleosome units (Figure 3.8). This may be possible due to the histone citrullination that occurs during NETosis by PAD4, which is a process that weakens the DNA-histone interactions by reducing the positive charge on histones (Franck et al., 2018). Incubation of NETs with DNase I (0.5 μM) for only 5 minutes was sufficient for complete degradation (Figure 3.10). We lowered the concentration of DNase I by 10-fold and 50-fold to see an intermediate pattern of degradation, instead of an all or nothing effect

that we were seeing with 0.5 μM of DNase I. Degradation with 50 nM of DNase I was more effective at degrading the DNA component of NETs compared to 10 nM of DNase I (Figure 3.9). Treating NETs with the lowest concentration of DNase I (10 nM) was still able to degrade majority of the DNA component of the NETs, suggesting that DNase I has potential to prevent micro- and macro-vascular thrombosis in diseases associated with excessive NET formation. DNase I would degrade the large structural NETs down to smaller components, such as nucleosomes, thereby preventing NETs from occluding vessels.

To test if neutrophil-derived proteases, such as neutrophil elastase or cathepsin G, are acting as cofactors for DNase I-mediated degradation of NETs, we treated NETs with DNase I (0.5 μM) in the presence of a protease inhibitor cocktail. Inhibition of the neutrophil-derived proteases by the protease inhibitor cocktail did not affect the activity of DNase I because the NETs were still fully degraded (Figure 3.10). This experiment suggests that the other NETs components do not act as cofactors in DNase I-mediated NET degradation, rules out the possibility that the proteases are degrading the NETs, and further supports the use of DNase I as a potential therapy to target NETs, thereby preventing their harmful effects within the host.

With respect to DNase1L3, treatment with DNase1L3 alone or in combination with fondaparinux resulted in the most effective degradation of DNA-histone complexes (Figure 3.7) and NETs (Figures 3.9). When DNase1L3 was combined with UFH, enoxaparin, or Vasoflux, this reduced its ability to degrade the DNA-histone complexes (Figure 3.7) and NETs (Figure 3.9). It has previously been reported that UFH inhibits DNase1L3, but our

results suggest that enoxaparin and Vasoflux may also be novel inhibitors of DNase1L3. The ability of GAGs to inhibit the activity of DNase1L3 is size-dependent and independent of the AT-binding region. GAGs are negatively charged molecules, which we believe allows them to bind to the positively charged DNase1L3 enzyme, and sterically inhibit its nuclease site.

Interestingly, DNase I was more efficient at degrading the NETs compared to DNase1L3, despite using a higher concentration of DNase1L3 (Figure 3.9A, 3.10E). This finding may be due to DNase I having greater enzymatic activity compared to DNase1L3. In the context of sepsis, it is possible that DNase1L3 would be more effective at degrading NETs because PAI-1 has previously been reported to slightly activate the activity of DNase1L3, and PAI-1 levels are elevated in septic patients (Napirei et al., 2005; Saracco et al., 2011).

Next we measured the plasma levels of DNase I and DNase1L3 in septic patients longitudinally to determine why the levels of DNA are elevated in some septic patients. We found that the levels of DNase I were significantly lower in septic patients compared to healthy controls, and remained low over time (Figure 3.12). We also found that DNase1L3 levels were significantly higher in septic patients compared to healthy controls, and remained elevated over time (Figure 3.12). We determined that the plasma levels of DNA are inversely correlated with levels of DNase I, suggesting that the clearance of circulating DNA is impaired during sepsis (Figure 3.13). Conversely, the positive correlation we found between DNA and DNase1L3 levels may be due to a potential induced expression of DNase1L3 in response to elevated DNA levels, or in response to a proinflammatory state

characteristic of sepsis (Figure 3.13). The origin of DNase I and DNase1L3 is different: DNase I is secreted by non-hematopoietic endocrine and exocrine glands mainly in the gastrointestinal and urogenital tract, while immune cells (especially dendritic cells and macrophages) secrete DNase1L3 (Onuora., 2016). This can potentially explain why DNase I levels are decreased in septic patients, while DNase1L3 levels are elevated. The organ damage that occurs in sepsis may impair the secretion of DNase I by various organs. Conversely, the inflammatory response in sepsis leads to an excessive activation of immune cells, which may explain why DNase1L3 levels are elevated (Ren., 2011).

A previous study by Napirei et al. demonstrated that plasmin inhibits DNase1L3 by proteolysis (Napirei et al., 2009). PAI-1, which is a serine protease inhibitor that inhibits the formation of plasmin through inhibiting tPA, is known to be increased in sepsis (Saracco et al., 2011). The increased PAI-1 levels may be a potential explanation for why we found significantly higher DNase1L3 levels in septic patients compared to healthy controls, as plasmin formation is inhibited and can no longer proteolyze DNase1L3. However, elevated DNase1L3 levels in sepsis may not retain normal endonuclease activity. As shown in Figure 3.13, we found that plasma levels of DNA and DNase1L3 were not significantly correlated, which may be explained by the presence of other physiological inhibitors that prevent this enzyme from functioning, and thereby being unable to clear the DNA.

We also discovered that there is a significant positive correlation between the levels of DNase I and DNase1L3 on days 14 and 21 in septic patients, but no significant correlation on the remaining days, which may be due to the low n-value on these days

(Figure 3.14). The positive correlation pattern suggests that patients with low levels of either endonuclease may benefit the most from therapeutic administration of DNase I or DNase1L3 due to low antigen levels of both enzymes. The presence of either DNase I or DNase1L3 has been shown to be sufficient in degrading NETs in mice during sterile neutrophilia and septicemia; however, the absence of both DNases lead to vascular occlusion and organ damage (Jiménez-Alcázar et al., 2017). Nonetheless, patients with elevated levels of both endonucleases may still benefit from therapeutic administration of DNase I or DNase1L3 because the activity of these enzymes may be impaired, despite elevated antigen levels. Our studies suggest that DNase1L3 does not serve as a compensatory endonuclease for the decreased DNase I levels in septic patients given the positive correlation, which further supports the use of these endonucleases in the treatment of sepsis.

Some limitations of our present study include the use of DNA-histone complexes that we formed by incubating purified genomic DNA with unfractionated bovine histones, which is unlikely to form the actual nucleosome structure present *in vivo*. Another limitation is that the DNA-histone complexes in our agarose gels were sometimes stained poorly with RedSafe. Alternatively, we tried EtBr due to its smaller size compared to RedSafe, and saw improved staining. However, the DNA was still stained faintly in some gels, which we believe is due to the histones binding tightly and masking the DNA, thereby rendering the DNA inaccessible to the staining reagents. Lastly, we were unable to determine exact binding affinity values using the BLITz for some interactions that were in the picomolar range, because the system only determines precise values above 1 nM.

Taken together, our study reveals novel findings with respect to how GAGs modulate the activities of DNase I and DNase1L3. By looking at four different heparin variants with different sizes and AT-binding capacities, we were able to determine that the ability of GAGs to act as a cofactor for DNase I-mediated degradation of DNA-histone complexes is size-dependent and does not require the pentasaccharide sequence of GAGs. Further, we determined that UFH, enoxaparin, and Vasoflux have high binding affinities for histones H2A, H2B, H3, and H4, which suggests that these heparins can bind and displace histones, thereby allowing DNase I access to DNA-cleavage sites. On the other hand, we found that the ability of GAGs to inhibit the activity of DNase1L3 is also size-dependent and independent of the AT-binding pentasaccharide. Although DNase I and DNase1L3 were able to degrade NETs on their own, the addition of heparins in the context of diseases with increased NETosis can help improve outcomes by binding and neutralizing the free histones that are released, thereby preventing their harmful effects. Lastly, we showed that host DNase levels are altered in sepsis pathophysiology; specifically, DNase I levels are significantly decreased, while DNase1L3 levels are significantly increased, which suggests that recombinant human DNase I can be a potential therapeutic strategy to improve outcomes in septic patients.

A schematic diagram summarizing our findings is provided in Figure 4.1.

Figure 4.1. Schematic diagram summarizing our findings. Non-hematopoietic endocrine cells (yellow) release DNase I (light purple) (A). DNase I cannot digest DNA-histone complexes, but can digest NETs down to individual nucleosomes on its own, thereby preventing vascular occlusion (A). Immune cells, especially macrophages (grey) and dendritic cells (purple) release DNase1L3 (green) (B). DNase1L3 digests DNA-histone complexes on its own, and significantly degrades NETs, but not as effectively as DNase I (B). The ability of GAGs to enhance DNase I-mediated digestion of histone-bound DNA is size-dependent, and independent of the AT-binding pentasaccharide of GAGs (C). Conversely, the ability of GAGs to impair the activity of DNase1L3 is size-dependent, and independent of the AT-binding pentasaccharide of GAGs (C). Source: biorender.com

A.

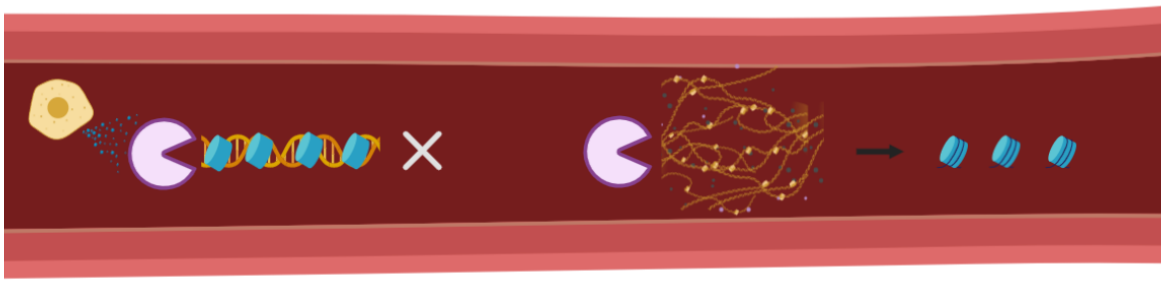

B.

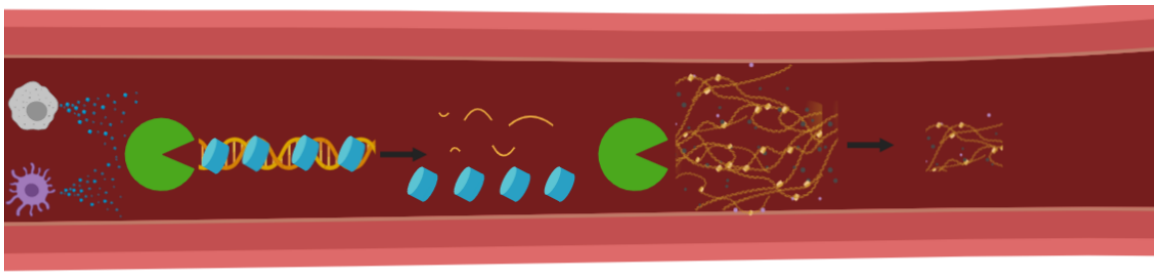

C.

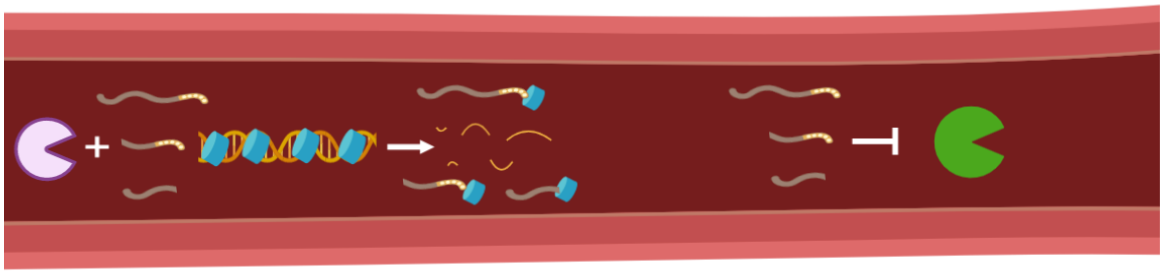

5.0 Future Studies

In this study, we have measured the levels of DNase I and DNase1L3 in septic patients in a longitudinal manner (days 1, 3, 7, 14, 21, and 28). The patients included in our experiments were part of our DYNAMICS study, which is a prospective, multi-centre observational study. We measured DNase I and DNase1L3 antigen levels of both septic survivors and non-survivors admitted to the ICU, and compared these values to healthy controls. Future studies can measure DNase I and DNase1L3 levels in non-septic ICU patients as an additional control using a sandwich ELISA. These experiments would address whether the significant reduction in DNase I levels compared to healthy controls are specific to sepsis, or a general characteristic of patients admitted to the ICU. Similarly, these future studies would reveal whether the significant increase in DNase1L3 levels compared to healthy controls are specific to sepsis, or general to patients in the ICU. Immune cells, especially dendritic cells and macrophages, secrete DNase1L3; therefore, it would be interesting to determine if the elevated levels of DNase1L3 are common to diseases with a state of increased inflammation. These studies can potentially inform and direct future management of patients in the ICU, and determine which patients would most benefit from DNase I treatment. In addition to measuring the levels of DNase I and DNase1L3 in non-septic ICU patients, future studies can also measure the levels of these endonucleases in patients in the emergency room as another control using a sandwich ELISA. These results would determine whether the decrease in DNase I levels and increase in DNase1L3 levels are correlated with sickness severity. The therapeutic potential of

DNase I may also benefit patients in the emergency room if we determine that there is a significant reduction of this endonuclease.

We have found that the levels of DNase I are significantly decreased in septic patients. To better understand the mechanisms by which this endonuclease is decreased, future studies can measure the levels of actin, the only known inhibitor of DNase I, in these septic patients using an ELISA. This experiment can explain if the levels of DNase I are caused by an elevation in actin levels due to cell death that occurs in sepsis, or if there is another explanation, such as impaired secretion of DNase I due to organ damage, or a consumption of this endonuclease in response to degrading the increased levels of DNA.

Existing literature states that DNase I is unable to cleave DNA that is bound to protein in the absence of either a serine protease or UFH. Our studies revealed that enoxaparin and Vasoflux are also able to help DNase I degrade DNA-protein complexes in a purified system. Interestingly, we have shown that DNase I can degrade NETs on its own, most likely down to individual nucleosomes. The decondensation of chromatin that occurs by PAD4 during NETosis, which weakens the DNA-histone interactions, may explain why DNase I can degrade NETs but not nucleosomes. The linker region between nucleosomes might become more open and accessible to DNase I during decondensation, thereby allowing DNase I to cleave this site. To test this hypothesis, future studies can repeat our purified experiments, but modify the histones *in vitro* with PAD4 to form looser DNA-histone complexes to see if DNase I can degrade the complexes.

Our preliminary studies reveal that UFH, enoxaparin, and Vasoflux can inhibit the activity of DNase1L3, but fondaparinux does not. Future studies can repeat the agarose gel

experiments using lower concentrations of the different GAGs in the presence of DNase1L3 to determine how a titration of GAGs affect the activity of DNase1L3.

Lastly, future studies can determine the K_D values between histones H2B, H3, and H4 with fondaparinux using the OctetRED384 System (FortéBio, Fremont, CA). Similar to the BLITz, the OctetRED384 also uses BLI technology to determine binding affinities between molecules; however, the OctetRed384 is able to determine binding affinities of smaller molecules (as small as 150 Da), such as fondaparinux (1.7 kDa), with greater accuracy than the BLITz. Using the OctetRED384 can overcome the limitations of the BLITz that we encountered when finding the interactions with histones and fondaparinux. Our preliminary results show that fondaparinux has low affinity for histone H2A (Table 2), and we will confirm this by finding the remaining K_D values using the OctetRED384. Histones H2B, H3, and H4 will be biotinylated and immobilized to a streptavidin-coated biosensor. Different concentrations of the analyte, fondaparinux, will be added to the solution. The binding interactions between the histones and fondaparinux will be measured in real-time using BLI technology, as described above in section 2.0.13. These experiments will allow us to better understand why fondaparinux is unable to assist with DNase I-mediated degradation of DNA-histone complexes. GAGs appear to enhance the activity of DNase I for DNA-histone complexes by binding to histones and displacing them from DNA, thereby allowing DNase I to gain access to DNA-cleavage sites. Additionally, our findings suggest that the cofactor activity of GAGs is size-dependent and does not require the AT-binding region, which will be further confirmed by determining the remaining K_D values of fondaparinux and histones.

6.0 References

Abrams, S. T., Zhang, N., Dart, C., Wang, S. S., Thachil, J., Guan, Y., Wang, G., & Toh, C.-H. (2013). Human CRP Defends against the Toxicity of Circulating Histones. *The Journal of Immunology*, *191*(5), 2495–2502.

Al-Mayouf, S. M., Sunker, A., Abdwani, R., Abrawi, S. Al, Almurshedi, F., Alhashmi, N., Al Sonbul, A., Sewairi, W., Qari, A., Abdallah, E., Al-Owain, M., Al Motywee, S., Al-Rayes, H., Hashem, M., Khalak, H., Al-Jebali, L., & Alkuraya, F. S. (2011). Loss-of-function variant in DNASE1L3 causes a familial form of systemic lupus erythematosus. *Nature Genetics*, *43*(12), 1186–1188.

Ammollo, C. T., Semeraro, F., Xu, J., Esmon, N. L., & Esmon, C. T. (2011). Extracellular histones increase plasma thrombin generation by impairing thrombomodulin-dependent protein C activation. *Journal of Thrombosis and Haemostasis*, *9*(9), 1795–1803.

Bajzar, L. (2000). Thrombin Activatable Fibrinolysis Inhibitor and an Antifibrinolytic Pathway. *Arteriosclerosis, Thrombosis, and Vascular Biology*, *20*(12), 2511–2518.

Barliya, T., Dardik, R., Nisgav, Y., Dachbash, M., Gaton, D., Kenet, G., Ehrlich, R., Weinberger, D., & Livnat, T. (2017). Possible involvement of NETosis in inflammatory processes in the eye: Evidence from a small cohort of patients. *Molecular Vision*, *23*, 922–932.

Barranco-Medina, S., Pozzi, N., Vogt, A. D., & Di Cera, E. (2013). Histone H4 promotes prothrombin autoactivation. *Journal of Biological Chemistry*, *288*(50), 35749–35757.

Barthel, S. R., Gavino, J. D., Descheny, L., & Dimitroff, C. J. (2007). Targeting selectins and selectin ligands in inflammation and cancer. *Expert Opinion on Therapeutic Targets*, *11*(11), 1473–1491.

Bernard, G. R., Vincent, J. L., Laterre, P. F., LaRosa, S. P., Dhainaut, J. F., Lopez-Rodriguez, A., Steingrub, J. S., Garber, G. E., Helterbrand, J. D., Ely, E. W., & Fisher, C. J. (2001). Efficacy and safety of recombinant human activated protein C for severe sepsis. *New England Journal of Medicine*, *344*(10), 699–709.

Blair, P., & Flaumenhaft, R. (2009). Platelet α-granules: Basic biology and clinical correlates. *Blood Reviews*, *23*(4), 177–189.

Bock, S. C., Wion, L. L., Vehar, G. A., Lawn, R. M., & Bock, S. C. (1982). Cloning and expression of the cDNA for human antithrom, bin III. *Nucleic Acids Research*, *10*(24), 8113–8125.

Bouma, B. N., & Mosnier, L. O. (2006). Thrombin activatable fibrinolysis inhibitor (TAFI)—How does thrombin regulate fibrinolysis? *Annals of Medicine*, *38*(6), 378–388.

Bounameaux, H. (1998). Unfractionated versus low-molecular-weight heparin in the treatment of venous thromboembolism. *Vascular Medicine*, *3*(1), 41–46.

Brinkmann, V., Reichard, U., Goosmann, C., Fauler, B., Uhlemann, Y., Weiss, D. S., Weinrauch, Y., & Zychlinsky, A. (2004). Neutrophil Extracellular Traps Kill Bacteria. *Science*, *303*(5663), 1532–1535.

Bronkhorst, A. J., Ungerer, V., & Holdenrieder, S. (2019). The emerging role of cell-free DNA as a molecular marker for cancer management. *Biomolecular Detection and Quantification*, *17*, 1–14.

Butenas, S., Bouchard, B. A., Brummel-Ziedins, K. E., Parhami-Seren, B., & Mann, K. G. (2005). Tissue factor activity in whole blood. *Blood*, *105*(7), 2764–2770.

Canadian Sepsis Foundation. (2019). https://canadiansepsisfoundation.ca/Understanding-Sepsis

Canales, J. F., & Ferguson, J. J. (2008). Low-molecular-weight heparins : mechanisms, trials, and role in contemporary interventional medicine. *American Journal of Cardiovascular Drugs : Drugs, Devices, and Other Interventions*, *8*, 15–25.

Cesarman-Maus, G., & Hajjar, K. A. (2005). Molecular mechanisms of fibrinolysis. *British Journal of Haematology*, *129*, 307–321.

Chapin, J. C., & Hajjar, K. A. (2015). Fibrinolysis and the control of blood coagulation. *Blood Reviews*, *29*(1), 17–24.

Chen, Q. X., Ye, L., Jin, Y. H., Zhang, N., Lou, T. Z., Qiu, Z. L., Jin, Y., Cheng, B. L., & Fang, X. M. (2012). Circulating nucleosomes as a predictor of sepsis and organ dysfunction in critically ill patients. *International Journal of Infectious Diseases*, *16*(7), 558–564.

Chen, Y., Yuan, Y., & Li, W. (2018). Sorting machineries: How platelet-dense granules differ from α-granules. *Bioscience Reports*, *38*(5), 1–9.

Chernysh, I. N., Nagaswami, C., Purohit, P. K., & Weisel, J. W. (2012). Fibrin clots are equilibrium polymers that can be remodeled without proteolytic digestion. *Scientific Reports*, *2*(1), 1–6.

Choay, J., Lormeau, J. C., Petitou, M., Sinaÿ, P., & Fareed, J. (1981). Structural studies on a biologically active hexasaccharide obtained from heparin. *Annals of the New York Academy of Sciences*, *370*, 644–649.

Clark, S. R., Ma, A. C., Tavener, S. A., McDonald, B., Goodarzi, Z., Kelly, M. M., Patel, K. D., Chakrabarti, S., McAvoy, E., Sinclair, G. D., Keys, E. M., Allen-Vercoe, E., DeVinney, R., Doig, C. J., Green, F. H. Y., & Kubes, P. (2007). Platelet TLR4 activates neutrophil extracellular traps to ensnare bacteria in septic blood. *Nature Medicine*, *13*(4), 463–469.

Conners, M. S., & Money, S. R. (2002). The new heparins. *The Ochsner Journal*, *4*, 41–47.

Dager, W. E., Andersen, J., & Nutescu, E. (2004). Special considerations with fondaparinux therapy: Heparin-induced thrombocytopenia and wound healing. *Pharmacotherapy*, *24*, 88–94.

Dahlback, B. (2005). Blood coagulation and its regulation by anticoagulant pathways: genetic pathogenesis of bleeding and thrombotic diseases. *Journal of Internal Medicine*, *257*(3), 209–223.

Davis, J. C., Manzi, S., Yarboro, C., Rairie, J., McInnes, I., Averthelyi, D., Sinicropi, D., Hale, V. G., Balow, J., Austin, H., Boumpas, D. T., & Klippel, J. H. (1999). Recombinant human Dnase I (rhDNase) in patients with lupus nephritis. *Lupus*, *8*(1), 68–76.

de Bont, C. M., Boelens, W. C., & Pruijn, G. J. M. (2019, January 1). NETosis, complement, and coagulation: a triangular relationship. In *Cellular and Molecular Immunology*. Chinese Soc Immunology.

Decker, P., Wolburg, H., & Rammensee, H. G. (2003). Nucleosomes induce lymphocyte necrosis. *European Journal of Immunology*, *33*(7), 1978–1987.

Dekker, L. V, Leitges, M., Altschuler, G., Mistry, N., McDermott, A., Roes, J., & Segal, A. W. (2000). Protein kinase C-beta contributes to NADPH oxidase activation in neutrophils. *Biochemical Journal*, *347*(1), 285.

Denning, N. L., Aziz, M., Gurien, S. D., & Wang, P. (2019). Damps and nets in sepsis. *Frontiers in Immunology*, *10*(2536), 1–15.

Dennis Lo, Y. M., Zhang, J., Leung, T. N., Lau, T. K., Chang, A. M. Z., & Magnus Hjelm, N. (1999). Rapid clearance of fetal DNA from maternal plasma. *American Journal of Human Genetics*, *64*(1), 218–224.

Dolin, H. H., Papadimos, T. J., Chen, X., & Pan, Z. K. (2019). Characterization of Pathogenic Sepsis Etiologies and Patient Profiles: A Novel Approach to Triage and Treatment. *Microbiology Insights*, *12*(1), 1–8.

Döring, Y., Libby, P., & Soehnlein, O. (2020). Neutrophil Extracellular Traps Participate in Cardiovascular Diseases. *Circulation Research*, *126*(9), 1228–1241.

Downing, L. J., Strieter, R. M., Kadell, A. M., Wilke, C. A., Greenfield, L. J., & Wakefield, T. W. (1998). Low-dose low-molecular-weight heparin is anti-inflammatory during venous thrombosis. *Journal of Vascular Surgery*, *28*(5), 848–854.

Durrant, T. N., Van Den Bosch, M. T., & Hers, I. (2017). Integrin αIIbβ3 outside-in signaling. *Blood*, *130*(14), 1607–1619.

Dwivedi, D. J., Toltl, L. J., Swystun, L. L., Pogue, J., Liaw, K.-L., Weitz, J. I., Cook, D. J., Fox-Robichaud, A. E., Liaw, P. C., & Canadian Critical Care Translational Biology Group. (2012). Prognostic utility and characterization of cell-free DNA in patients with severe sepsis. *Critical Care (London, England)*, *16*(4), R151.

Ernofsson, M., Thelin, S., & Siegbahn, A. (1997). Monocyte tissue factor expression, cell activation, and thrombin formation during cardiopulmonary bypass: A clinical study. *Journal of Thoracic and Cardiovascular Surgery*, *113*(3), 576–584.

Esmon, C. T. (2003). The protein C pathway. *Chest*, *124*(3), 26S-32S.

Estevez, B., & Du, X. (2017). New Concepts and Mechanisms of Platelet Activation Signaling. *Physiology*, *32*(2), 162–177.

Fan, Y., Jiang, M., Gong, D., & Zou, C. (2016). Efficacy and safety of low-molecular-weight heparin in patients with sepsis: A meta-analysis of randomized controlled trials. *Scientific Reports*, *6*(1), 1–8.

Farrera, C., & Fadeel, B. (2013). Macrophage Clearance of Neutrophil Extracellular Traps Is a Silent Process. *The Journal of Immunology*, *191*(5), 2647–2656.

Foley, J. H., & Conway, E. M. (2016). Cross Talk Pathways between Coagulation and Inflammation. *Circulation Research*, *118*(9), 1392–1408.

Franck, G., Mawson, T. L., Folco, E. J., Molinaro, R., Ruvkun, V., Engelbertsen, D., Liu, X., Tesmenitsky, Y., Shvartz, E., Sukhova, G. K., Michel, J. B., Nicoletti, A., Lichtman, A., Wagner, D., Croce, K. J., & Libby, P. (2018). Roles of PAD4 and netosis in experimental atherosclerosis and arterial injury implications for superfcial erosion. *Circulation Research*, *123*(1), 33–42.

Frank, R. D., Schabbauer, G., Holscher, T., Sato, Y., Tencati, M., Pawlinski, R., & Mackman, N. (2005). The synthetic pentasaccharide fondaparinux reduces coagulation, inflammation and neutrophil accumulation in kidney ischemia-reperfusion injury. *Journal of Thrombosis and Haemostasis*, *3*(3), 531–540.

Fraser, S. R., Booth, N. A., & Mutch, N. J. (2011). The antifibrinolytic function of factor XIII is exclusively expressed through α2-antiplasmin cross-linking. *Blood*, *117*(23), 6371–6374.

Fredenburgh, J. C., & Nesheim, M. E. (1992). Lys-plasminogen is a significant intermediate in the activation of Glu-plasminogen during fibrinolysis in vitro. *The Journal of Biological Chemistry*, *267*(36), 26150–26156. http://www.ncbi.nlm.nih.gov/pubmed/1464625

Fuchs, T. A., Abed, U., Goosmann, C., Hurwitz, R., Schulze, I., Wahn, V., Weinrauch, Y., Brinkmann, V., & Zychlinsky, A. (2007). Novel cell death program leads to neutrophil extracellular traps. *Journal of Cell Biology*, *176*(2), 231–241.

Fuchs, T. A., Bhandari, A. A., & Wagner, D. D. (2011). Histones induce rapid and profound thrombocytopenia in mice. *Blood*, *118*(13), 3708–3714.

Gaertner, F., & Massberg, S. (2016). Blood coagulation in immunothrombosis—At the frontline of intravascular immunity. *Seminars in Immunology*, *28*(6), 561–569.

Gailani, D., & Renné, T. (2007). The intrinsic pathway of coagulation: a target for treating thromboembolic disease? *Journal of Thrombosis and Haemostasis*, *5*(6), 1106–1112.

Gando, S. (2013). Role of fibrinolysis in sepsis. *Seminars in Thrombosis and Hemostasis*, *39*(4), 392–399.

Gauthier, V. J., Tyler, L. N., & Mannik, M. (1996). Blood clearance kinetics and liver uptake of mononucleosomes in mice. *Journal of Immunology*, *156*(3), 1151–1156.

http://www.ncbi.nlm.nih.gov/pubmed/8557992

Giaglis, S., Hahn, S., & Hasler, P. (2016). "The NET outcome": Are neutrophil extracellular traps of any relevance to the pathophysiology of autoimmune disorders in childhood? *Frontiers in Pediatrics*, *4*(97), 1–8.

Giansily-Blaizot, M., & Schved, J.-F. (2017). Recombinant human factor VIIa (rFVIIa) in hemophilia: mode of action and evidence to date. *Therapeutic Advances in Hematology*, *8*(12), 345–352.

Goldhaber, S. Z. (2012). Venous thromboembolism: Epidemiology and magnitude of the problem. *Best Practice and Research: Clinical Haematology*, *25*(3), 235–242.

Gould, T. J., Lysov, Z., & Liaw, P. C. (2015). Extracellular DNA and histones: Double-edged swords in immunothrombosis. *Journal of Thrombosis and Haemostasis*, *13*(1), S82–S91.

Gould, T. J., Lysov, Z., Swystun, L. L., Dwivedi, D. J., Zarychanski, R., Fox-Robichaud, A. E., Liaw, P. C., & Group, C. C. C. T. B. (2016). Extracellular Histones Increase Tissue Factor Activity and Enhance Thrombin Generation by Human Blood Monocytes. *Shock*, *46*(6), 655–662.

Gould, T. J., Vu, T. T., Stafford, A. R., Dwivedi, D. J., Kim, P. Y., Fox-Robichaud, A. E., Weitz, J. I., & Liaw, P. C. (2015). Cell-Free DNA Modulates Clot Structure and Impairs Fibrinolysis in Sepsis. *Arteriosclerosis, Thrombosis, and Vascular Biology*, *35*(12), 2544–2553.

Gould, T. J., Vu, T. T., Swystun, L. L., Dwivedi, D. J., Mai, S. H. C., Weitz, J. I., & Liaw, P. C. (2014). Neutrophil extracellular traps promote thrombin generation through platelet-dependent and platelet-independent mechanisms. *Arteriosclerosis, Thrombosis, and Vascular Biology*, *34*(9), 1977–1984.

Griffin, J. H., Fernandez, J. A., Gale, A. J., & Mosnier, L. O. (2007). Activated protein C. *Journal of Thrombosis and Haemostasis*, *5*(1), 73–80.

Guan, Y., Xu, X., Liu, X., Sheng, A., Jin, L., Linhardt, R. J., & Chi, L. (2016). Comparison of Low-Molecular-Weight Heparins Prepared From Bovine Lung Heparin and Porcine Intestine Heparin. *Journal of Pharmaceutical Sciences*, *105*(6), 1843–1850.

Guéroult, M., Picot, D., Abi-Ghanem, J., Hartmann, B., & Baaden, M. (2010). How Cations Can Assist DNase I in DNA Binding and Hydrolysis. *PLoS Computational Biology*, *6*(11), 1–11.

Guitton, C., Gérard, N., Sébille, V., Bretonnière, C., Zambon, O., Villers, D., & Charreau, B. (2011). Early rise in circulating endothelial protein C receptor correlates with poor outcome in severe sepsis. *Intensive Care Medicine*, *37*(6), 950–956.

Gyawali, B., Ramakrishna, K., & Dhamoon, A. S. (2019). Sepsis: The evolution in definition, pathophysiology, and management. *SAGE Open Medicine*, *7*(1), 1–13.

Hajjar, K. A., & Nachman, R. L. (1988). Endothelial cell-mediated conversion of Glu-

plasminogen to Lys-plasminogen. Further evidence for assembly of the fibrinolytic system on the endothelial cell surface. *J Clin Invest*, *82*(5), 1769.

Harter, K., Levine, M., & Henderson, S. O. (2015). Anticoagulation drug therapy: A review. *Western Journal of Emergency Medicine*, *16*, 11–17.

Haynes, L. M., Dubief, Y. C., & Mann, K. G. (2012). Membrane binding events in the initiation and propagation phases of tissue factor-initiated zymogen activation under flow. *Journal of Biological Chemistry*, *287*(8), 5225–5234.

Healy, L. D., Puy, C., Fernández, J. A., Mitrugno, A., Keshari, R. S., Taku, N. A., Chu, T. T., Xu, X., Gruber, A., Lupu, F., Griffin, J. H., & McCarty, O. J. T. (2017). Activated protein C inhibits neutrophil extracellular trap formation in vitro and activation in vivo. *The Journal of Biological Chemistry*, *292*(21), 8616–8629.

Hepner, M., & Karlaftis, V. (2013). Antithrombin BT - Haemostasis: Methods and Protocols. *Methods in Molecular Biology*, *992*(1), 355–364.

Hirsh, J., Dalen, J. E., Deykin, D., & Toller, L. (1992). Heparin: Mechanism of Action, Pharmacokinetics, Dosing Considerations, Monitoring, Efficacy, and Safety. *Chest*, *102*(4), 337S-351S.

Houston, B. L., Dwivedi, D. J., Grin, P., Kwong, M., Rullo, E., Khan, M. A., Asma, S., Pare, G., Liaw, P. C., Zarychanski, R., & Fox-Robichaud, A. E. (2015). Biological Rational for the Use of Heparin in Septic Shock: Translational Data from the Halo Pilot RCT. *Blood*, *126*(23), 2336–2336.

Iba, T., Hashiguchi, N., Nagaoka, I., Tabe, Y., Kadota, K., & Sato, K. (2015). Heparins attenuated histone-mediated cytotoxicity in vitro and improved the survival in a rat model of histone-induced organ dysfunction. *Intensive Care Medicine Experimental*, *3*(1), 1–11.

Iba, T., Watanabe, E., Umemura, Y., Wada, T., Hayashida, K., Kushimoto, S., & Wada, H. (2019). Sepsis-associated disseminated intravascular coagulation and its differential diagnoses. *Journal of Intensive Care*, *7*(1), 1–13.

Ibbotson, T., & Goa, K. L. (2002). Enoxaparin: an update of its clinical use in the management of acute coronary syndromes. *Drugs*, *62*, 1407–1430.

Jackson, S. P. (2007). The growing complexity of platelet aggregation. *Blood*, *109*(12), 5087–5095.

Jiménez-Alcázar, M., Rangaswamy, C., Panda, R., Bitterling, J., Simsek, Y. J., Long, A. T., Bilyy, R., Krenn, V., Renné, C., Renné, T., Kluge, S., Panzer, U., Mizuta, R., Mannherz, H. G., Kitamura, D., Herrmann, M., Napirei, M., & Fuchs, T. A. (2017). Host DNases prevent vascular occlusion by neutrophil extracellular traps. *Science*, *358*(6367), 1202–1206.

Jin, L., Abrahams, J. P., Skinner, R., Petitou, M., Pike, R. N., & Carrell, R. W. (1997). The anticoagulant activation of antithrombin by heparin. *Proceedings of the National Academy of Sciences of the United States of America*, *94*(26), 14683–14688.

Jones, S. J., Worrall, A. F., & Connolly, B. A. (1996). Site-directed mutagenesis of the catalytic residues of bovine pancreatic deoxyribonuclease I. *Journal of Molecular Biology*, *264*(5), 1154–1163.

Jorch, S. K., & Kubes, P. (2017). An emerging role for neutrophil extracellular traps in noninfectious disease. *Nature Medicine*, *23*(3), 279–287.

Kaplan, M. J., & Radic, M. (2012). Neutrophil Extracellular Traps: Double-Edged Swords of Innate Immunity. *The Journal of Immunology*, *189*(6), 2689–2695.

Kempker, J. A., & Martin, G. S. (2020). A global accounting of sepsis. *The Lancet*, *395*(10219), 168–170.

Keshari, R. S., Silasi, R., Popescu, N. I., Georgescu, C., Chaaban, H., Lupu, C., McCarty, O. J. T., Esmon, C. T., & Lupu, F. (2020). Fondaparinux pentasaccharide reduces sepsis coagulopathy and promotes survival in the baboon model of Escherichia coli sepsis. *Journal of Thrombosis and Haemostasis*, *18*(1), 180–190.

Keyel, P. A. (2017). Dnases in health and disease. *Developmental Biology*, *429*(1), 1–11.

Lakshmikanth, C. L., Jacob, S. P., Chaithra, V. H., de Castro-Faria-Neto, H. C., & Marathe, G. K. (2016). Sepsis: in search of cure. *Inflammation Research*, *65*(8), 587–602.

Lauková, L., Konečná, B., Bábíčková, J., Wagnerová, A., Melišková, V., Vlková, B., & Celec, P. (2017). Exogenous deoxyribonuclease has a protective effect in a mouse model of sepsis. *Biomedicine and Pharmacotherapy*, *93*, 8–16.

Lechtenberg, B. C., Murray-Rust, T. A., Johnson, D. J. D., Adams, T. E., Krishnaswamy, S., Camire, R. M., & Huntington, J. A. (2013). Crystal structure of the prothrombinase complex from the venom of Pseudonaja textilis. *Blood*, *122*(16), 2777–2783.

Levi, M., van der Poll, T., & Schultz, M. (2012). Infection and inflammation as risk factors for thrombosis and atherosclerosis. *Seminars in Thrombosis and Hemostasis*, *38*(5), 506–514.

Ley, K., Rivera-Nieves, J., Sandborn, W. J., & Shattil, S. (2016). Integrin-based therapeutics: Biological basis, clinical use and new drugs. *Nature Reviews Drug Discovery*, *15*(3), 173–183.

Li, X., & Ma, X. (2017). The role of heparin in sepsis: much more than just an anticoagulant. *British Journal of Haematology*, *179*(3), 389–398.

Liaw, P. C., Fox-Robichaud, A. E., Liaw, K.-L., McDonald, E., Dwivedi, D. J., Zamir, N. M., Pepler, L., Gould, T. J., Xu, M., Zytaruk, N., Medeiros, S. K., McIntyre, L., Tsang, J., Dodek, P. M., Winston, B. W., Martin, C., Fraser, D. D., Weitz, J. I., Lellouche, F., … Marshall, J. (2019). Mortality Risk Profiles for Sepsis. *Critical Care Explorations*, *1*(8), e0032.

Longstaff, C., & Kolev, K. (2015). Basic mechanisms and regulation of fibrinolysis. *Journal of Thrombosis and Haemostasis*, *13*(S1), S98–S105.

Longstaff, Colin, Hogwood, J., Gray, E., Komorowicz, E., Varjú, I., Varga, Z., & Kolev, K. (2016). Neutralisation of the anti-coagulant effects of heparin by histones in blood plasma and purified systems. *Thrombosis and Haemostasis*, *115*(3), 591–599.

Lood, C., Blanco, L. P., Purmalek, M. M., Carmona-Rivera, C., De Ravin, S. S., Smith, C. K., Malech, H. L., Ledbetter, J. A., Elkon, K. B., & Kaplan, M. J. (2016). Neutrophil extracellular traps enriched in oxidized mitochondrial DNA are interferogenic and contribute to lupus-like disease. *Nature Medicine*, *22*(2), 146–153.

Loof, T. G., Deicke, C., & Medina, E. (2014). The role of coagulation/fibrinolysis during infection. *Front Cell Infect Microbiol*, *4*(1), 128.

Mackman, N., Tilley, R. E., & Key, N. S. (2007). Role of the extrinsic pathway of blood coagulation in hemostasis and thrombosis. *Arteriosclerosis, Thrombosis, and Vascular Biology*, *27*(8), 1687–1693.

Mai, S. H. C., Khan, M., Dwivedi, D. J., Ross, C. A., Zhou, J., Gould, T. J., Gross, P. L., Weitz, J. I., Fox-Robichaud, A. E., & Liaw, P. C. (2015). Delayed but not early treatment with dnase reduces organ damage and improves outcome in a murine model of sepsis. *Shock*, *44*(2), 166–172.

Malíčková, K., Ďuricová, D., Bortlík, M., Hrušková, Z., Svobodová, B., Machková, N., Komárek, V., Fučíková, T., Janatková, I., Zima, T., & Lukáš, M. (2011). Impaired Deoxyribonuclease I Activity in Patients with Inflammatory Bowel Diseases. *Autoimmune Diseases*, *2011*(1), 1–5.

Mannherz, H. G., Peitsch, M. C., Zanotti, M. C., Paddenberg, R., & Polzar, B. (1995). A new function for an old enzyme: The role of DNase I in apoptosis. *Current Topics in Microbiology and Immunology*, *198*(2), 161–174.

Mariño-Ramírez, L., Kann, M. G., Shoemaker, B. A., & Landsman, D. (2005). Histone structure and nucleosome stability. *Expert Review of Proteomics*, *2*(5), 719–729.

Markiewski, M. M., Deangelis, R. A., & Lambris, J. D. (2008). Complexity of complement activation in sepsis: Crossroads in Sepsis Research Review Series. *Journal of Cellular and Molecular Medicine*, *12*(6), 2245–2254.

Maroney, S. A., Ellery, P. E., Wood, J. P., Ferrel, J. P., Martinez, N. D., & Mast, A. E. (2013). Comparison of the inhibitory activities of human tissue factor pathway inhibitor (TFPI)α and TFPIβ. *Journal of Thrombosis and Haemostasis*, *11*(5), 911–918.

Marsman, G., Zeerleder, S., & Luken, B. M. (2016). Extracellular histones, cell-free DNA, or nucleosomes: Differences in immunostimulation. *Cell Death and Disease*, *7*(12), 2518–2527.

Martinod, K., Demers, M., Fuchs, T. A., Wong, S. L., Brill, A., Gallant, M., Hu, J., Wang, Y., & Wagner, D. D. (2013). Neutrophil histone modification by peptidylarginine deiminase 4 is critical for deep vein thrombosis in mice. *Proceedings of the National Academy of Sciences of the United States of America*,

110(21), 8674–8679.

Massberg, S., Grahl, L., Von Bruehl, M. L., Manukyan, D., Pfeiler, S., Goosmann, C., Brinkmann, V., Lorenz, M., Bidzhekov, K., Khandagale, A. B., Konrad, I., Kennerknecht, E., Reges, K., Holdenrieder, S., Braun, S., Reinhardt, C., Spannagl, M., Preissner, K. T., & Engelmann, B. (2010). Reciprocal coupling of coagulation and innate immunity via neutrophil serine proteases. *Nature Medicine*, *16*(8), 887–896.

Mast, A. E. (2016). Tissue Factor Pathway Inhibitor: Multiple Anticoagulant Activities for a Single Protein. *Arteriosclerosis, Thrombosis, and Vascular Biology*, *36*(1), 9–14.

McCord, J. J., Harsini, F., Sutton, R. B., & Keyel, P. A. (2018). Structural characteristics of the serum endonuclease Dnase1L3. *The Journal of Immunology*, *200*(1 Supplement), 100.

McCoy, A. J., Pei, X. Y., Skinner, R., Abrahams, J. P., & Carrell, R. W. (2003). Structure of beta-antithrombin and the effect of glycosylation on antithrombin's heparin affinity and activity. *Journal of Molecular Biology*, *326*(3), 823–833.

McCoy, K., Hamilton, S., & Johnson, C. (1996). Effects of 12-week administration of dornase alfa in patients with advanced cystic fibrosis lung disease. *Chest*, *110*(4), 889–895.

McDonald, B., Davis, R. P., Kim, S. J., Tse, M., Esmon, C. T., Kolaczkowska, E., & Jenne, C. N. (2017). Platelets and neutrophil extracellular traps collaborate to promote intravascular coagulation during sepsis in mice. *Blood*, *129*(10), 1357–1367.

Meneghetti, M. C. Z., Hughes, A. J., Rudd, T. R., Nader, H. B., Powell, A. K., Yates, E. A., & Lima, M. A. (2015). Heparan sulfate and heparin interactions with proteins. *Journal of the Royal Society Interface*, *12*(110), 1–13.

Metzler, K. D., Fuchs, T. A., Nauseef, W. M., Reumaux, D., Roesler, J., Schulze, I., Wahn, V., Papayannopoulos, V., & Zychlinsky, A. (2011). Myeloperoxidase is required for neutrophil extracellular trap formation: Implications for innate immunity. *Blood*, *117*(3), 953–959.

Metzler, K. D., Goosmann, C., Lubojemska, A., Zychlinsky, A., & Papayannopoulos, V. (2014). Myeloperoxidase-containing complex regulates neutrophil elastase release and actin dynamics during NETosis. *Cell Reports*, *8*(3), 883–896.

Minami, T., Sugiyama, A., Wu, S. Q., Abid, R., Kodama, T., & Aird, W. C. (2004). Thrombin and Phenotypic Modulation of the Endothelium. *Arteriosclerosis, Thrombosis, and Vascular Biology*, *24*(1), 41–53.

Moss, J., Magenheim, J., Neiman, D., Zemmour, H., Loyfer, N., Korach, A., Samet, Y., Maoz, M., Druid, H., Arner, P., Fu, K. Y., Kiss, E., Spalding, K. L., Landesberg, G., Zick, A., Grinshpun, A., Shapiro, A. M. J., Grompe, M., Wittenberg, A. D., … Dor, Y. (2018). Comprehensive human cell-type methylation atlas reveals origins of

circulating cell-free DNA in health and disease. *Nature Communications*, *9*(1), 1–12.

Müller, F., Gailani, D., & Renné, T. (2011). Factor XI and XII as antithrombotic targets. *Current Opinion in Hematology*, *18*(5), 349–355.

Mulloy, B., Hogwood, J., Gray, E., Lever, R., & Page, C. P. (2015). Pharmacology of Heparin and Related Drugs. *Pharmacological Reviews*, *68*, 76–141.

Nadano, D., Yasuda, T., & Kishi, K. (1993). Measurement of deoxyribonuclease I activity in human tissues and body fluids by a single radial enzyme-diffusion method. *Clinical Chemistry*, *39*(3), 448–452.

Napirei, M., Karsunky, H., Zevnik, B., Stephan, H., Mannherz, H. G., & Möröy, T. (2000). Features of systemic lupus erythematosus in Dnase1-deficient mice. *Nature Genetics*, *25*(2), 177–181.

Napirei, M., Ludwig, S., Mezrhab, J., Klöckl, T., & Mannherz, H. G. (2009). Murine serum nucleases - contrasting effects of plasmin and heparin on the activities of DNase1 and DNase1-like 3 (DNase1l3). *The FEBS Journal*, *276*(4), 1059–1073.

Napirei, M., Wulf, S., Eulitz, D., Mannherz, H. G., & Kloeckl, T. (2005). Comparative characterization of rat deoxyribonuclease 1 (Dnase1) and murine deoxyribonuclease 1-like 3 (Dnase1l3). *The Biochemical Journal*, *389*(2), 355–364.

Narayanan, S. (1999). Multifunctional roles of thrombin. *Annals of Clinical and Laboratory Science*, *29*(4), 275–280.

Neeli, I., Khan, S. N., & Radic, M. (2008). Histone Deimination As a Response to Inflammatory Stimuli in Neutrophils. *The Journal of Immunology*, *180*(3), 1895–1902.

Ni, H., & Freedman, J. (2003). Platelets in hemostasis and thrombosis: Role of integrins and their ligands. *Transfusion and Apheresis Science*, *28*(3), 257–264.

Oefner, C., & Suck, D. (1986). Crystallographic refinement and structure of DNase I at 2 Å resolution. *Journal of Molecular Biology*, *192*(3), 605–632.

Okamoto, K., Tamura, T., & Sawatsubashi, Y. (2016). Sepsis and disseminated intravascular coagulation. *Journal of Intensive Care*, *4*(1), 1–23.

Onuora, S. (2016). Autoimmunity: DNASE1L3 prevents anti-DNA responses. *Nature Reviews Rheumatology*, *12*(8), 437.

Palta, S., Saroa, R., & Palta, A. (2014). Overview of the coagulation system. *Indian Journal of Anaesthesia*, *58*, 515–523.

Pan, C. Q., Ulmer, J. S., Herzka, A., & Lazarus, R. A. (1998). Mutational analysis of human DNase I at the DNA binding interface: Implications for DNA recognition, catalysis, and metal ion dependence. *Protein Science*, *7*(3), 628–636.

Pannekoek, H., Veerman, H., Lambers, H., Diergaarde, P., Verweij, C. L., van Zonneveld, A. J., & van Mourik, J. A. (1986). Endothelial plasminogen activator inhibitor (PAI): a new member of the Serpin gene family. *The EMBO Journal*, *5*(10), 2539–2544.

Paolucci, F., Claviés, M.-C., Donat, F., & Necciari, J. (2002). Fondaparinux sodium mechanism of action: identification of specific binding to purified and human plasma-derived proteins. *Clinical Pharmacokinetics*, *41*, 11–18.

Papayannopoulos, V., Metzler, K. D., Hakkim, A., & Zychlinsky, A. (2010). Neutrophil elastase and myeloperoxidase regulate the formation of neutrophil extracellular traps. *Journal of Cell Biology*, *191*(3), 677–691.

Paschoa, A. F. (2016). Heparin: 100 years of pleiotropic effects. *Journal of Thrombosis and Thrombolysis*, *41*, 636–643.

Perry, D. J. (1994). Antithrombin and its inherited deficiencies. *Blood Reviews*, *8*(1), 37–55.

Pryzdial, E. L. G., Lee, F. M. H., Lin, B. H., Carter, R. L. R., Tegegn, T. Z., & Belletrutti, M. J. (2018). Blood coagulation dissected. *Transfusion and Apheresis Science : Official Journal of the World Apheresis Association : Official Journal of the European Society for Haemapheresis*, *57*, 449–457.

Reinhart, K., Daniels, R., Kissoon, N., Machado, F. R., Schachter, R. D., & Finfer, S. (2017). Recognizing Sepsis as a Global Health Priority — A WHO Resolution. *New England Journal of Medicine*, *377*(5), 414–417.

Remick, D. G. (2007). Pathophysiology of sepsis. *American Journal of Pathology*, *170*(5), 1435–1444.

Ren, H. (2011). Sepsis and immune response. *World Journal of Emergency Medicine*, *2*(2), 127.

Repetto, O., & De Re, V. (2017). Coagulation and fibrinolysis in gastric cancer. *Ann. N.Y. Acad. Sci*, *1404*(1), 27–48.

Rhodes, A., Evans, L. E., Alhazzani, W., Levy, M. M., Antonelli, M., Ferrer, R., Kumar, A., Sevransky, J. E., Sprung, C. L., Nunnally, M. E., Rochwerg, B., Rubenfeld, G. D., Angus, D. C., Annane, D., Beale, R. J., Bellinghan, G. J., Bernard, G. R., Chiche, J. D., Coopersmith, C., … Dellinger, R. P. (2017). Surviving Sepsis Campaign: International Guidelines for Management of Sepsis and Septic Shock: 2016. *Intensive Care Medicine*, *43*(3), 304–377.

Rollins, M. R., Larson, E. A., Larson, H. J., & Taylor, J. A. (2016). Factor XIII Contributes to Clot Formation and Thrombin Generation. *Blood*, *128*(22), 208–208.

Rosales, C. (2018). Neutrophil: A cell with many roles in inflammation or several cell types? *Frontiers in Physiology*, *9*(113), 1–17.

Sabbione, F., Keitelman, I. A., Iula, L., Ferrero, M., Giordano, M. N., Baldi, P., Rumbo, M., Jancic, C., & Trevani, A. S. (2017). Neutrophil Extracellular Traps Stimulate Proinflammatory Responses in Human Airway Epithelial Cells. *Journal of Innate Immunity*, *9*(4), 387–402.

Saffarzadeh, M., Juenemann, C., Queisser, M. A., Lochnit, G., Barreto, G., Galuska, S. P., Lohmeyer, J., & Preissner, K. T. (2012). Neutrophil extracellular traps directly

induce epithelial and endothelial cell death: A predominant role of histones. *PLoS ONE*, *7*(2), 1–14.

Saracco, P., Vitale, P., Scolfaro, C., Pollio, B., Pagliarino, M., & Timeus, F. (2011). The coagulopathy in sepsis: Significance and implications for treatment. *Pediatric Reports*, *3*(4), 119–121.

Schneider, M., & Nesheim, M. (2004). A Study of the Protection of Plasmin from Antiplasmin Inhibition within an Intact Fibrin Clot during the Course of Clot Lysis. *Journal of Biological Chemistry*, *279*(14), 13333–13339.

Scully, M., & Levi, M. (2019). How we manage haemostasis during sepsis. *British Journal of Haematology*, *185*(2), 209–218.

Semeraro, F., Ammollo, C. T., Esmon, N. L., & Esmon, C. T. (2014). Histones induce phosphatidylserine exposure and a procoagulant phenotype in human red blood cells. *Journal of Thrombosis and Haemostasis*, *12*(10), 1697–1702.

Semeraro, N., Ammollo, C. T., Semeraro, F., & Colucci, M. (2015). Coagulopathy of Acute Sepsis. *Seminars in Thrombosis and Hemostasis*, *41*(6), 650–658.

Shah, B. H., Rasheed, H., Rahman, I. H., Shariff, A. H., Khan, F. L., Rahman, H. B., Hanif, S., & Saeed, S. A. (2001). Molecular mechanisms involved in human platelet aggregation by synergistic interaction of platelet-activating factor and 5-hydroxytryptamine. *Experimental and Molecular Medicine*, *33*(4), 226–233.

Shiokawa, D., Tanaka, M., Kimura, T., Hashizume, K., Takasawa, R., Ohyama, H., Fujita, K., Yamada, T., & Tanuma, S. ichi. (2000). Characterization of two DNase γ-specific monoclonal antibodies and the in situ detection of DNase γ in the nuclei of apoptotic rat thymocytes. *Biochemical and Biophysical Research Communications*, *275*(2), 343–349.

Silk, E., Zhao, H., Weng, H., & Ma, D. (2017). The role of extracellular histone in organ injury. *Cell Death & Disease*, *8*(5), 2812–2822.

Simmons, J., & Pittet, J. F. (2015). The coagulopathy of acute sepsis. *Current Opinion in Anaesthesiology*, *28*(2), 227–236.

Singer, M., Deutschman, C. S., Seymour, C., Shankar-Hari, M., Annane, D., Bauer, M., Bellomo, R., Bernard, G. R., Chiche, J. D., Coopersmith, C. M., Hotchkiss, R. S., Levy, M. M., Marshall, J. C., Martin, G. S., Opal, S. M., Rubenfeld, G. D., Poll, T. Der, Vincent, J. L., & Angus, D. C. (2016). The third international consensus definitions for sepsis and septic shock (sepsis-3). *JAMA - Journal of the American Medical Association*, *315*(8), 801–810.

Sisirak, V., Sally, B., D'Agati, V., Martinez-Ortiz, W., Özçakar, Z. B., David, J., Rashidfarrokhi, A., Yeste, A., Panea, C., Chida, A. S., Bogunovic, M., Ivanov, I. I., Quintana, F. J., Sanz, I., Elkon, K. B., Tekin, M., Yalçınkaya, F., Cardozo, T. J., Clancy, R. M., … Reizis, B. (2016). Digestion of Chromatin in Apoptotic Cell Microparticles Prevents Autoimmunity. *Cell*, *166*(1), 88–101.

Smith, S. A., Travers, R. J., & Morrissey, J. H. (2015). How it all starts: Initiation of the

clotting cascade. *Critical Reviews in Biochemistry and Molecular Biology*, *50*, 326–336.

Soni, C., & Reizis, B. (2019). Self-DNA at the epicenter of SLE: Immunogenic forms, regulation, and effects. *Frontiers in Immunology*, *10*, 1601.

Springer, T. A. (2014). Von Willebrand factor, Jedi knight of the bloodstream. *Blood*, *124*(9), 1412–1425.

Standeven, K. F., Ariëns, R. A. S., Whitaker, P., Ashcroft, A. E., Weisel, J. W., & Grant, P. J. (2002). The effect of dimethylbiguanide on thrombin activity, FXIII activation, fibrin polymerization, and fibrin clot formation. *Diabetes*, *51*(1), 189–197.

Stroun, M., Lyautey, J., Lederrey, C., Olson-Sand, A., & Anker, P. (2001). About the possible origin and mechanism of circulating DNA: Apoptosis and active DNA release. *Clinica Chimica Acta*, *313*(2), 139–142.

Swystun, L. L., Mukherjee, S., & Liaw, P. C. (2011). Breast cancer chemotherapy induces the release of cell-free DNA, a novel procoagulant stimulus. *Journal of Thrombosis and Haemostasis*, *9*(11), 2313–2321.

Tatsiy, O., & McDonald, P. P. (2018). Physiological stimuli induce PAD4-Dependent, ROS-Independent NETosis, with early and late events controlled by discrete signaling pathways. *Frontiers in Immunology*, *9*(2036), 1–12.

Vancevska, A., & Nikolic, A. (2013). Assessment of Deoxyribonuclease Activity in Biological Samples by a Fluorescence Detection-Based Method. *Laboratory Medicine*, *44*(2), 125–128.

Versteeg, H. H., Heemskerk, J. W. M., Levi, M., & Reitsma, P. H. (2013). New Fundamentals in hemostasis. *Physiological Reviews*, *93*(1), 327–358.

von Brühl, M.-L., Stark, K., Steinhart, A., Chandraratne, S., Konrad, I., Lorenz, M., Khandoga, A., Tirniceriu, A., Coletti, R., Köllnberger, M., Byrne, R. A., Laitinen, I., Walch, A., Brill, A., Pfeiler, S., Manukyan, D., Braun, S., Lange, P., Riegger, J., … Massberg, S. (2012). Monocytes, neutrophils, and platelets cooperate to initiate and propagate venous thrombosis in mice in vivo. *The Journal of Experimental Medicine*, *209*(4), 819–835.

Walker, C. K., Sandmann, E. A., Horyna, T. J., & Gales, M. A. (2017). Increased Enoxaparin Dosing for Venous Thromboembolism Prophylaxis in General Trauma Patients. *Annals of Pharmacotherapy*, *51*(4), 323–331.

Wang, Y., Gallant, R. C., & Ni, H. (2016). Extracellular matrix proteins in the regulation of thrombus formation. *Current Opinion in Hematology*, *23*(3), 280–287.

Weitz, J., Young, E., Johnston, M., Stafford, A. R., Fredenburgh, J. C., & Hirsh, J. (1999). Vasoflux, a new anticoagulant with a novel mechanism of action. *Circulation*, *99*(5), 682–689.

Wildhagen, K. C. A. A., De Frutos, P. G., Reutelingsperger, C. P., Schrijver, R., Aresté, C., Ortega-Gómez, A., Deckers, N. M., Hemker, H. C., Soehnlein, O., & Nicolaes,

G. A. F. (2014). Nonanticoagulant heparin prevents histone-mediated cytotoxicity in vitro and improves survival in sepsis. *Blood*, *123*(7), 1098–1101.

Wood, J. P., Bunce, M. W., Maroney, S. A., Tracy, P. B., Camire, R. M., & Mast, A. E. (2013). Tissue factor pathway inhibitor-alpha inhibits prothrombinase during the initiation of blood coagulation. *Proceedings of the National Academy of Sciences of the United States of America*, *110*(44), 17838–17843.

Wood, J. P., Ellery, P. E. R., Maroney, S. A., & Mast, A. E. (2014). Biology of tissue factor pathway inhibitor. *Blood*, *123*(19), 2934–2943.

Xu, J., Zhang, X., Monestier, M., Esmon, N. L., & Esmon, C. T. (2011). Extracellular histones are mediators of death through TLR2 and TLR4 in mouse fatal liver injury. *Journal of Immunology (Baltimore, Md. : 1950)*, *187*(5), 2626–2631.

Xu, J., Zhang, X., Pelayo, R., Monestier, M., Ammollo, C. T., Semeraro, F., Taylor, F. B., Esmon, N. L., Lupu, F., & Esmon, C. T. (2009). Extracellular histones are major mediators of death in sepsis. *Nature Medicine*, *15*(11), 1318–1321.

Xu, X. R., Carrim, N., Neves, M. A. D., McKeown, T., Stratton, T. W., Coelho, R. M. P., Lei, X., Chen, P., Xu, J., Dai, X., Li, B. X., & Ni, H. (2016). Platelets and platelet adhesion molecules: Novel mechanisms of thrombosis and anti-thrombotic therapies. *Thrombosis Journal*, *14*(1), 37–49.

Yang, S., Qi, H., Kan, K., Chen, J., Xie, H., Guo, X., & Zhang, L. (2017). Neutrophil extracellular traps promote hypercoagulability in patients with sepsis. *Shock*, *47*(2), 132–139.

Yeung, E. N. W., Treskes, P., Martin, S. F., Manning, J. R., Dunbar, D. R., Rogers, S. M., Le Bihan, T., Lockman, K. A., Morley, S. D., Hayes, P. C., Nelson, L. J., & Plevris, J. N. (2015). Fibrinogen production is enhanced in an in-vitro model of non-alcoholic fatty liver disease: an isolated risk factor for cardiovascular events? *Lipids in Health and Disease*, *14*, 86.

Young, E. (2008). The anti-inflammatory effects of heparin and related compounds. *Thrombosis Research*, *122*(6), 743–752.

Yu, X., & Diamond, S. L. (2019). Fibrin Modulates Shear-Induced NETosis in Sterile Occlusive Thrombi Formed under Haemodynamic Flow. *Thrombosis and Haemostasis*, *119*(4), 586–593.

Yusuf, S., Mehta, S. R., Chrolavicius, S., Afzal, R., Pogue, J., Granger, C. B., Budaj, A., Peters, R. J. G., Bassand, J. P., Wallentin, L., Joyner, C., & Fox, K. A. A. (2006). Comparison of fondaparinux and enoxaparin in acute coronary syndromes. *New England Journal of Medicine*, *354*, 1464–1476.

Zarychanski, R., Abou-Setta, A. M., Kanji, S., Turgeon, A. F., Kumar, A., Houston, D. S., Rimmer, E., Houston, B. L., McIntyre, L., Fox-Robichaud, A. E., Hébert, P., Cook, D. J., & Fergusson, D. A. (2015). The efficacy and safety of heparin in patients with sepsis: A systematic review and metaanalysis. *Critical Care Medicine*, *43*(3), 511–518.

Zhang, L., Gong, Y., Grella, D. K., Castellino, F. J., & Miles, L. A. (2003). Endogenous plasmin converts Glu-plasminogen to Lys-plasminogen on the monocytoid cell surface. *Journal of Thrombosis and Haemostasis*, *1*(6), 1264–1270.

Zhao, L., Wu, M., Xiao, C., Yang, L., Zhou, L., Gaoa, N., Li, Z., Chen, J., Chen, J., Liu, J., Qin, H., & Zhao, J. (2015). Discovery of an intrinsic tenase complex inhibitor: Pure nonasaccharide from fucosylated glycosaminoglycan. *Proceedings of the National Academy of Sciences of the United States of America*, *112*(27), 8284–8289.

Zucoloto, A. Z., & Jenne, C. N. (2019). Platelet-Neutrophil Interplay: Insights Into Neutrophil Extracellular Trap (NET)-Driven Coagulation in Infection. *Frontiers in Cardiovascular Medicine*, *6*(85), 1–8.

7.0 Appendix

7.0.1 Determining the affinity between histones and UFH, enoxaparin, fondaparinux, and Vasoflux

The affinity between individual human histones and UFH, enoxaparin, fondaparinux, and Vasoflux were determined using the BLITz. Figure 7.1 shows the raw binding curves for UFH (A), enoxaparin (B), Vasoflux (C), or fondaparinux (D). UFH, enoxaparin, and Vasoflux have high binding affinities for histones, while fondaparinux has a low binding affinity for histones.

Figure 7.1. Raw binding curves of the BLITz data. Interactions between histones and either: UFH (A), enoxaparin (B), Vasoflux (C), or fondaparinux (D) are shown.

A.

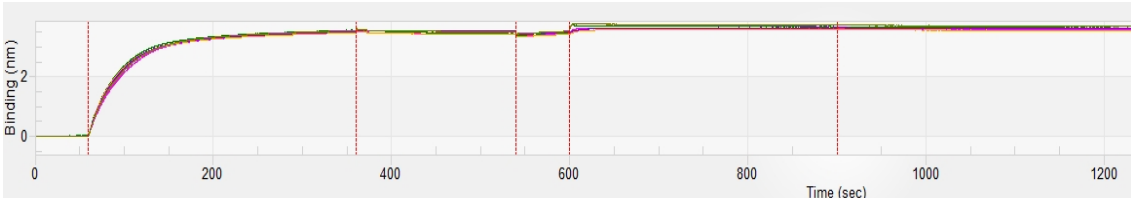

B.

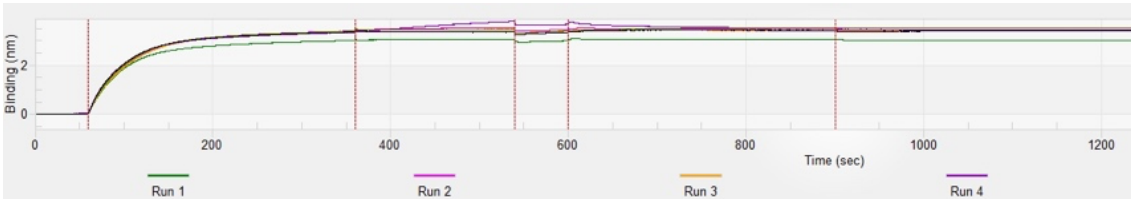

C.

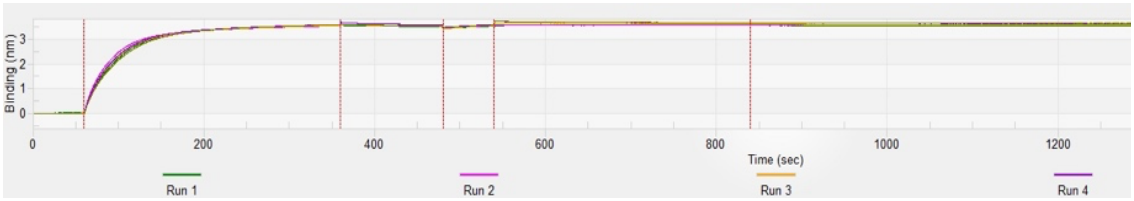

D.

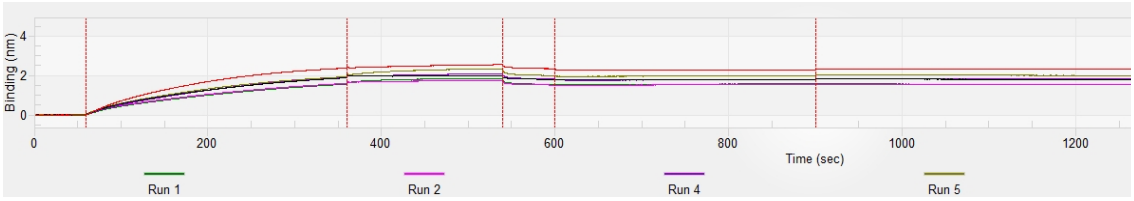

7.0.2 Comparing APC and plasmin on DNase I-mediated degradation of DNA-histone complexes and NETs

In addition to determining the effects of GAGs on enhancing DNase I-mediated degradation of DNA-histone complexes and NETs, we also tested the ability of APC or plasmin to accelerate the activity of DNase I. When APC was added with DNase I, the complexes were degraded (Figure 7.2, Lanes 9, 10, 11, 12). Notably, only 2 nM of APC was required for complete complex degradation. The presence of plasmin also enabled DNase I to degrade the DNA-histone complexes, with 0.1 μM of plasmin being sufficient for complete complex degradation (Figure 7.2, Lane 10).

Figure 7.2. Effects of APC or plasmin on DNase I activity. DNA (3 nM) and histones (3 μM) were incubated for 1 hour at 37°C to form DNA-histone complexes. DNase I (0.5 μM) was added to the complexes either alone or in combination with increasing concentrations of (A) APC, or (C) plasmin for 30 minutes at 37°C. The samples were run on a 1.8% agarose gel stained with RedSafe for 1 hour at 110 V. Each image is representative of n = 3 gels. Gels were quantified using densitometry, and the percent DNA in the wells was reported as mean ± SEM (n = 3) (B, D). Next, neutrophils were isolated from healthy human whole blood, added to coverslips, and 100 nM PMA was added. Coverslips were incubated for 4 hours at 37°C and 5% CO_2 to allow for NETosis as visualized by SYTOX Green. DNase I (0.5 μM) was added to the NETs in combination with APC (0.8 nM) (E) or plasmin (2 μM) (F). Images were obtained using a fluorescence microscope. Each image is representative of n = 3 experiments with three different blood donors.

A.

APC (nM)	1 kb ladder	2	-	-	-	-	-	-	0.1	0.8	2	3	2
DNase I (0.5 μM)		-	+	-	-	+	-	+	+	+	+	+	-
DNA (3 nM)		-	-	+	-	+	+	+	+	+	+	+	+
Histones (3 μM)		-	-	-	+	-	+	+	+	+	+	+	+
Lane Number	1	2	3	4	5	6	7	8	9	10	11	12	13

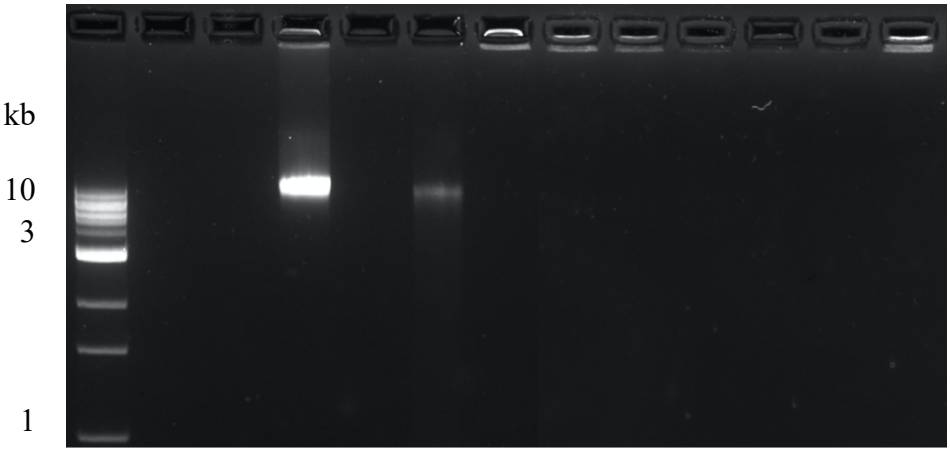

B.

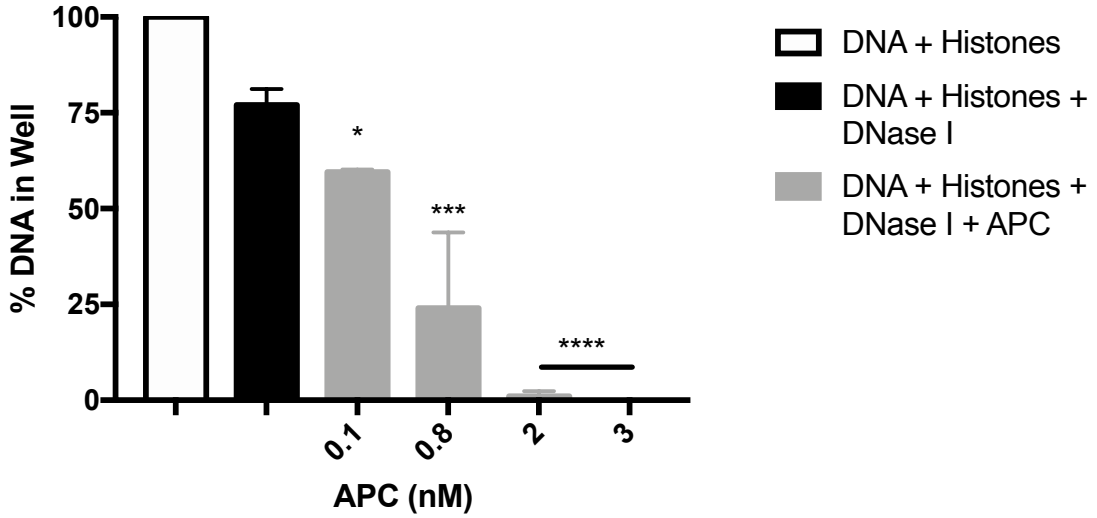

C.

Plasmin (μM)	1 kb ladder	2	-	-	-	-	-	-	0.01	0.1	1	2	1
DNase I (0.5 μM)		-	+	-	-	+	-	+	+	+	+	+	-
DNA (3 nM)		-	-	+	-	+	+	+	+	+	+	+	+
Histones (3 μM)		-	-	-	+	-	+	+	+	+	+	+	+
Lane Number	1	2	3	4	5	6	7	8	9	10	11	12	13

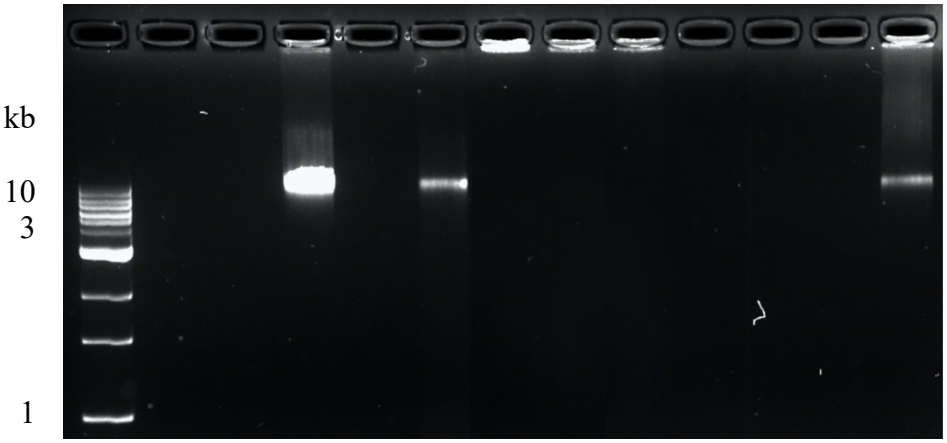

D.

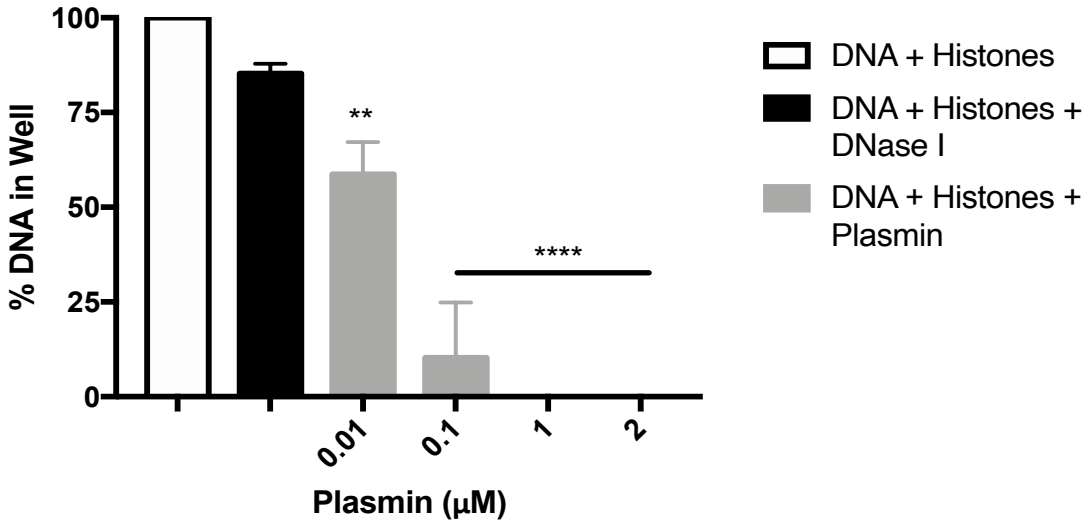

E. NETs + DNase I + APC (0.8 nM)

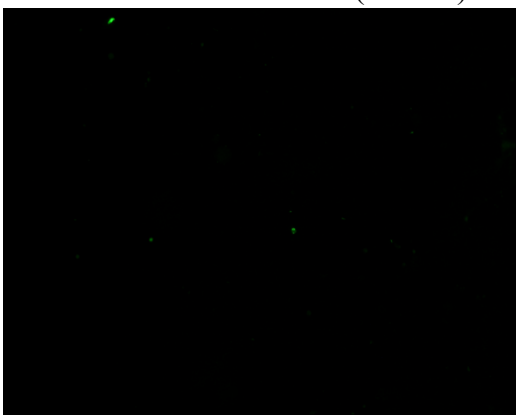

F. NETs + DNase I + Plasmin (2 μM)

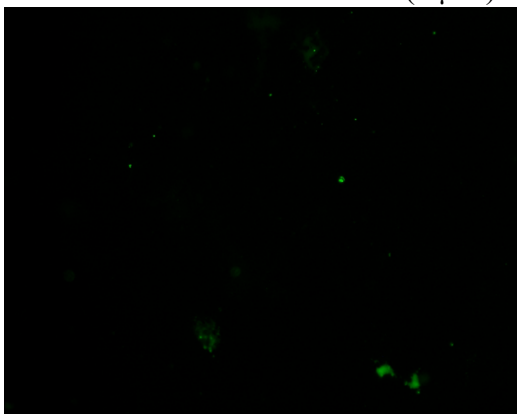

7.0.3 Measuring the levels of APC in plasma of septic patients

In addition to understanding how DNA levels are regulated in sepsis, we are also interested in understanding the regulation and clearance of histones, which is a major component of NETs. APC is a serine protease that inhibits NETosis and also degrades histones. These functions make APC an important enzyme to study as a potential therapeutic strategy to reduce the mortality rates associated with sepsis. In this study, we measured plasma APC levels in healthy controls (n =17), septic survivors (n = 9 – 21), and non-survivors (n = 3 – 23) longitudinally (on days 1, 3, 7, 14, 21, 28). There were no statistically significant differences between the groups (Figure 7.3). We also determined the correlation between protein C and APC levels in these patients (Figure 7.3). The correlation showed a positive trend on all the days except for day 7. Protein C and APC levels were statistically significant only on day 21. These findings can be attributed to patient variability, and give support to the need for a more personalized medicine approach to treating septic patients.

APC attenuates many pathophysiological states present in sepsis, such as hypercoagulability. APC is a natural anticoagulant enzyme due to its ability to inactivate FVa and FVIIIa, thereby reducing thrombin generation (Esmon., 2003). Another protective effect of APC is its ability to inhibit the formation of NETs, which prevents multiple organ damage, as well as micro- and macro-vascular thrombosis (McDonald et al., 2017). We also showed that APC can enhance DNase I-mediated digestion of DNA-protein complexes in a purified system (Figure 7.2). Therefore, the combination of APC with DNase I can be a potential therapeutic strategy for targeting many harmful molecules in sepsis.

Figure 7.3. Plasma APC levels in septic patients (days 1 to 28). APC levels were measured in healthy controls (n = 17), septic survivors (n = 9 – 21), and non-survivors (n = 3 – 23) longitudinally (on days 1, 3, 7, 14, 21, 28) using an APC enzyme capture assay (A). Correlations between protein C levels and APC levels in the septic patients were made using Pearson's correlation coefficient (B, C, D, E, F, G). Significant differences between groups were determined using a one-way ANOVA followed by Tukey's multiple comparisons test. P-values < 0.05 were considered significant. Values are expressed as mean ± SEM.

A.

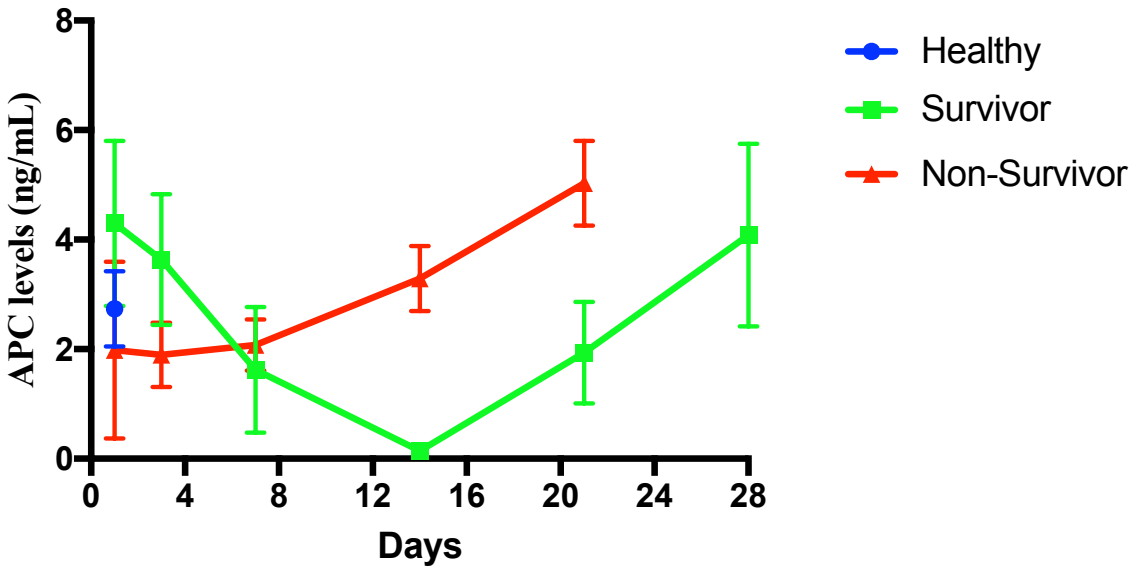

B.

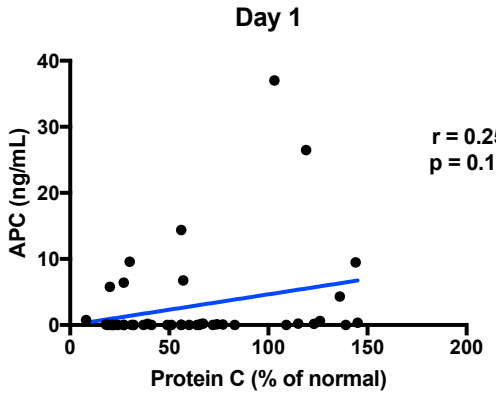
Day 1
APC (ng/mL)
Protein C (% of normal)
r = 0.25
p = 0.10

C.

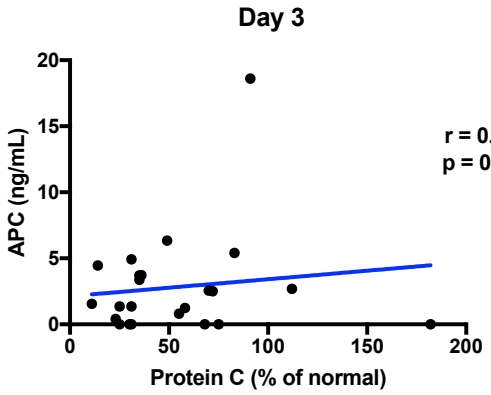
Day 3
APC (ng/mL)
Protein C (% of normal)
r = 0.13
p = 0.57

D.

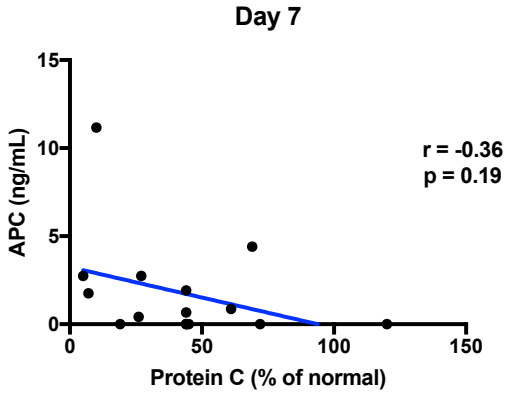
Day 7
APC (ng/mL)
Protein C (% of normal)
r = -0.36
p = 0.19

E.

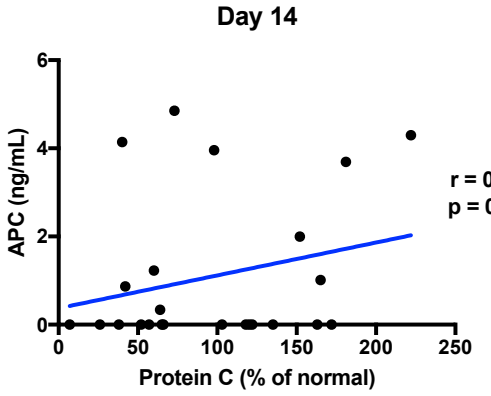
Day 14
APC (ng/mL)
Protein C (% of normal)
r = 0.25
p = 0.24

F.

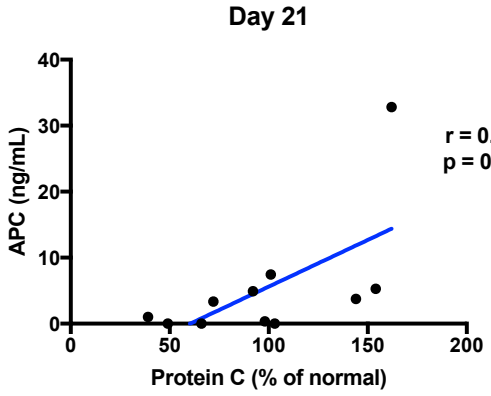
Day 21
APC (ng/mL)
Protein C (% of normal)
r = 0.62
p = 0.04

G.

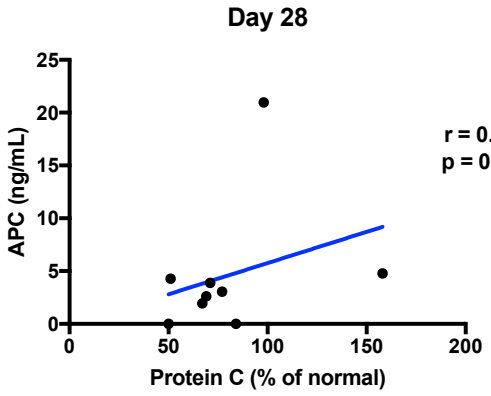
Day 28
APC (ng/mL)
Protein C (% of normal)
r = 0.30
p = 0.43

7.0.4 Determining the effects of age on the levels of DNA in healthy mice

We have previously reported that DNA has high prognostic value in predicting mortality in septic patients (Dwivedi et al., 2012). The role of aging and its effects on the levels and clearance of DNA have not been reported in literature. To determine the effects of age on the levels of DNA, we collected plasma from healthy mice of different age groups over time using a retro-orbital blood collection technique. We measured DNA levels using the PicoGreen dsDNA quantitation assay. The levels of DNA were not statistically significant between mice of different age groups, nor did the levels of DNA change over time (Figure 7.4). The average body weight of each age group did not differ statistically over time (Figure 7.4). Taken together, this suggests that aging does not affect the clearance of DNA in healthy conditions.

Figure 7.4. Plasma levels of cfDNA in healthy mice in an aging study. Plasma levels of DNA were measured in healthy mice of different age groups (n = 3 – 6 in each group) using the PicoGreen dsDNA quantitation assay (A). Different colours represent the different age groups (blue = 6 weeks, red = 12 weeks, black = 29 weeks, and green = 86 weeks old, at the beginning of the study). Results are representative of n = 3 different experiments. The body weight of each mouse was measured (B). Significant differences between groups were determined using a one-way ANOVA followed by Tukey's multiple comparisons test. Values are expressed as mean ± SEM.

A.

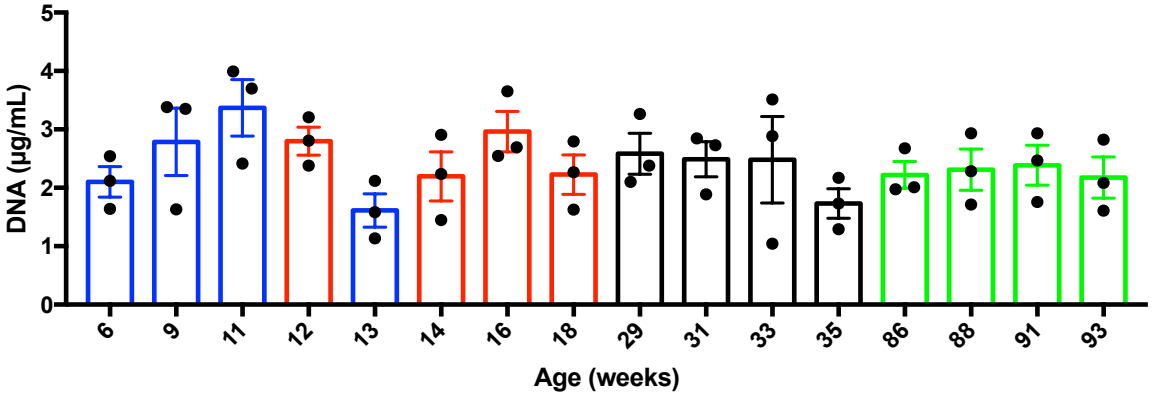

B.